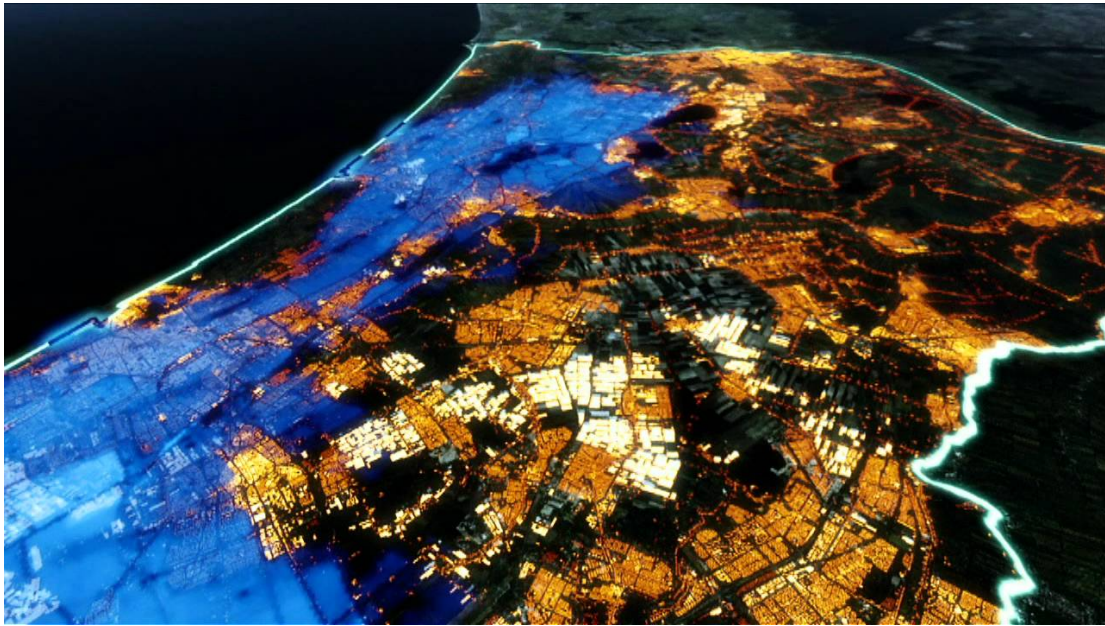DELFT UNIVERSITY OF TECHNOLOGY

Impact assessment for the area dikering 14 under the influence of sea level rise

MSc Thesis

Koen van der Vaarst

Graduation Committee:
Prof.dr.ir. M. Kok - TU Delft
Dr.ir. R.C. Lanzafame - TU Delft
Dr.ir. M.M. Rutten - TU Delft
ir. M. Bos - Royal HaskoningDHV
ir. R. Huting - Royal HaskoningDHV

TUDelft Delft University of Technology

November 26, 2021

Royal **HaskoningDHV**
Enhancing Society Together

Impact assessment for the area dikering 14 under the influence of sea level rise

by

K.T. (Koen) van der Vaarst

to obtain the degree of Master of Science

at the Delft University of Technology,

to be defended publicly on Friday December 3, 2021 at 03:45 PM.

Student number: 4468228
Thesis committee: Prof. dr. ir. M. Kok,   TU Delft, chair
                    Dr. ir. R. C. Lanzafame,   TU Delft
                    Dr. ir. M. M. Rutten,   TU Delft
                    Ir. M. Bos,   Royal HaskoningDHV, daily supervisor
                    Ir. R. Huting,   Royal HaskoningDHV

An electronic version of this thesis is available at http://repository.tudelft.nl/.

TUDelft Delft University of Technology

Preface

With this thesis I complete my time at TU Delft and this thesis contains 2 years of knowledge of the Master Hydraulic Engineering. During this period, I became more and more aware of the threats posed by climate change and the challenges that will come to protect the Netherlands against rising water levels. I quickly found out that my interest are mainly with the theme of flood risk, where not only the safety of the flood defences must be considered, but also the potential economic and societal consequences.

The chairman of my graduation committee, Matthijs Kok, was able to put me in contact with my supervisors from Royal HaskoningDHV, Matthijs Bos and Ric Huting, who together have extensive experience in the field of flood risk management and climate adaptation. Together with Matthijs and Ric, we came up with a subject that both suited my interests and was socially relevant. I would like to thank Matthijs Bos and Ric Huting for their guidance during my graduation in this difficult COVID times. Although we mainly saw each other through video calls, I noticed that I could always call you and ask you questions when I needed some help. I would also like to thank Matthijs Kok for the many interesting conversations and feedback, in which you always made me think critically about my own assumptions and developed methods. I would also like to thank the other members of my graduation committee, Robert Lanzafame and Martine Rutten, who during my progress meetings and green light meeting always came up with interesting critical questions and comments that made me look at the problem in other ways and investigate the effect of my own assumptions.

During my thesis, I learned to work with various software programs which enabled me to assess the safety of flood defences. It often took me a relatively long time to understand the progams because I ran into frustrating errors. Several specialists helped me a lot in understanding these errors so I could continue with my thesis. I would like to thank Robert Slomp and Thomas van Walsum from Rijkswaterstaat and Joost Veer from the Water Board Rijnland especially for helping me understand the MorphAn and Hydra-NL programs.

I also received a lot of help from colleagues who were very involved during my graduation. I would like to thank Maarten Schoenmaker for the interesting conversations and his help with the Hydra-NL program. Without the help of Friso Dam and Almar Joling I would still be stuck in a programming code and the conversations with Sam Westerhof gave me a lot of insights into the loss of life estimation.

My family and friends have always supported me throughout my thesis, and I could always turn to them when I needed some distraction. I would like to thank my parents and brother Niels for supporting me throughout my study. Finally, I would like to thank my girlfriend, Saskia, who always made me laugh during difficult times.

K.T. (Koen) van der Vaarst

Rotterdam, November 2021

Abstract

Climate change is a major problem for today's society, which has a huge impact on water safety issues. Recent IPCC scenarios show that sea level rises of 1m by 2100 and 2m beyond 2200 should be seriously considered. Several scenarios show an increase in river discharge of between 10 and 20 percent of the Rhine generated by extreme precipitation by the year 2050. The combination of the sea level rise and the increase in river discharge has consequences for the flood risk in the Netherlands. The area where most people live, about 3,5 million, and where most of the gross national product, around 65 percent, is earned is the area of dikering 14. This thesis determines how the flood risk changes for future climate change scenarios, considering a sea level rise up to 2m and an associated increase in river discharge. One base case scenario with the current situation and four future scenarios with a sea level rise up to 2m with increments of 0,5m were evaluated. The river dikes along the trajectories of the Hollandse Ijssel, Nieuwe Maas and Nieuwe Waterweg and the dunes between Hoek van Holland and Ijmuiden were assessed and the consequences of flooding due to a dune or dike breach were investigated for all scenarios.

Flood risk is determined by the probability of failure of a flood defence and the consequences in case of a flood, which are expressed in economic damage, casualties and affected persons. The influence of climate change on the probability of failure of 8 river dike profiles was investigated by assessing the failure mechanism overtopping and overflow, using a relationship between height shortage and the probability of failure. The height shortage was determined by subtracting the hydraulic load level from the crest level of the dike. The safety of the dunes was evaluated using the Duros-plus model, with which dune erosion calculations were made. The results show that climate change has a big impact on the probability of failure, which is highest for the trajectory along the Hollandse Ijssel with a probability of failure of 1/370.000 per year in the current situation and 1/170 per year in the scenario involving a 2 m sea level rise. Although the failure probabilities of the dunes are very low in the current situation, the influence of sea level rise is shown for the dunes with failure probabilities that are a factor of 2000-3000 higher in a scenario with 2m sea level rise compared to the base case scenario.

For determining the consequences, both existing flood scenarios for the river side and new flood scenarios for the seaside were used. The new flood scenarios show the effect of sea level rise on the increased flood extent caused by a dune breach for each scenario. The potential economic damage is determined by combining the flood depth, damage curves and the land use map and is highest, 14.300 million Euros, for a dike failure along the Hollandse Ijssel, as the highest flood depths are reached in these deep polders. The highest number of casualties, 7900, determined by the mortality rates based on flood depth, flow velocity, rise rate and evacuation factor, are expected in case of a dike failure along the Nieuwe Maas, as the densely populated cities of Rotterdam and Schiedam are flooded. By assigning monetary values for casualties and affected persons, the total damage is determined, to which the damages resulting from casualties and affected persons contribute most.

After determining the costs of several reinforcement projects, these costs and the potential total damage were used as input in a cost-benefit analysis, where economic optimums were determined expressed in a probability of failure and associated investment costs. The conclusion is that it is economically efficient to reinforce all flood defences except for the trajectory along the Nieuwe Waterweg in case of a scenario corresponding to 2m sea level rise. It was also examined whether the economic optimums met the requirement that everyone should have a maximum risk of dying due to a flood of 10^{-5} per year. A total length of 40,5 km river dikes and 63,5 km of dunes will need to be reinforced, for which the costs of reinforcing the river dikes are significantly higher than for the dunes, approximately 20 and 3,8 million euros/km respectively. The total estimated costs determined in this study are around 1 billion euros for a 2m sea level rise scenario, but these costs for keeping the area safe will be a factor of 2-3 higher, as the method used in this study for determining the costs of river dike reinforcements leads to an underestimation of the total costs in reality. In addition, hydraulic structures and future subsidence are not included, which will also lead to higher total costs. With these investments the flood risk will remain acceptable and the river dikes and dunes will continue to offer sufficient protection against floods with a total potential damage of 230 billion euros, consisting of 70 billion euros in economic damage, 20.000 casualties and 2,5 million affected persons.

Contents

List of Figures

List of Tables

1. Introduction

1.1. General context

Climate change is a global threat and also results in a change in the outcomes of the flood risk approach. Rising water levels in the rivers and at sea result in higher hydraulic loads on the flood defences, increasing the probability of failure and therefore both the economic risks and the risk of casualties. These rise of the sea level and water levels in the rivers as a result of climate change will present the Netherlands with an enormous challenge. The pressure on the flood defences and the entire water system will increase over this century. It is important to map out the possible solutions so that a policy for ensuring water safety can be created to prevent a disaster like the flooding in 1953 called the 'watersnoodramp'. Not only should the solutions be considered, but also the effectiveness and the costs of these solutions. Not only should solutions be considered, but also the effectiveness and costs of these solutions. By looking at the reduction of the failure probability or the reduction of the consequences, the effectiveness of certain solutions can be measured. In this study, the focus will be on reducing the probability of failure. The combination of the probability and the consequences of the flooding will result in the flood risk, see Figure 1.1. In a government policy, a trade-off can then be made between the amount of investments needed for solutions and the safety level.

Figure 1.1: The risk of flooding can be determined by multiplying the flooding probability and the consequences, which are expressed in both economic damages and casualties and affected persons (Vergouwe, 2015).

The Netherlands is divided into several dikerings, which are flood prone areas, where dikering 14 protects the Randstad. Dikering 14 is threatened by storm surges from the North Sea and flooding from the Rijnmond. Within dikering 14 there are places which are 6 meters below sea level. The fact that this area is one of the lowest lying parts of the Netherlands and the enormous social and economic activity that takes place in the Randstad, result in an enormous potential damage for this area in case of a dike breach (S. Jonkman, 2007). This enormous potential damage is mainly due to the large number of people living in this area, around 3,5 million people, and to the fact that around 65 percent of the gross national product is earned there (Traa, 2012).

This potential damage will increase as a result of higher expected water levels in the future scenarios determined by the Royal Netherlands Meteorological Insitute (KNMI) . These scenarios contain various uncertainties, including the amount of emission of greenhouse gases. A high emissions scenario may lead to a sea level rise of around 1,1 m in the year 2100 and the long-term scenario gives an estimate of between 2,3 and 5,4 m in the year 2300 (KNMI, 2019), see Figure 1.2.
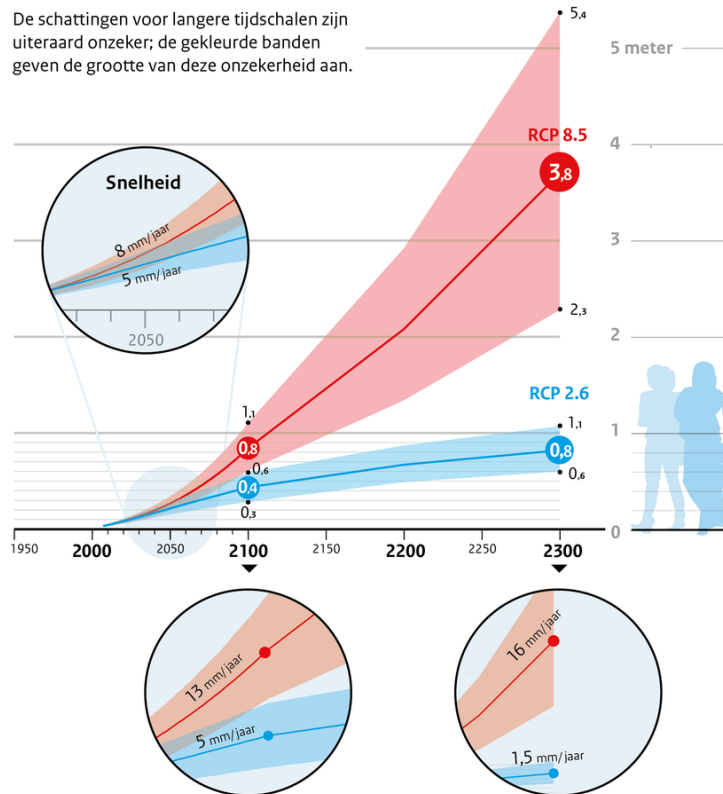
Figure 1.2: Expected sea level rise [m] and rise rate [mm/yr] from now to 2300 determined by the KNMI with two different scenarios. 1) RCP 85 is the scenario with the highest greenhouse gas emissions and 2) RCP 2.6 is the scenario with the lowest greenhouse gas emissions (KNMI, 2019)

This study will look at possible consequences for several scenarios of sea level rise up to 2 m. A sea level rise of 1 m by 2100 will have to be seriously taken into account and for the long term, from 2200, even sea level rise of more than 2 m will have to be considered, see Figure 1.2. Increased river discharge due to climate change will also be taken into account.

To get insight in the possible consequences of the aforementioned sea level rise and increase in river discharge, a complete impact assessment of the increased water levels has to be made. Consequences of flooding have impact on economic, political, social, psychological, ecological and environmental aspects. This consequences can be divided in direct, indirect, tangible and intangible damages. An incomplete overview from S. Jonkman (2007) is included in Table 1.1.

	Tangible	**Intangible**
Direct	Residences Other buildings Cars Infrastructure Business interruption (inside flooded area)	Fatalities Injuries Animals Loss of cultural heritage ...
Indirect	Damage for companies outside flooded area ...	Societal disruption Damage to government

Table 1.1: Classification of flood damage (S. Jonkman, 2007)

To ensure an appropriate level of safety in the Netherlands and especially in the area of dikering 14, a careful analysis of flood risks must be completed, whereby a trade-off must made between the costs, in-

2

vestments in flood defences, and the allowable flood risk. The growing threats from climate change like increasing potential damages require a well-thought and detailed impact assessment. As many factors as possible has to be included to improve the future decision making process for water safety. With an impact assessment that is as complete as possible, the timing and extent of investments in water safety of in this specific case dike ring 14 can be determined.

1.2. Problem definition

Prior to this thesis, a study by Ranneft (2020) was conducted into strengthening and/or raising the height of the dunes in dikering 14, which could be necessary because of the expected rise in sea level. For the three different locations assessed in this study, see Figure 1.3. An economic optimum was found for the safety levels, looking at possible direct and indirect damage. The Kijkduin and Monster locations met the required safety level of a flooding probability of 1/10.000 per year. The economic optimum for Noordwijk came out slightly below this standard. However, if the dependency of the entire dike ring is included, the conclusion is that both the northern part and the southern part have an economic optimum whereby the flood risks are above the safety standard (Ranneft, 2020). However, nowadays there are different standards for the safety levels for the primary flood defences. The old requirement for dike ring 14, the flood defences had to be able to withstand a hydraulic load level that would occur once every 10.000 years, no longer applies. The new standards are explained later in this section.

Figure 1.3: Overview area of dikering 14 with the three dots as the locations from North to South: Noordwijk, Kijkduin and Monster.

This is not the complete story, since, among other things, as the loss of life estimation is not included in this analysis. The goal of this thesis is to supplement Meyer's thesis with more aspects, such as the loss of life estimation, and so to result in a more complete story. The consequences of a potential flood can be briefly expressed in two different ways: the potential economic damage, which was examined in the aforementioned study, and the potential number of casualties and fatalities. In this thesis the probability of death in the event of a potential flood is considered, which is influenced by the evacuation rate, the flood characteristics, and the behavior and vulnerability of those left behind. The probability that an individual will die as a result of a possible flood must not exceed 1/100.000 per year ('Local Individual Risk (LIR)'), which means that each individual must have a minimum protection level of 10-5 per year. This minimum protection level is stated in the Water Act. This means that the LIR is a measure of risk for a location which expresses the probability that a person who is present at a particular location will die as a result of flooding (ENW, 2017). In this LIR, potential evacuation is taken into account. Setting a limit to this probability gives a minimum protection to everyone living in areas in the Netherlands protected by flood defences. In addition, a higher level of protection is applied for locations with potentially large economic damage, large impact on vital infrastructure and/or a potentially large number of casualties.

In order to achieve a more complete study, an analysis of the potential casualties and affected persons will be added to the previous thesis (Ranneft, 2020). This will involve looking at both the individual risk and the loss of life estimation as a result of a possible threats of flooding. Due to the increase in water

levels as a result of climate change, these aforementioned risks will also increase. The question is therefore whether in the future this risk will not fall below the safety standards. New standards have applied since 2017. Previously, a certain water level was defined that a flood defence had to withstand. This standard focused mainly on the hydraulic load on the flood defence and not on its strength. For dikering 14, this standard was the most strict, which meant that the primary flood defences had to withstand a water level that occurred 1/10.000 per year. Other areas in the country had lower standards, see Figure 1.4. These standards applied to the entire dikering 14. The high norm was based on the high economic value that this area represents, 65 percent of the country GNP. This high economic value in combination with a large part of the area laying below sea level, results in high potential damages (Vergouwe, 2015).
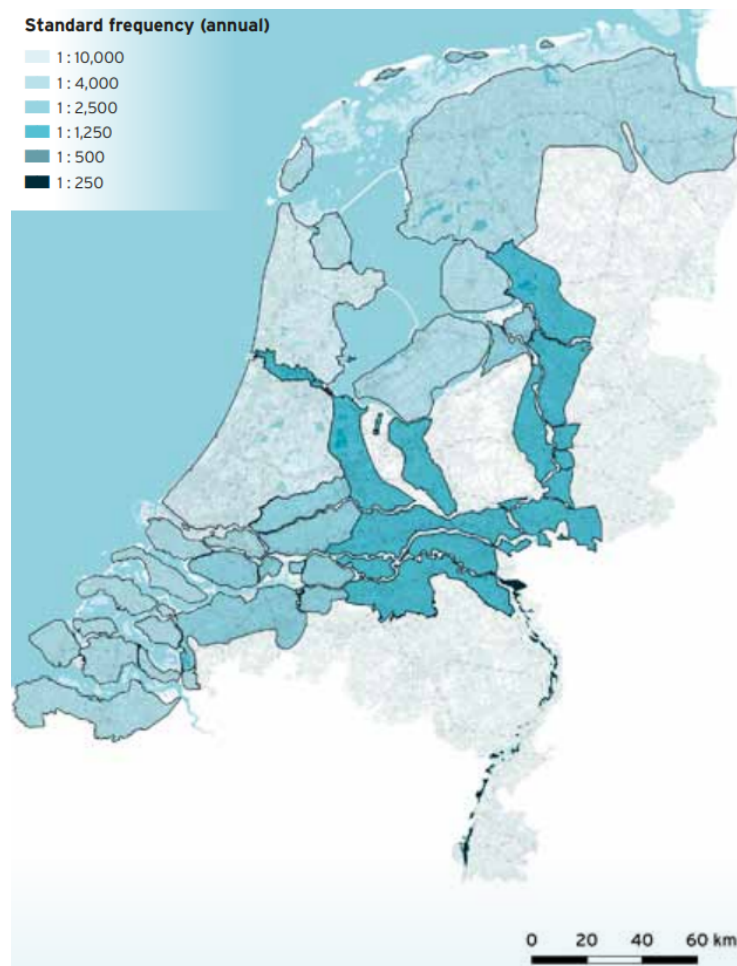
Figure 1.4: Old standards expressed as an exceedance probability of the waterlevels for each dikering. The flood defences protecting dikering 14 had to withstand water levels that may occur 1/10.000 per year (Vergouwe, 2015).

From 2017, the standards have been defined as a probability of flooding that is considered acceptable. These standards have been determined by the government following advice from risk assessments and cost-benefit studies. This probability of flooding depends not only on the hydraulic load, but also on the strength of the flood defence. The new standard is based on the risk of flooding. This risk consists of the economic risk (cost-benefit analyses), the societal risk and the individual risk (LIR). Together, these risks form the basis for the new standards which are included in the Water Act for primary flood defences. In short, the greater the total consequences of a flood, the stricter the standard and the smaller the probability of flooding. Another difference is that the standards are no longer set for a whole dikering, but for each seperate dike trajectory. A dike trajectory is defined as length of dikes exposed to the same threat and, in the event of the failure of a dike in the dike trajectory, this would result in similar consequences (ENW, 2017).

The Water Act defines two different flooding probabilities for primary water defences (ENW, 2017):

1. Signaling value (in Dutch 'signaleringswaarde'): If the probability of flooding of a dike trajectory is greater than this value, this should be reported to the government at the Minister of Infrastructure and the Environment. If this value is reached there is still sufficient time to take measures until the lower limit is reached.

2. Threshold (in Dutch 'grenswaarde'): The flood defences have to be designed at least for this probability of flooding. This is the basic protection level.

An overview of the signal value and the threshold is given in Figure 1.5. From Figure 1.5 it can be seen that the northern part of the coast has lower threshold limit than the southern part of the coast, 1/30.000 and 1/10.000 per year respectively. The dune breach location Noordwijk is located in the northern part and the dune breach locations Monster and Kijkduin in the southern part. On the river side, the part near Rotterdam, trajectory 14-2, has the most strict threshold, 1/30.000 per year. Trajectory 14-1 and 14-3 both have a lower limit of 1/10.000 per year. The signal value of trajectory 14-1, 14-2 and 14-3 are 1/30.000, 1/100.000 and 1/10.000 per year respectively.
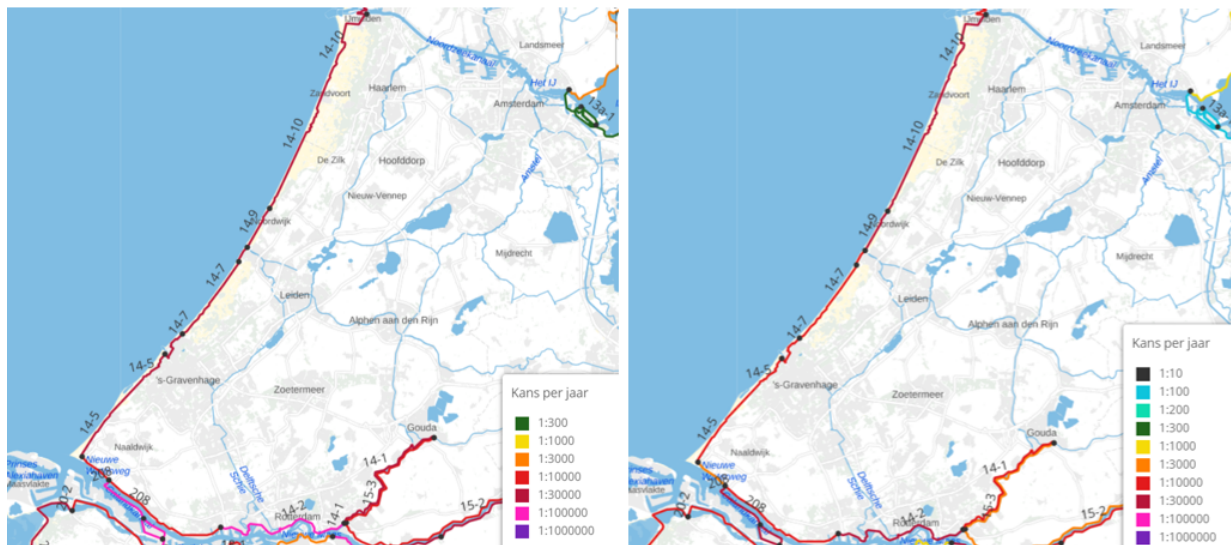
Figure 1.5: New standards expressed as two different probabilities of flooding [per year] (Waterveiligheidsportaal, n.d.). On the left sight, an overview is given of the signal value and the right sight of the lower limit. The figure includes the primary flood defences of dikering 14.

Both the sea water levels at the Dutch coast and the water levels in the rivers become higher due to sea level rise and rising river discharge. With these rising water levels, the consequences for the area behind the flood defences becomes severe. It is plausible that the probability of death given a flood caused by a dike breach will increase. This is because a potential flood event will reach higher water levels, velocities and rise rates with a rise in sea level. In general, it is likely that higher water levels will result in higher inundation depths in the area in the case of a dike or dune breach. It does not mean that 1 m sea level rise results in 1 m higher flood inundation depths. From the hydrodynamic models designed by Ranneft (2020), it can be concluded that a 2 m sea level rise will approximately result in a higher flood depth of 0.5m for most places. In addition, the extent of flooding increases per scenario of sea level rise. These higher inundation depths and increase in the extent of flooding result in higher economic and a higher amount of potential casualties and affected persons.

Because a possible flood caused by rising sea levels results in higher flood depths and a greater extent of flooding, more people are affected. Therefore, a casualty analysis / loss of life estimation due to flood risk have to be made in the area of dikering 14 to see what happens to the loss of life estimation. This will examine whether the risk still meets the standard (LIR) for the various steps in sea level rise (steps of 0.5 m).

In the previous thesis (Ranneft, 2020) only the seaside boundary was considered. Dune erosion due to waves is the dominant process at the coastal dunes that could cause flooding (ENW, 2017). However, the dunes on the Dutch coast are very wide, so this contribution to the flood risks could be very limited. Instead of the dunes the hydraulic structures in the dunes could be the weak spots for the coastal flood defences. Moreover, other weak spots in the system could be formed by the existing engineering structures

(e.g. The Measlant barrier) or by the river dikes. So, the other boundaries should be included in the impact assessment as well. The southern boundary of dikering 14 is formed by the Nieuwe Waterweg, Nieuwe Maas and Hollandse IJssel. The northern boundary is formed by the Amsterdam-Rhine Canal and the North Sea Canal. This study focuses on the primary flood defences of dikering, see Figure 1.6. Due to time constraints only the river dikes for the river side and the dunes for the sea side are considered.
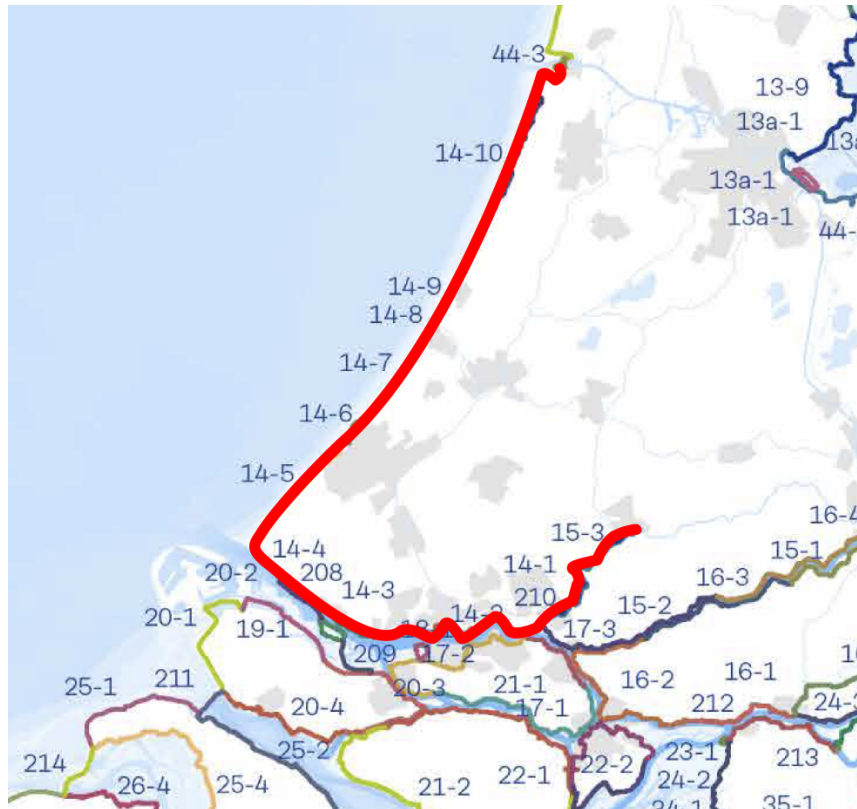
Figure 1.6: A representation of the part of the primary flood defences that are included in this study in red. The different levee segments in the Netherlands are also indicated (ENW, 2017).

If the required threshold are not met, see Figure 1.5, several options for reinforcements must be considered. This should include consideration of the spatial location, the costs and the timing of the investment. The costs for possible dune and dike strengthening could be better substantiated for example by means of a design. With a design of dune reinforcements, the number of m^3 of sand needed for reinforcements for the dunes can be estimated.

By implementing more data and more locations to the impact assessment, it is possible that the economic optimum expressed in a flooding probability derived in the previous study is shifted. Therefore a new economic optimization problem has to be solved in order to see if these economic optima do meet the required new safety standard, see Figure 1.5. The loss of life estimation, the economic risk and the investments needed to increase the safety level should be considered in this economic optimization problem. This will lead to a better understanding of the consequences of climate change in terms of flood risk,. The goal of this study is to derive a more detailed and integral impact assessment that will allow better conclusions to be drawn and to provide help for future decision-making for the policy of water safety.

1.3. Objectives

From the general context and the problem definition the necessity for an impact assessment as complete as possible becomes clear. In this thesis the economic risks and the loss of life estimation will be included. Moreover, the thesis is expanded with not only considering the seaside, but also the threats from other boundaries such as flooding of the rivers Hollandse IJssel, Nieuwe Maas and Nieuwe Waterweg (the river-side / southern boundary). Besides the three breach locations Noordwijk, Kijkduin and Monster, other breach locations at the southern boundary are considered. These other breach locations are available in the National Informationsystem Water and Floods (in Dutch 'Landelijke informatiesysteem Water en Overstromingen (LIWO)). This information system contains map layers for professionals, which are necessary to prepare for flooding in the Netherlands (Rijkswaterstaat, n.d.-a). These map layers with flood scenarios will then be linked to a methodology for determining the influence of climate change which is described in the following chapters. In this study, climate change refers to a sea level rise of up to 2m and an increase in river discharge. The increase in river discharge is only important when looking at the breach locations along the riverside and not for the breach locations on the seaside. This results in the main research question below:

How does climate change affect the flood risk for the area protected by the primary flood defences of dikering 14 and which investments can optimally ensure the future safety of this area?

This main question can be divided into several sub-questions regarding the different locations (seaside or riverside) and different impacts (loss of life estimation and economic damages). Sea level rise up to 2m is included in this study. For every sub-question below increments of 0,5 m will be taken for each location resulting in a set with five different scenarios: 1 basic case with 0 meter sea level rise and four scenarios where sea level rise is included.

1. **How does climate change affect the probability of failure of the primary flood defences at the seaside and riverside of dikering 14?**

   In this question, a total of 11 different cross sections are considered. Eight cross-sections along the rivers and three cross sections along the coast. The most recent failure probabilities per dike/dune trajectory and dike/dune sections are extracted from assessment reports. Present day hydraulic load on the flood defences is compared with the expected hydraulic load in the future for the different scenarios up to 2m sea level rise. For the rivers this can be determined using the program Hydra-NL. In the calculation of the flooding probability of the river dikes, both sea level rise and rise in river peak discharge taken into account. The hydraulic loads on the coasts are used as input for the application MorphAn (Rijksoverheid, n.d.-c) to determine the situation that a dune can no longer withstand the sea water level. This is the situation that a dune breach will occur and in this way the probability of failure can be determined for the different scenarios.

2. **To what extent does climate change affect the loss of life estimation for the area on both the river side and the sea side?**

   For this question, maps containing the flood depth, flood velocity and the rise rate will first need to be formed for the various scenarios. For this purpose, the flood scenarios from LIWO will be used (Rijkswaterstaat, n.d.-a), whereby an overview should be made of the maximum values for the previously mentioned flooding characteristics. These maps are made for the three trajectories 14-1 to 14-3. Since the flood depth, flow velocity and the rise rate have to be considered for each trajectory, this results in 9 total input maps. The flooding probabilities determined in the previous question will be used for this question. For the seaside, the hydrodynamic models designed by Ranneft (2020) are used instead of the LIWO maps. In these models flood depths and velocities are simulated for each sea level rise scenario. To produce the rise rate maps, assumptions have to be made which are explained in Chapter 5. When the maps for the different scenarios are complete, they will be used in combination with the method of S. Jonkman (2007) to determine the number of fatalities and casualties for the three different breach locations at the seaside and the three trajectories at the riverside.

3. **To what extent does climate change affect the expected damage for the area on the river side?**

   This question will be addressed the same as in the previous research (Ranneft, 2020), in which the expected damages were visualized using a land use map, damage curves and the Global Flood Risk

Tool. Since the potential damage on the seaside has already been mapped by Ranneft (2020), only the potential damage on the river side needs to be examined for this study. For this purpose the maps from LIWO will be used for the flood depths, whereby a map is formed with the maximum flood depth. This will be done for the three different trajectories, which maps with flood depths are the same used in the previous question. The same land use map will be used as in the economic analysis for the sea side. These two maps combined with the damage functions will give an overview of the expected damages in case of a flood. These damage maps will be formed for the five different scenarios, whereby the damages will be visualized with the Global Flood Risk Tool.

4. **What are the expected costs for specific dune and dike reinforcements that would increase the safety levels?**

The KosWat program is used to determine the costs of dike reinforcements along the riverside. This program is based on a spatial analysis in which the locations of buildings, (rail) roads and large water bodies are known. This makes it possible to determine the applicability of a certain reinforcement measure (Rijksoverheid, n.d.-b). Based on the applicable reinforcement measures and cross-sections of the reinforced dike profiles, KosWat can determine the total costs for a certain reinforcement project. The costs for dune reinforcements are determined by the number of m^3 of sand required. To determine the amount of sand required, cross-sections of the reinforced dune profiles are made to determine the number of m^3/m. With the lengths of the sections and the costs per m^3 of sand, the total costs for particular dune reinforcements can then be determined. The costs for reaching different safety levels are determined in this question and will be used as input in the optimisation problem.

5. **What are the economic optimums for the safety level expressed as a probability of failure?**

The results of the loss of life estimation and economic risk are used to determine an (economic) optimum for the safety level expressed as a probability of failure. These optimal flooding probabilities are determined for each trajectory 14-1 to 14-3 and each breach location along the seaside: Noordwijk, Kijkduin and Monster. The loss of life estimation will be included in the optimization by attaching a monetary value to a fatality, whereby a same value will be used as in previous studies, see Table 2.5. In this way, the total number of casualties and fatalities will be added to the economic damages. This economic optimisation is derived by considering both the costs and the investments for increasing the safety level expressed as a probability of failure. The costs are determined in the previous question. Afterwards, the economic optimum safety levels expressed as a probabilities of failure are compared to the thresholds, see Figure 1.5. In this way, it is possible to determine when and which reinforcement measures will be needed in the future.

The goal of this thesis is to make a more complete impact assessment of future flood scenario's that will provide help for future decision-making for the policy of water safety.

1.4.   Research method

In this section the methodology used in this study is explained, which is chosen after a detailed literature study. The needed formulas are not included in this section, but are shown in the next chapter. As explained earlier, five flood scenario's will be evaluated. As explained earlier, a base scenario with 0 m sea level rise and 4 future scenarios up to and including 2 m sea level rise in increments of 0,5 m are considered resulting in a 5 different scenarios.

Creating maps with flood characteristics
Maps with flood characteristics from LIWO (Rijkswaterstaat, n.d.-a) will be used for this study, whereby the breach locations available in the LIWO database on the riverside will be included. Different dike breach locations are combined to create maps showing the maximum value of the flooding characteristic per grid cell. A map will be formed with ArcMap for the flood depth, the flow velocity and the rise rate, as in the maximum flood depths shown in Figure 1.7. For the maps for the seaside the hydrodynamic models for the breach locations Noordwijk, Kijkduin and Monster will be used.
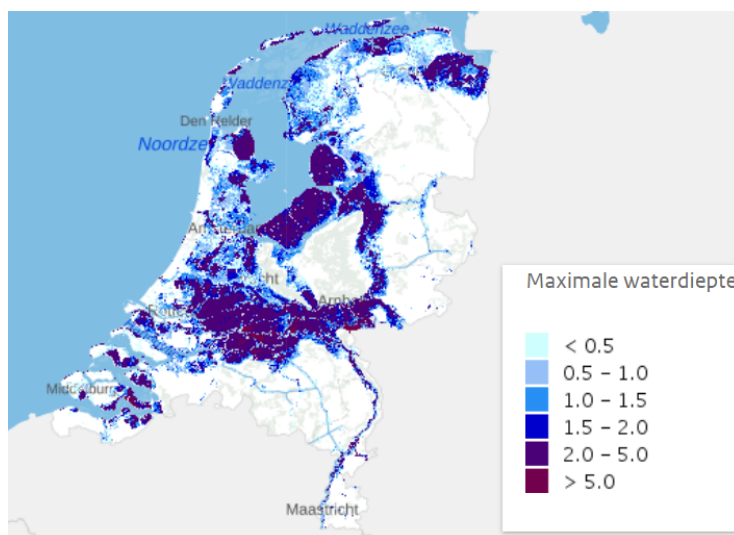
Figure 1.7: Maximum flood depth for the Netherlands based on based on individual flood scenarios from the LIWO database where this floods may occur 1/10.0000 per year. In reality, this floods do not occur at the same time (Rijkswaterstaat, n.d.-a). The flood depths are in meters.

Flooding probability

The flood scenarios are held constant for the riverside and the probability of flooding is then varied per sea level scenario. Ranneft (2020) assumed that the probability of flooding of the dunes rises with a factor 10 per m sea level rise, which will be examined in more detail in this study. New hydrodynamic topographic models are designed by Ranneft (2020) for the seaside which do not include the steadfastness of barriers. Some research has already been done on the change of flood probabilities under the influence of sea level rise of 35 cm and 85 cm. The maximum flood depth of a 1/1.000 year flood in 2015 is approximately comparable to a 1/300 per year flood with 35 cm sea level rise and 1/100 per year with 85 cm sea level rise for the Waal-Eemhaven in Rotterdam. The probability of flooding increases by about a factor around a factor of 3 with 35cm sea level rise and again a factor of 3 in case of sea level rise of 85 cm (Van de Visch & Bos, 2018), see Table 2.1. Table 2.2 and Table 2.3 show the water levels inside and outside the Maeslantbarrier determined by Rijkswaterstaat used for 35 cm and 85 cm sea level rise (Boersen et al., 2017). However, this study will asses different cross-sections for scenarios up to 2 m sea level rise. This is done with the erosion profile and the boundary profile for the dunes using the Duros-plus calculation method which is integrated in the Morphan program, which is an application for making dune erosion calculation to test the safety of dunes against flooding (Rijksoverheid, n.d.-c). For the river dikes, the flood probability will be determined with Hydra-NL and information from recent assessments. Hydra-NL is a probabilistic model that calculates the statistics of hydraulic loads for the assessment of the primary dikes of the Netherlands (Rijksoverheid, n.d.-a). An relationship between flooding probability and height shortage that is obtained from recent assessments reports is used to estimate the flooding probabilities for the different scenario's and different cross-sections, which is explained in more detail in Chapter 3. This study only includes the failure mechanisms dune erosion for the dunes and wave overtopping and overflow for the river dikes.

Loss of life estimation

For the question the maps created with LIWO data will be used as input for the loss of life estimation. The specific parameters that are needed are the extent of the flood with the water depth, velocity, and the rise rate of the water for each breach location. The maps with flood characteristics are created for each different scenario and for each different trajectory.

These flood characteristics are the input for the loss of life estimation according to the method developed by Jonkman (2007). First of all for each specific breach location the number of people at risk should be determined. In addition the evacuation fraction and the fraction of people that could find shelter before the flood are needed to result in the number of people exposed.

The extent of the flood make a distinction between three different zones based on the flood characteristics. Jonkman derived three mortality functions for each zone, which will be used in this study although later a fourth mortality function was derived by Maaskant et al. (2009). Lastly, the individual risk will be

determined with the probability of a given flood scenario and the mortality given that flood scenario and will be visualized with ArcMap.

Expected damage riverside dikering 14

First of all, it is necessary to know what could possibly be destroyed in the area by a flood. For this purpose it is necessary to assign areas a certain possible economic damage (e.g. EUR/m^2). The same damages per category will be used as in the thesis of Ranneft (2020) in order to get the same input in the final impact assessment, see Table 2.4. The categories are obtained by combining 26 categories from CBS (Central Office for Statistics in The Netherlands) into 11 different categories. For example, the categories houses, gardens and pavements will be combined into one bigger category, residential area. This is done by using an average value of the possible economic damage of the original categories for the combined (Ranneft, 2020). For the area at the riverside the same land use map created by Ranneft (2020) will be used, Figure 1.8. In addition to the direct economic damage, the indirect economic damage is also taken into account.
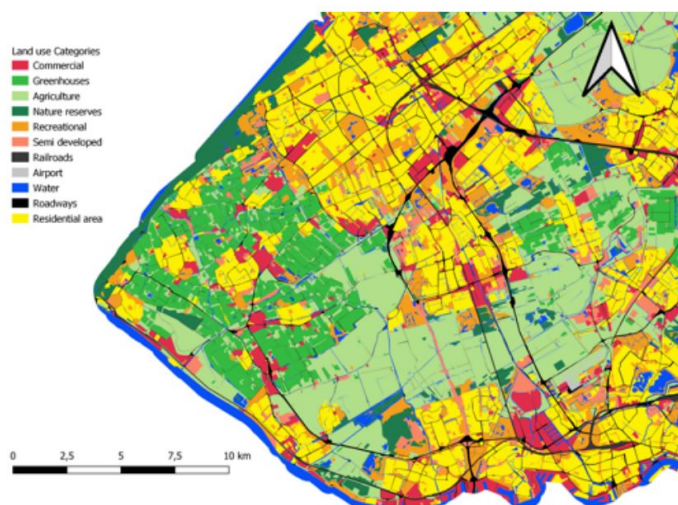
Figure 1.8: An example of a land use map using the 11 different combined categories (Ranneft, 2020).

The most important flood characteristic for the damage modelling approach is the flood depth. The flood depths are obtained by LIWO data. The estimated damages for each flood scenario are visualized with the Global Flood Risk Tool from Royal HaskoningDHV. In the Global Flood Risk Tool, the created maps of the maximum flood depths and the land use map are combined with a damage function based on the flood depths per grid cell. The damage function for commercial use, residential use and infrastructure used in Ranneft (2020) will be used in this study as well. An example of a damage curved is shown in Figure 1.9, which shows that the percentage damage for stores is the highest, followed by industry and offices. 100 percent of the damages will occur when the flood reaches depths of around 2,5 m, 4,2 m, 8 m for stores, industry and offices respectively.
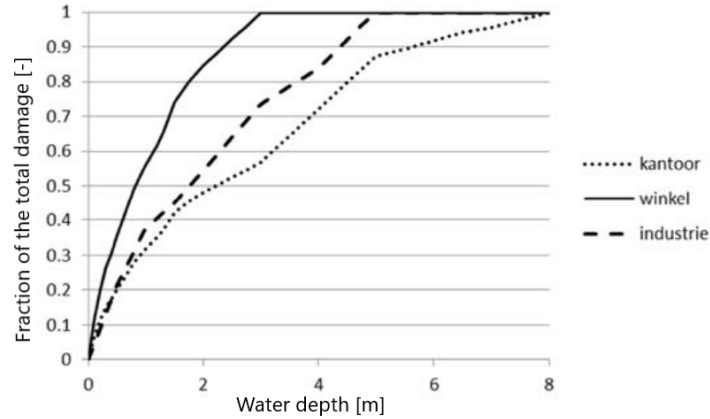
Figure 1.9: An example of a damage curve for an office ('kantoor' in Dutch), store ('winkel' in Dutch) and industry ('industrie' in Dutch). These three are combined in one single category: commercial use. Therefore an average of the three damage functions will be used for the category commercial use. The y-axis shows the factor of damage occurred and the x-axis shows the flood depth in meters (Ranneft, 2020).

Expected costs of specific reinforcements
In this question, the costs for different dike reinforcement projects are determined using the program KosWat. The most recently available price level will be used and converted to today's price level. The re-inforced and therefore higher dikes will result in a lower probability of failure according to the relationship between probability of failure and height shortage, which is explained in Chapter 3. For the dunes, the sand required to reinforce the cross-section is calculated. The required amount of sand is multiplied by the length of the dune section for which that specific cross-section is normative. Broader and higher dunes resulting from the sand supplements will result in lower probability of failures. Ultimately, the costs and associated probability of failure can be determined for various reinforcement projects. The effect of each measure on the probability of flooding and consequently on the flood risk will be shown in the results. This will be done for each section and will be used as input for the economic optimisation problem. This thesis only considers the consequences of a single dune failure and therefore only includes the costs of reinforcing the dunes. Hard flood defences such as the dike in the dunes near Katwijk and the boulevard are not included in this study.

Economic optimization
The first step is to determine the total damage per flood scenario. This will include both economic and damages due to the loss of life estimation. The number of casualties and affected persons per flood scenario will have to be expressed in monetary terms so that the two aspects (economic and loss of life estimation) can be combined in one optimization problem. Because this thesis will not evaluate the unethical side of attaching a price to a fatality, a value that has been used in other previous studies will be also used in this thesis, see Table 2.5. These two aspects will then result in a total damage per flood scenario for each trajectory. The total costs depend on the investments to reach a higher safety level and the total flood risk. The next step is to evaluate investments to raise the level of safety. Higher investments will result in higher investment costs, but in lower risks. The costs needed for investments are obtained from the previous question. Finally, an optimum must be obtained per flood scenario between these investments for strengthening the dikes and the potential damages associated with flood risks. The economic optimum per flood scenario can be determined by varying the probability of flooding. The basic principle of the economic optimisation is shown in Figure 2.7. These obtained optima of safety levels are compared to the thresholds for eacht trajectory, see Figure 1.5.

Conclusion, discussion and recommendations
The final part of this thesis consist of a conclusion, discussion and some recommendations. In the conclusion the research questions, introduced in section 1.3, are answered. Possible uncertainties in this thesis are discussed in the discussion. Some ideas for future research are given in the recommendations.

2. Background

In this chapter an overview is given of the background information used in this thesis. This chapter is divided into five sections. The first and second sections are about the probability of flooding and the loss of life estimation respectively. The third section discusses the method to determine the economic damage. And the determination of the costs for reinforced project and the optimization problem are discussed in section four and five respectively.

2.1. Probability of failure

The part of the Netherlands that is at risk of flooding due to storm surges and high river discharges is around 60 percent (ENW, 2017). It is expected that this percentage will grow in the future with higher river discharges and higher sea levels.

An assumption in this study is that failure of a flood defence will cause a flood, which means that the probability of failure of a flood defence is equal to the probability of flooding. The probability of flooding depends both on the hydraulic loads and the strength of the particular defence. The most important loads are the water levels and the wave impacts. The height, width and type of material used for the defence determine the strength.

The new standard for water safety is based on the flood risk which is influenced by the probability of flooding and the impact of flooding. It is not possible to reduce this risk to zero, which means that the level of risk which is indicated as safe enough is obtained by societal and political decisions. This minimum safety level expressed in an exceedance probability is a result of balancing the investments for strengthening and the reduce in flood risk. The old standards were based on the decision of the Delta Commission that the water levels with an annual exceedance probability of 1/10.000 are the minimum water levels that the flood defences have to withstand in the west of the Netherlands. Lower requirements were given for other parts of the country (ENW, 2017). However, nowadays new standards apply, whereby the same safety level no longer applies to the entire dikering. The safety requirements are determined per dike trajectory, see Figure 1.5. These safety levels are for primary defences. A breach in other defences, regional defences along canals and man-made lakes, will have a smaller impact and therefore decisions for the minimum safety levels are proposed by the provincial authorities instead of the Delta Commission (ENW, 2017).

Research has already been done by Boersen et al. (2017) and Van de Visch & Bos (2018) on the change in flooding probability for sea level rise up to 85 cm by 2100. In Table 2.1 is shown that the flood scenario of 1/3000 years in 2015 is equal to the flood scenario of 1/1000 years in 2050 and 1/300 years in 2100 with the KNMI scenario W+. The probability of flooding increases by a factor of 3 for 2050 (35 cm sea level rise) and again by a factor of 3 for 2100 (85 cm sea level rise) (Van de Visch & Bos, 2018). In another report, water levels at the Hartel barrier (SVKH) and the Maeslantbarrier (SVKW) under sea level rise of 35 cm and 85 cm were included. These future water levels were determined by Rijkswaterstaat by carrying out a hydraulic assessment based on a quantitative analysis, using model calculations with river modelling tools: the GIS application Baseline and the 2D flow model WAQUA (Boersen et al., 2017), see Table 2.2 and Table 2.3.

	Year		
Recurrence time [years]	**2015**	**2050(W+)/2100(G)**	**2100(W+)**
10	3,0	3,1	3,3
100	3,2	3,3	3,4
300	3,3	3,4	3,5
1.000	3,4	3,5	3,7
3.000	3,5	3,6	4,0
10.000	3,6	3,9	4,3

Table 2.1: Development of the water depth in time in meters for the Waal-Eemhaven under the KNMI scenarios W+ and G. W+ represents a scenario with accelerated sea level rise and G represents a slower scenario. At W+, the sea level rise is 35 cm in 2050 and 85 cm in 2100. For the G scenario. the sea level rise is 15 cm in 2050 and 35 cm in 2100 (Van de Visch & Bos, 2018).

SVKW outside	Year		
Recurrence time [years]	2015	2050	2100
3.000	4,80	5,03	5,55
10.000	5,17	5,45	5,95

Table 2.2: Development of the water levels outside the Maeslantbarrier for sea level rise of 35 cm in 2050 and 85 cm in 2100. The water levels are in meters (Boersen et al., 2017).

SVKH outside	Year		
Recurrence time [years]	2015	2050	2100
3.000	5,01	5,21	5,64
10.000	5,36	5,58	5,98

Table 2.3: Development of the water levels outside the Hartelbarrier for sea level rise of 35 cm in 2050 and 85 cm in 2100. The water levels are in meters (Boersen et al. (2017)).

The probability of flooding of dikering 14 is 1/16.0000 per year (Vergouwe, 2015). The Dutch coast of dikering 14 can be divided into two coastal sections: Rijnland and Delftland. The probbability of flooding are 1/33.0000 and 1/150.000 for Rijnland and Delftland respectively (Vuik & van Balen, 2012).

2.2. Loss of life estimation

A method of loss of life estimation due to floods is estimated by S. Jonkman (2007) and improved by Maaskant et al. (2009). The method is based on three elements: 1) The flood characteristics and the exposed area, 2) The number of people exposed and 3) The mortality fraction calculated with a dose response function/mortality function. Based on historical data from floods (such as the Dutch flood in 1953), a rule of thumb is derived which says that 1 percent of the exposed people will not survive the flood. There are many different definitions for individual. Risk can be seen as a function of probabilities and consequences of a set of undesired events, which can include both social consequences (fatalities), economical, ecological aspects. The definition for individual risk used in this study are (S. Jonkman (2007)): The probability (per year) of being killed at a certain location assuming permanent presence of the population.

In the method of S. Jonkman (2007), three regions or zones are distinguished based on their flood characteristics: 1) breach zone, 2) zone with rapidly rising water, 3) the remaining zone. The first zone has the highest mortality (close to the dike breach). This is due to rapidly rising water and high velocities resulting in collapsing buildings. Another reason for the high mortality is that the exposed people do not have many time to evacuate or to find shelter. For each zone a different mortality function is applied derived with historical characteristics from floods. The mortality functions are based on the flood characteristics and do not take into account the building types. Because today's buildings are of better quality than during the historic flooding, these mortality functions can be somewhat conservative. A further discussion of this used method is included in Chapter 5.
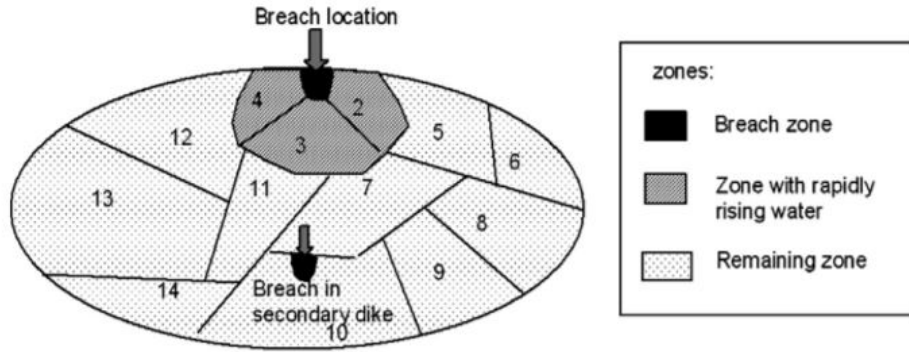
Figure 2.1: Different zones that has to be distinguished during a dike breach (S. Jonkman, 2007)

The number of people exposed, $N_{EXP}(c)$, can be calculated with the evacuation fraction, F_E, the fraction that could find shelter, F_S and the number of people at risk, $N_{PAR}(c)$. The physical effects, c, and the extent of the flood influence these characteristics. The number of people exposed can be determined using the following formula (S. Jonkman, 2007).:

$$N_{EXP}(c) = (1 - F_E(c))(1 - F_s(c))N_{PAR}(c) \qquad (2.1)$$

An overview of the number of exposed people for different flood scenarios is shown in Table 5.1.

Flood scenario	People exposed in flooded area	Fatalities			
		Unexpected flood		Predicted flood	
		No evacuation	Disorganised evacuation	Disorganised evacuation	Organised evacuation
Rotterdam – Kralingen	180.880	1070	1060	900	860
Den Haag - Boulevard	112.140	110	100	100	100
Den Haag - Scheveningen	179.270	230	220	210	210
Katwijk	205.960	400	380	340	330
Hoek van Holland	102.690	110	100	100	100
Katwijk and Den Haag	299.280	550	530	470	460
Den Haag and Ter Heijde	706.650	3460	3290	3210	3170
Rotterdam West	107.440	190	180	170	170
Rotterdam East	187.840	600	600	510	480
Katwijk, Den Haag and Ter Heijde	1.016.560	5090	4850	4720	4670

Figure 2.2: Number of exposed people for different flood scenarios and different evacuation types (S. Jonkman, 2007)

The number of people exposed is used as input to determine the number of fatalities. A flow chart of the loss of life estimation derived by S. Jonkman (2007) can be seen in Figure 2.3.
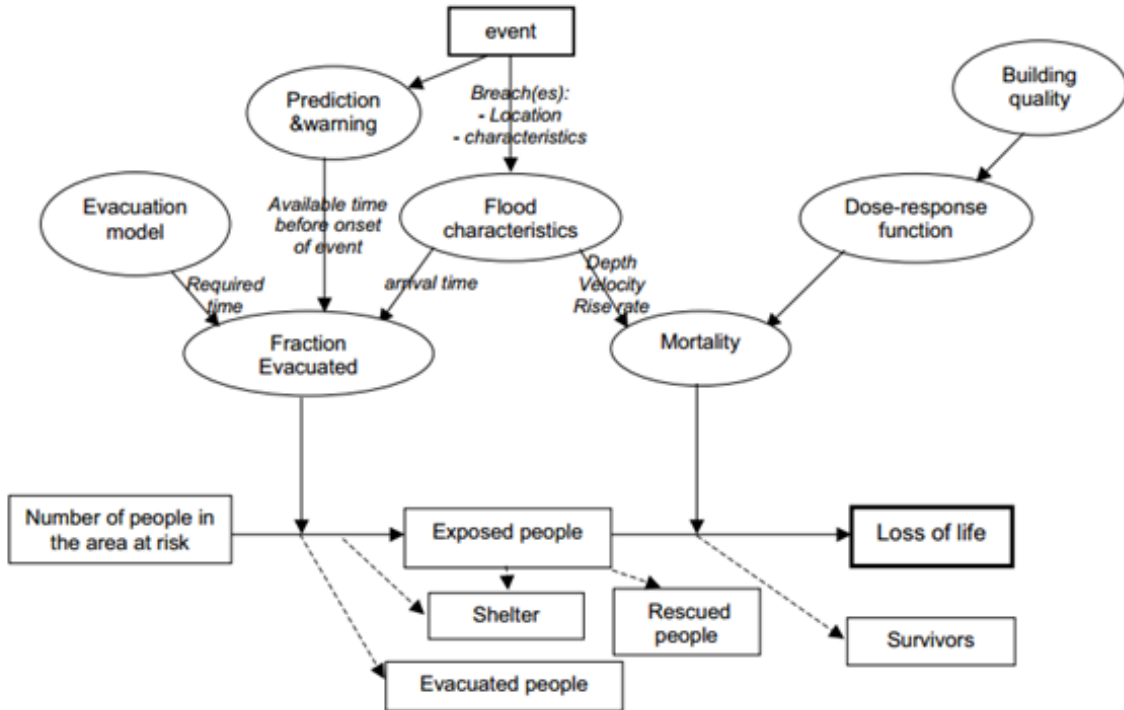
Figure 7-2: General approach for loss of life estimation for floods, The variables used as input are shown in italics.

Figure 2.3: Flow chart of the loss of life estimation pS. Jonkman (2007)

One of the most important variables of the loss of life estimation is the rise rate of the water, since this influences the possibility for the people at risk to find shelter. In the context of loss of life estimation it is proposed to estimate the average rise rate at a location from initiation of flooding up to a depth of 1,5 metres (S. Jonkman, 2007). This is the water depth when it becomes harmful for the exposed people.

Now it is known how to determine the number of exposed people, the next step is to include this number of people in the mortality function. This mortality function is influenced by the flood characteristics and the specific zone of the flood, shown in Figure 2.1.

An important indicator for these zones is the depthvelocity product (hv). It is stated that there will be a total destruction of masonry, concrete and brick houses if (S. Jonkman, 2007):

$$ hv \geq 7\frac{m^2}{s} \quad \text{and} \quad v \geq 2\frac{m}{s} \tag{2.2}$$

One of the assumptions in this method is that the exposed people stay inside buildings. When the buildings collapse, the people will not survive and therefore F_d will be 1 (in the breach zone). A discussion of the assumption such the destruction of houses in the breach zone and the permanent presence of people inside buildings is included in Chapter 3. The radius of the breach zone, R, is dependent on the breach discharge, Q, and can be calculated with the simple formula and the model calculation versus the analytical estimate is shown in Figure 2.4 :

$$ Q(R) = \pi R h(R) v(R) \tag{2.3}$$
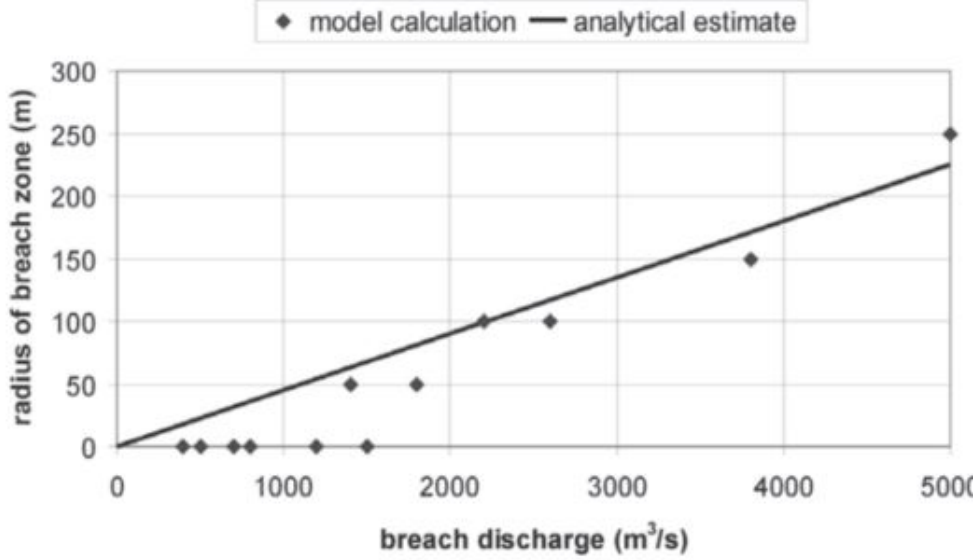
Figure 2.4: Radius of the breach zone versus the breach discharge (S. Jonkman (2007))

The method for loss of life estimation by S. Jonkman (2007) can be summarized in a couple equations for the different zones using log-normal distributions:

Mortality in the breach zone:

$$F_d = 1 \quad \text{if} \quad hv \geq 7\frac{m^2}{s} \quad \text{and} \quad v \geq 2\frac{m}{s} \tag{2.4}$$

Mortality in the zone with rapidly rising water:

$$F_d(h) = \Phi_N\left(\frac{ln(h) - \mu_N}{\sigma_N}\right) \quad \text{with} \quad \mu_N = 1.46 \quad \text{and} \quad \sigma_N = 0.28 \tag{2.5}$$

$$\text{if} \quad (h \geq 2,1m \quad and \quad w \geq 0.5\frac{m}{hr}) \quad and \quad (hv \geq 7\frac{m^2}{s} \quad or \quad v < 2\frac{m}{s}) \tag{2.6}$$

This function will only be used if the resulting mortality is higher than when using the formulas for the remaining zone. The buildings do have better quality compared with the situations for the historical floods. To take this improved building quality into account $\mu_N = 1.68$ and $\sigma_N = 0.37$ will be used.

Mortality in the remaining zone:

$$F_d(h) = \Phi_N\left(\frac{ln(h) - \mu_N}{\sigma_N}\right) \quad \text{with} \quad \mu_N = 7.6 \quad \text{and} \quad \sigma_N = 2.75 \tag{2.7}$$

$$\text{if} \quad (w < 0.5\frac{m}{hr} \quad or \quad (w \geq 0.5\frac{m}{hr} \quad and \quad h < 2.1m) \quad and \quad (hv < 7\frac{m^2}{s} \quad or \quad v < 2\frac{m}{s}) \tag{2.8}$$

These three mortality equations are extended and revised by Maaskant et al. (2009) with a fourth interpolation equation. They distinguished 4 zones: 1) the breach zone, 2) zone with high rise rates and high depths, 3) zone with low rise rates and low depths and 4) a remaining zone where linear interpolation is used (Westerhof, 2019). So a complete overview is given in the following equations.

Mortality in the breach zone:

$$F_{D,B}(d) = 1 \quad \text{if} \quad dv \geq 7\frac{m^2}{s} \quad \text{and} \quad v \geq 2\frac{m}{s} \tag{2.9}$$

Mortality in the zone with high rise rates and depths:

$$F_{D,FR}(d) = \Phi_N\left(\frac{ln(d) - \mu_N}{\sigma_N}\right) \quad \text{with} \quad \mu_N = 1.46 \quad \text{and} \quad \sigma_N = 0.28 \tag{2.10}$$

16

$$if \quad d > 2.1m \quad and \quad w > 4.0\frac{m}{hr} \tag{2.11}$$

Mortality in the zone with low rise rates and depths:

$$F_{D,SR}(d) = \Phi_N(\frac{ln(d) - \mu_N}{\sigma_N}) \quad with \quad \mu_N = 7.6 \quad and \quad \sigma_N = 2.75 \tag{2.12}$$

$$if \quad d < 2.1m \quad or \quad w < 4.0\frac{m}{hr} \tag{2.13}$$

In the remaining zones:

$$F_{D,RZ}(d) = F_{D,SR} + (w - 0.5)\frac{F_{D,FR} - F_{D,SR}}{3.5} \tag{2.14}$$

When the mortality of the different floods are known, the individual risk can be determined using the probability of occurrence of that particular flood scenario (S. Jonkman, 2007):

$$IR(x,y) = \Sigma P_{f,i} F_{D|i}(x,y) \tag{2.15}$$

2.3. Economic damages

The economic damages can be calculated by making use of the damage module (S. Jonkman, 2007), see Figure 2.5. The land use map has to be created for the potential floods for the riverside of dikering 14. For the seaside the land use map created by Ranneft (2020) can be used. The inundation depth and other flood characteristics are given by the LIWO data. The Global Flood Risk Tool of Royal HaskoningDHV can visualize the estimated damages for the potential floods using the land use map, flood characteristics and damage functions as input. In this study the same damage functions as in the study of Ranneft (2020) will be used. An example of a damage function is given in Figure 1.9.
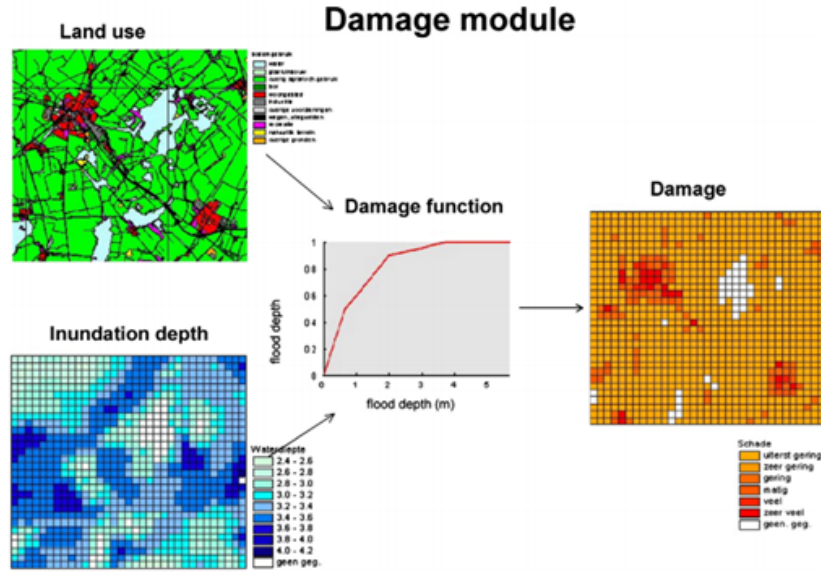
Fig. 2 – Schematization of the assessment of direct physical damages due to catastrophe flooding (source: Rijkswaterstaat).

Figure 2.5: Overview of the damage module designed by Rijkswaterstaat (S. Jonkman, 2007).

The land use map is used to estimate the different potential damages in EUR/m^2. The same monetary values are used as in Meyer's thesis, because in that case the results of the potential damages at the seaside under sea level rise derived by Ranneft (2020) can be used as input for this integral impact assessment as well. Damages per category were determined by using the model of the Flood Information System module Damages and Victims (in Dutch 'Hoogwater Informatie Systeem module Schade en Slachtoffers' (HIS-SSM)). With this model, the expected total damage during a flooding can be estimated on the basis of flood depths.

Use category	Estimated damages in EUR per squared meter
Residential	212
Commercial	433
Recreational	108
Semi developed	13
Agriculture	2
Water	-
Greenhouses	52
Airport	155
Railroads	353
Roadways	109
Nature reserve	11

Table 2.4: Estimated damages used in the previous thesis (Ranneft, 2020) from estimated with the model HIS-SSM.

2.4.   Determination of the expected costs of reinforced projects

When the probability of failure for a levee section does not meet the requirements, there are several solutions. There are three different types of solutions: 1) Reducing the hydraulic load, 2) Increasing the strength, 3) Limiting the consequences in case of a flood through effective crisis management (ENW, 2017). In this research the focus will be on increasing the strength by creating a new design for a dike profile or dune profile.

For dikes, the program KOSWAT is used. KOSWAT is a tool whereby an estimate can be made of the costs of possible measures and solutions. In this way, the same cost basis is given for different dike reinforcement programs and projects. This makes it possible to compare different programs and projects. In this study, it will mainly be used to determine the costs of different reinforcements. The new chrest height of the reinforcement dikes is important, since the methodology for determining the probability of failure of dikes is based on the height shortage, which is explained in Chapter 3. A number of standard assumptions are made in KOSWAT, but possible variations can also be implemented to get a feel for the bandwidth around the estimate. To make cost estimates, KOSWAT needs information on the different dike sections, their characteristics, hydraulic loads, the required dimensions of the flood defence and information on the surroundings. Whether the reinforcement measure is actually possible depends on a number of factors in the environment, such as the presence of buildings, (rail) roads and large bodies of water. In KOSWAT, the locations of these objects are known, because the tool is based on a spatial analysis. KOSWAT assumes that existing buildings will not be demolished. In reality, there will be a consideration in deciding whether something is demolished, whereby not only costs have an influence (Deltares, 2014).

The cheapest measure and also the most sustainable solution is that the reinforcement is entirely ground-based, with the dike being raised and/or widened. If there is no room to place a long berm, a seepage screen can be placed in the toe of the dike. If there is no room, a stability wall can be placed in the crest of the dike to improve the stability of the dike. If a dike is completely between buildings and can therefore only be reinforced straight up, a cofferdam can be chosen. The choice for a reinforcement measure is dependent on the surroundings and at the end a mix of the aforementioned measured will be the result of a reinforcement project along an entire trajectory. An overview of these measures is given in Figure 2.6.
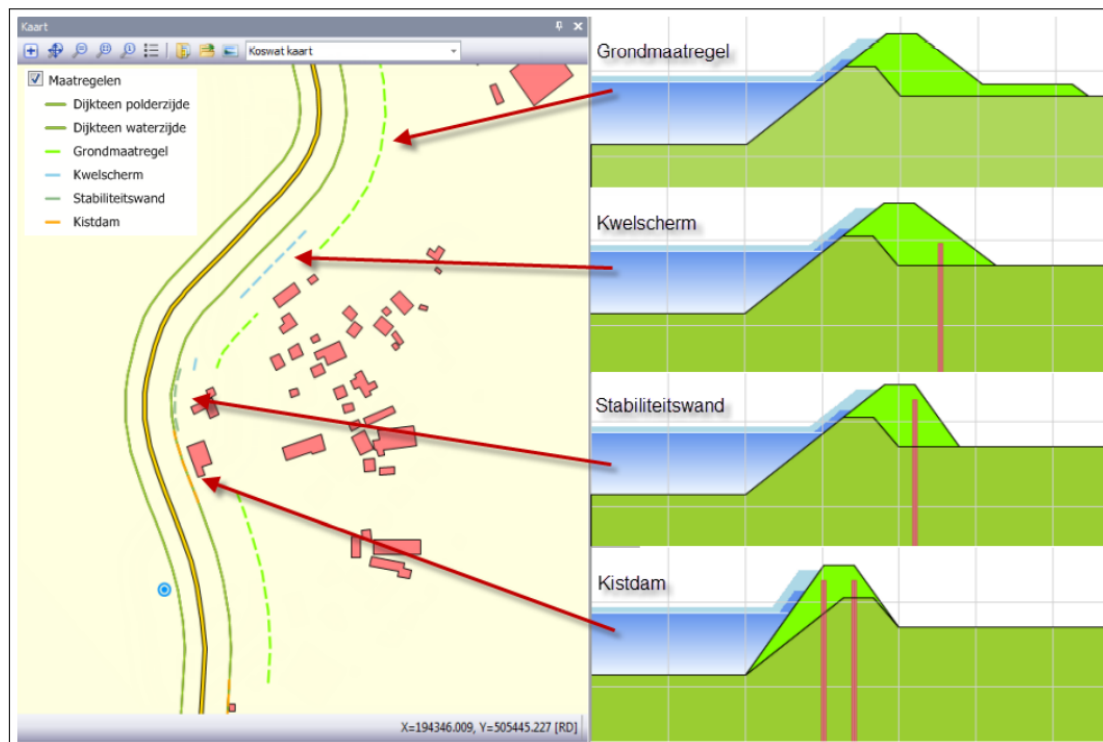
Figure 2.6: Different reinforcement measures included in KosWat: a ground-based solution (in Dutch: 'grondmaatregel'), a seepage screen (in Dutch: 'kwelscherm'), a stability wall (in Dutch: 'stabiliteitswand') and cofferdam (in Dutch: 'kistdam') (Deltares, 2014).

In addition to these measures, KOSWAT also has the possibility to design three other solutions which are more complex and are applied to situations where a complex constructive solution is needed. KOSWAT cannot make a dike design for these, but the costs for these measures are linked to the costs of a cofferdam by a factor.

The total investment costs are estimated using the SSK system (Standard System for Cost Estimates in the Civil Engineering sector). This estimate is made by multiplying the required quantities supplement factors and by adding these factors, the total project costs are determined instead of only the direct construction costs. In addition, not only the required materials are included, but also the costs of adapting or replacing the infrastructure, structures and dike revetments. KOSWAT uses the price book drawn up by the Expertise Centre for Costs and Benefits (ECK-B) of the Delta Program. In this study the most recent available price level from 2016 will be chosen and will be transformed to today's price level.

In order to determine the costs of reinforcing the dunes, the first step is to look at how much sand is needed for reaching different safety levels. In the MorphAn programme, different volumes of sand can be added to the original cross-section dune profile. Ultimately, three dune profiles will be evaluated along the coast. The amount of sand needed in $m^3./m$ will be multiplied with the length of the trajectory to obtain the total volume of sand in m^3. This volume will be multiplied by the unit costs of coastal defence measures. For beach nourishment this is 7,5 EUR per m^3 (S. N. Jonkman et al., 2013). This is a conservative method, because this research is from 2013. The price of 7,5 EUR per m^3 will be transformed to today's price level. The final reinforcement costs will be compared to the costs for increasing the safety level of the trajectories along the coast with a factor 10 (Slootjes & Wagenaar, 2016). This are also the costs that were used in the previous study of Ranneft (2020).

2.5. Optimization problem

To include both loss of life estimation and economic aspects in one optimization problem is a difficult problem. For many it is called unethical to put a price on a human life in flood risk analysis. However in other fields, this is also a necessity (e.g. in medicine and insurance decisions). These decisions are

usually made by the governments instead of by the experts themselves. An analysis of these decisions shows that a human life is never priceless in these kind of optimization problems (Vrijling, JK & Van Gelder, 2000).

One of the first optimization problems including the valuation of human life was performed by Van Danzig in the late 1950's (Vrijling, JK & Van Gelder, 2000). The total damage of a polder was estimated based on the total economic damage (D), the expected fatalities and the monetary value of a human life (d):

$$D + Nd \tag{2.16}$$

With this simple formulation of the total damage, a formula of the cost per year of (statistically) saving a human life (CSX) was determined with the P_f and P_f, opt which are the probabilities of flooding before and after dike reinforcements and the present value factor (PV). :

$$CSX = \frac{I}{(P_{f,0} - P_{f,opt})N * PV} \tag{2.17}$$

Another way to express the human life in monetary values in an optimization problem, is to use the Nett National Product (NNP) per head of the country. The NNP per head in the Netherlands is estimated at 19400 dollars per year. If a life span of 70 years is then taken, we arrive at a present value of this amount from 450.000 to 800.000 dollars, depending of the real rate of interest (Vrijling, JK & Van Gelder, 2000).

The result of this approach is that the value of a human life in a developing country is much lower. However, this study does not compare countries but only focuses on the Netherlands. The monetary value based on a macro-economic valuation is approximately 500.000 EUR (S. Jonkman, 2007). As this study dates from 2007, this seems a conservative value.

The safety standards determined for the Netherlands are based on the parameters in Table 2.5 and therefore this study will use these parameters as well. These parameters are fixed, so they do not change with new insights into the parameters. However, the standard is periodically evaluated (ENW, 2017).

Parameter	Value
Discount rate	5,5% per year
Fatality	6,7 million euros
Victim	12.000 EUR
Year	2050
Economic growth	1,9% per year

Table 2.5: Parameters used for the derivation of the safety standards (ENW, 2017)

Now that it is known how to express non-material damage, fatalities/casualties and affected persons/victims, in terms of monetary value, the loss of life estimation and economic risk analysis can be added in a single monetary value. The next step is to vary the flooding probability to arrive at an economic optimum per scenario. This economic optimum will be determined in the same way as in the previous thesis (Ranneft, 2020). The economic optimum is a optimum of the total costs (C) which depends on both the investments to reduce the flooding probability (I) and the associated risk (R).

$$C = I + R \tag{2.18}$$

The risk is dependent on the flooding probability (P_f) and the consequences of a potential flood, the expected damages (D).

$$R = P_f * D \tag{2.19}$$

The following should be added to the above equation: the growth rate (g) and the discount rate (r). The growth rate is a value for the expected increase in the economic value of the area in the future. Due

to economic growth, the area will represent an increasingly higher value and with that, the potential damages will also grow. By including the discount rate in the equation above, the devaluation of money in the future is taken into account. For the growth rate and the discount rate 1,9 percent and 5.5 percent are used respectively per year (i). This result in the following equation:

$$R = \sum \frac{1}{(1+r)^i} * D * (1+g)^i * P_f \tag{2.20}$$

Flood defences are designed and calculated for a whole number of years and therefore is a convenient rule to include a unbound time horizon. This rule can be applied to both the growth rate and the discount rate:

$$\sum \frac{1}{(1+r)^i} \rightarrow \frac{(1+r)^i}{1-(1+r)^i} = \frac{1}{r} \tag{2.21}$$

By substituting above rule in the equation for the risk, the following equation is obtained to calculate the total risk used in the economic optimization:

$$R = \frac{P_f * D}{r - g} \tag{2.22}$$

Now that the method of calculating the total risk is known, the next step is to determine the level of investments to reach a certain safety level expressed in a flooding probability. The higher the investments resulting in a lower the flooding probability, then lower the risk of flooding. In the study of Ranneft (2020) the investments to decrease the flooding probability by a factor 10 are 42 and 123 million euros for Monster/Kijkduin and Noordwijk respectively. The basic principle of economic optimisation is shown in Figure 2.7.
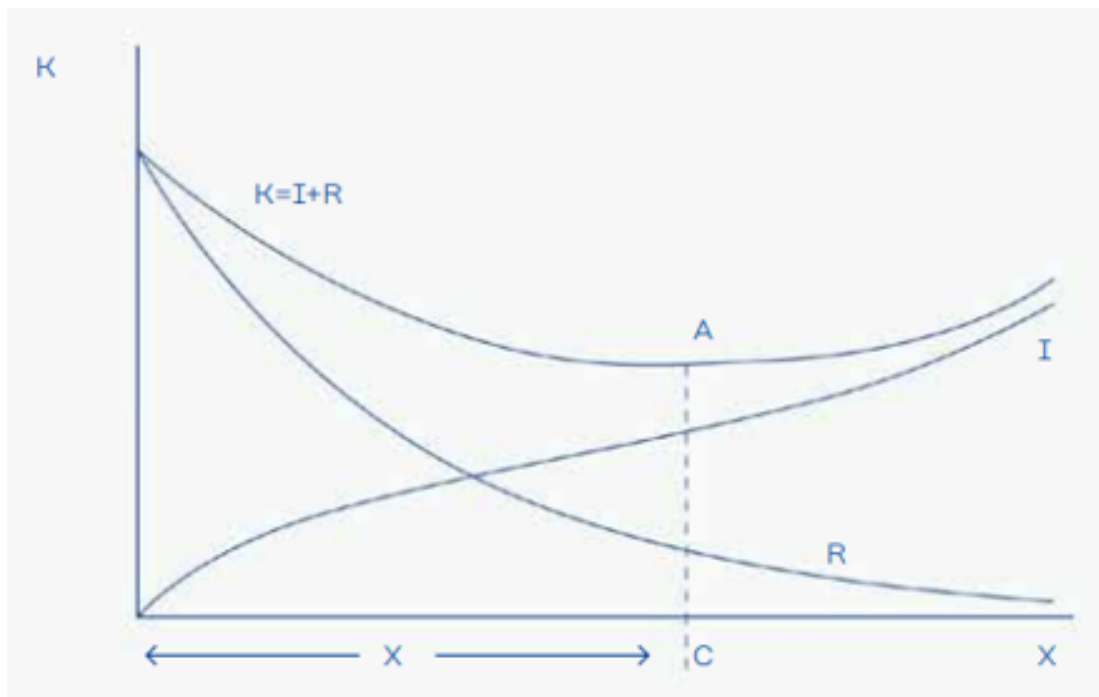
Figure 2.7: This is the basic principle of economic optimisation. The economic optimum is at the minimum of the total costs (K), which consists of the investments costs (I) and the present value of the risk (R). The safety level that corresponds with the economic optimum is point C (ENW, 2017)

By plotting the total costs, consisting of the risk and the investments, the economic optimum can be determined for each trajectory. This economic optimum is the minimum of the total costs. These economic optima will be compared to the threshold for each trajectory, see Figure 1.5.

3. Probability of failure

First, the probability of failure of the dunes along the coast of dikering 14 and the dikes along the Nieuwe Waterweg, Nieuwe Maas and Hollandse Ijssel will be examined. The assumption for this study is that failure of a flood defence will cause a flood. This means that the probability of failure of a flood defence is equal to the probability of flooding. The Hydra-NL tool will be used to determine the hydraulic load level for the dikes. Hydra-NL is a probabilistic tool which can be used to determine hydraulic loads for assessing primary flood defences. This tool is consistent with the WBI2017 (Rijksoverheid (n.d.-a)), which contains the procedure for assessment of primary flood defences, the calculation rules and the methods for deriving hydraulic loads. Only the failure mechanism wave overtopping and overflow is considered in this study and not the failure mechanisms piping, instability and revetment failure. The MorphAn application will be used to determine the failure probability of the dunes. This application allows calculations to be made for dune erosion which can be used for dune safety (Rijksoverheid (n.d.-c)).' Only the failure of the dunes due to dune erosion will be considered and not the failure of hard flood defences along the coast, such as the boulevard at Scheveningen. The Duros-plus model is used which is integrated in the MorphAn porgram. For detailed background of the Duros-plus model, see Appendix B.

For climate change, 1 base scenario and 4 future scenarios are considered. The base scenario corresponds to present-day conditions with 0 m sea level rise and current river discharge. Four different future scenarios with 0,5m, 1m, 1,5m and 2m sea level rise are considered. In addition, for these 4 future scenarios, the statistics for the sea-level at the Maas estuary and the river discharge at Lobith are determined by extrapolating the available datasets for 0, 35 and 85 cm sea-level rise. This way 4 combinations of datasets have been created with which the hydraulic load on the river dikes can be determined with the help of the Hydra-NL program. For the load conditions for the dunes an increase in significant wave height of 3,7 percent and an increase of 0,9 percent in wave period has also been included in future scenarios (HKV, 2018). In this way, in addition to the sea level rise, a corresponding river discharge and an increase in significant wave height and period are included. It is assumed that wind conditions will not change in future scenarios.

3.1. Description dikering 14

Dikering 14 is protected by many different flood defences. Each flood defence has a different dominant failure mechanism that needs to be considered. The coast is protected by the dunes managed by the Delfland and Rijnland Water Boards. The coast also contains several hydraulic structures, such as the boulevard and the locks at Scheveningen and Katwijk aan Zee. The primary flood defences at the southern boundary of dike ring 14 consist of the dikes along the Nieuwe Waterweg, Nieuwe Maas and Hollandse IJssel. There are also two storm-surge barriers which close in the event of high water levels in the river or at sea: the Maeslant barrier and the Hollandse Ijssel barrier. Moreover, there are various hydraulic structures in the trajectories 14-1 to 14-3, such as the locks at Vlaardingen, Schiedam, Maassluis, Gouda and Rotterdam. An overview of the trajectories 14-1 and 14-3 can be seen in Figure 3.1.
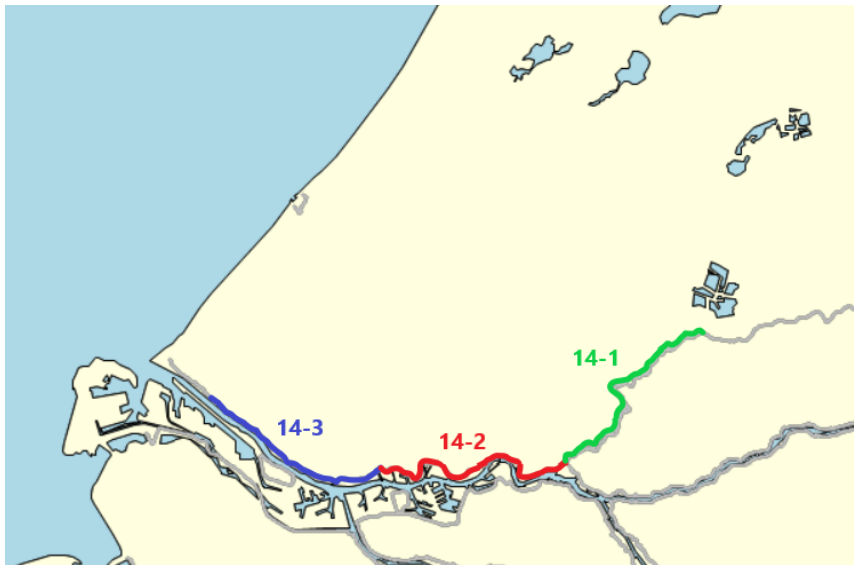
Figure 3.1: Overview of the 3 different trajectories included in this study. The primary flood defences along the rivers Hollandse IJssel, Nieuwe Maas and Nieuwe Waterweg form the trajectories 14-1, 14-2 and 14-3 respectively.

This study focuses on the probability of flooding of the dunes and river dikes. There is also a connection between the dike rings 14, 55 and 44. Dike rings 55 and 44 contribute to the flood risk in dike ring 14. In the event of a dike breach in dike rings 55 and 44 this will lead to a cascade effect, see Figure 3.2 (Ter Horst (2012)). However, this will not be considered in this thesis.
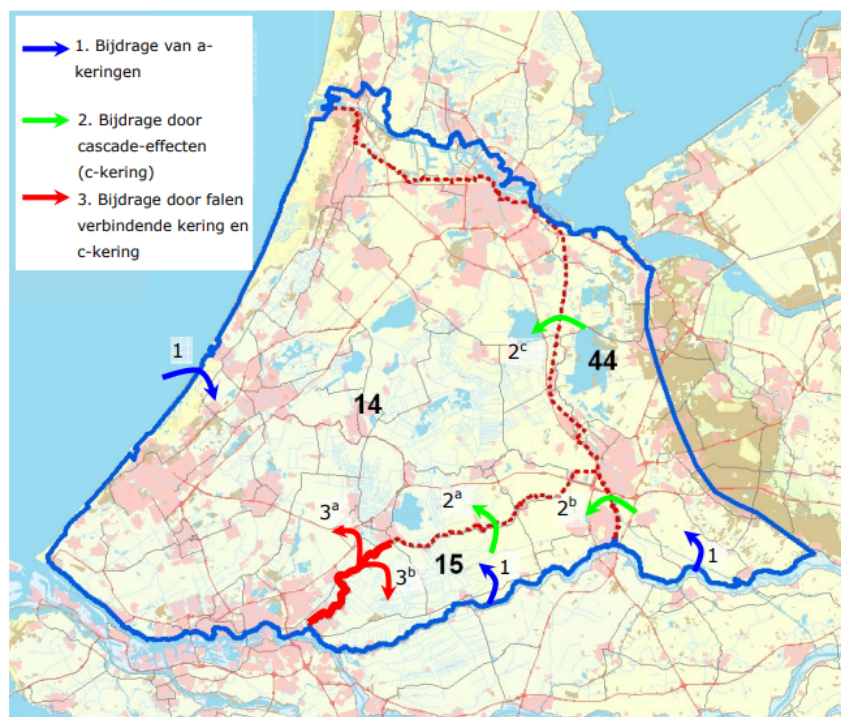
Figure 3.2: Representation of the contributions of the different flood defences and the cascade effect to the flood risk in the dike rings 14, 15 and 44 (Ter Horst (2012))

3.2. Hydra-NL

In this section the Hydra-NL programme will be discussed. With Hydra-NL it is possible to determine the hydraulic loads on the toe of the flood defence. First the different variables will be discussed. Hydra-NL

uses Hydra-ring, which will be discussed in the second subsection.

3.2.1. Stochastic variables and uncertainty

The boundary conditions used as input for Hydra-NL are calculated with another program: Hydra-Ring. Hydra-Ring is a computational kernel which incorporates the probabilistic calculation schemes, the statistical treatment of hydraulic data and the different failure mechanisms for flood defences (van Balen, 2013). For Hydra-Ring the set of variables and accompanying statistics are an important input. Some of these statistics are, for example, the sea level at the Maasmond, the wind speed and the peak discharge at Lobith, which are responsible for the variability of the water system (Chbab (2017)). The statistics of the random variables are derived from measurements, with the exception of the Rhine and Meuse discharge statistics. This discharge statistic is based on GRADE. Finally, these variables are converted to a hydraulic load on the flood defence. This is done with various hydrodynamic and wave models.

This section will take a closer look at the various random variables used to calculate the loads on the flood defences of dike trajectory 14-1 to 14-3.

In Hydra-Ring, exceeding probabilities are calculated from 1/300 to 1/100.000 per year. Probability distributions are added to this to take into account the uncertainty in the values of the small probabilities.For each load variable, a random variable is added expressed in an uncertainty distribution. These hydraulic loads are calculated by probabilistic Hydra models. The following aspects are taken into account in these calculations:

1. Statistics of the stochastic variables: wind, sea water level, discharge, lake level, state of the storm-surge barriers and offshore wave conditions

2. Conversion of these stochastic variables to hydraulic loads at the toe of the flood defence

3. Calculation of return periods of the hydraulic loads

4. Additional surcharges not considered in above aspects

The new standards of 2017 also led to a re-examination of the use of uncertainties in the determination of the hydraulic loads. The aim was to improve their use. Now, not only the uncertainty of the loads and strength are included, but also the knowledge uncertainty, which is a consequence of insufficient information or data. This knowledge uncertainty can be divided into statistical and model uncertainties. The former refers to uncertainty in certain coefficients and parameters used in the probability distributions of the stochastic variables. This often results from insufficient data. Model uncertainties are related to the settings of the model itself, thus indicating possible inaccuracies in the transformation of the variables into hydraulic loads. Furthermore, uncertainties on the strength side and on the load side are now implemented.

For each different water system different stochastic variables will be used. It will now briefly be discussed which ones are used for the sea-delta where the area of this thesis is part of. The coast which will be considered in this thesis as well is part of the Hollandse Kust Midden and the river area lies in the lower Rhine river area. In the end, the statistics of these stochastic variables used for these areas in combination with the databases of the model results of the water levels and wave conditions, the correlations and the associated statistical and model uncertainties will result in the hydraulic boundary conditions. This is also referred to as the load model, with which Hydra-Ring calculates the probability distributions of the loads on the toe of the flood defence (Chbab (2017)).

The area consists of the part of the dike trajectory on the outside of the Europoort and on the inside of the Europoort. The load model is the same for both sections, although the Europoort is included separately. For the trajectory outside the Europoort barrier it is not included as a stochastic variable, but it is for the trajectory inside the Europoort barrier. A failing Europoort barrier will cause very high water levels, which scenario must therefore be included in the risk analyses.

The stochastic variables for the downstream part of the Rhine are the wind direction in 16 different directions, the Rhine discharge at Lobith, the sea level in the Maas estuary, the wind speed at Schiphol and the error in the water level prediction of the Maas estuary (Chbab (2017)). For the Dutch coast 12 different wind directions are used, the water level at the dunes measured by different stations and the wave characteristics (height and period). In addition, a new stochastic variable has been added since 2017: the uncertainty in the seiche effect. Other parameters such as storm duration and storm surge duration are

included deterministic. A probabilistic approach will not lead to significant differences compared to the deterministic parameters. Using the storm surge duration as a stochastic factor has little effect on the hydraulic load. Storm surge duration is only relevant for the lower rivers. However, according to Tijssen (2010), including the storm surge duration at the Hoek van Holland as a stochastic factor hardly affects the hydraulic loads. This is why it was determined deterministic. The standard storm surge duration is 30 hours, which means that the design water level is only underestimated by a few centimeters on a few occasions.

The tidal phase is the difference between the astronomical high water and the straight storm surge (Chbab (2017)). This is also important for the tidal rivers included in this study. In the calculations it is assumed that the tide difference is 4.5 hours, which means that the maximum of the storm surge is 4.5 hours later than the astronomical high water. The choice for 4.5 hours is based on a database of measurements from 1976 - 2006. (Chbab (2017)). It was concluded that the tidal phases -4.5 hours and 3.0 hours occurred most frequently and that these two tidal phases have a similar course of the sea level. This combination of findings results in a safe choice for the deterministic value of -4.5 hours. The use of the tidal phase as a stochastic variable has not been investigated and therefore it has been used in the new assessment in the same way as in the previous assessment. This means that only in the area of the Eastern Scheldt the storm surge and the phase difference between the tide and this storm surge are included as a stochastic variable. This is not the case for the area of the Lower Rhine.

Because of the amount of extra work to include the soil roughness of the rivers as a stochastic variable, it was decided not to do so for the WBI-2017. Instead, this uncertainty is included in the model uncertainty. This model uncertainty also includes uncertainties in the SWAN model, which is used to convert the basic wind variable into wave conditions (wave height and period) (Chbab & Groeneweg (2017)).

The last uncertainty of importance for the downstream area is the water level predictions. Based on these water level predecitions, the Europoort barrier and Hollandse IJssel barrier are kept open or closed. An inaccuracy in the water level predictions can lead to a delay or even failure in the closure of the barriers, which in turn affects the water levels behind the barriers. The closure of the Europoort barrier is based on the predicted water levels at the Hoek van Holland. These predictions are uncertain. The Europoort barrier will close at a water level of +3.00m NAP near Rotterdam and +2.90m NAP near Dordrecht and the predictions at the Hoek van Holland are used to determine whether these water levels will be reached. The uncertainty of the sea-level prediction at the Hoek van Holland is taken into account by modelling the accuracy of the predictions with a normal distribution. The probability of failure of the Maeslant barrier is 1/100 per demand according to the WBI-2017.

The Hollandse IJssel barrier is located at the mouth of the Hollandse IJssel. The barrier consists of two doors and a lock. The closure criteria is +2.25 NAP at the location of the barrier and will be opened again when the water levels on both sides of the barrier are approximately equal. The failure probability per demand is 1/200 according to the WBI-2017.

3.2.2. Hydra-ring

Ultimately, the stochastic variables will be converted into hydraulic loads at the toe of the dike. For this, a probabilistic relationship is used between the variables and the loads. This is done with Hydra-ring. In Hydra-ring load models are formed. A detailed explanation how these load models are formed is given in (Diermanse et al. (2013)). In general, the load model is formed by using the probability distribution function of the random load variables, correlation models, hydrodynamic models and additional load parameters. Eventually, this load model can be used to determine the failure probability. However, the outputs of Hydra-NL only give the hydraulic load at the base of the flood defence. A general overview of the process in the load model can be found in Figure 3.3.
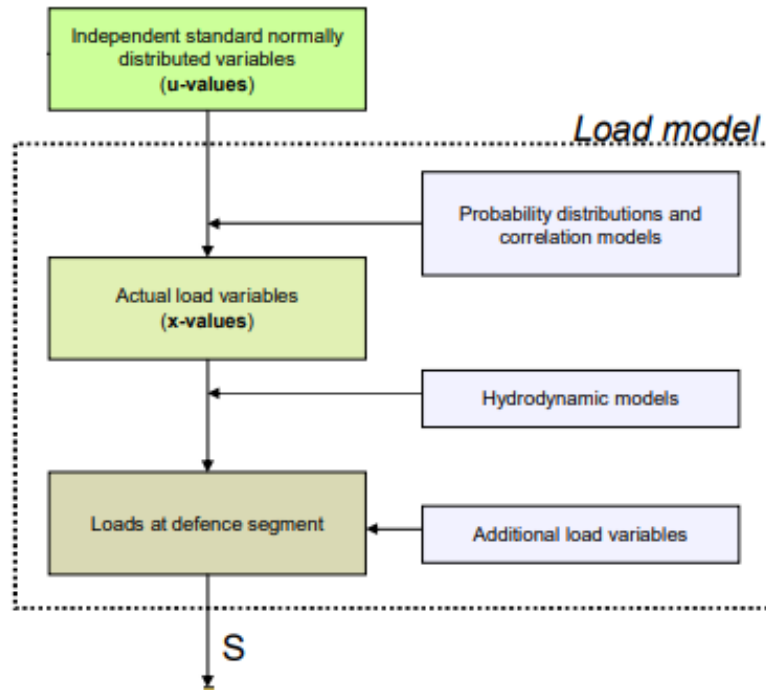
Figure 3.3: Overview of the calculation method of the hydraulic loads (S) on the foot of the flood defence (Diermanse et al. (2013)).

The independent variables consist of the river discharge, wind speed, sea water levels and the performance of the storm surge barriers, such as the Europoort barrier and the Hollandse IJssel barrier. The probability distributions of these variables consist of probabilities of exceedance of threshold values, duration of these threshold levels and the probabilities of occurrence of discrete events. A discrete event happens at a certain point in time, such as the failure of a storm surge barrier or the probability of a wind direction in a region. Together with correlation models, these are then formed into actual load variables. Statistical dependency is usually the result of the same meteorological cause. This dependency usually leads to an increased probability of high load variables and thus to an increased probability of flooding. The two different correlations taken into account in Hydra-ring are correlation in time and correlation in space. Many hydrodynamic simulations are used to transform the actual load variables into loads at the flood defence. In these hydrodynamic models physical relations are used to determine the final hydraulic loads on the toe of the flood defence from the possible realizations of the load variables. For tidal rivers, two-dimensional hydrodynamic models and wave simulation models are used to determine water levels and the wave characteristics respectively. Additional load variables are added in case it is relevant for a failure mechanism. For example in some cases the mean sea water level or the water level at the inner slope of the flood defence are needed. In Hydra-ring these additional load variables are used as completely independent of the other load variables, determined following the previous methods.

In Hydra-ring several types of water systems are distinguished. An overview of these types of water systems can be seen in Figure 3.4. The load models of the different types of water systems are formed in a similar way and within a type they will only differ in some details, such as the choice of certain measurement locations for certain variables.

Figure 3.4: An overview of the primary water systems that are distinguished in Hydra-ring (Diermanse et al. (2013))

Calculations for the tidal rivers (in red in Figure 3.4) contains influences of the storm surges on the North Sea and the performance of the storm surge barriers. The water levels at the Maas estuary are described according to a Weibull distribution function. This function shows the correlation between the wind characteristics and the sea water level. The wind characteristics are described with a modified Gumbel distribution function. The correlation between the wind and the sea water levels is described according to the 'Volkermodel'. In short, the extreme sea water levels are the result of storms at sea with northerly or westerly directions in combination with high tide. The closure of these barriers is based on the closure criterion, predicted water levels and the uncertainty of the predicted water levels. Both this uncertainty and the probability of closure failure are taken into account in the load models. Other variables are the river discharge, sea water level and wind characteristics. The correlation between the sea water level and the wind characteristics is also included in the load model. The hydrodynamic model that is used for the tidal rivers is the one-dimensional hydrodynamic model Sobek. This is calculated for different combinations of river discharge, sea water levels, wind characteristics and the state of the storm surge barriers. By using this model, water levels can be estimated per kilometer. The water levels between these locations are determined through interpolation between the closest water level downstream and upstream. In this model the relationship between discharge and water level is included. Additional effects on the water levels such as wind set up and seiches are written from the input database. The Brettschneider model is used to calculate the wave characteristics along the tidal rivers.

Eventually the hydraulic boundary conditions are formed per location which are given as output in Hydra-NL. These are the maximum water level, wave height, wave period and, when adding a profile, the hydraulic load level.

3.3. Distribution over failure mechanisms

With a distribution over the failure mechanisms, a flood probability standard is distributed among the different failure mechanisms of the flood defences (Knoeff, 2016). Correlations between failure mechanisms are not considered. The distribution over the failure mechanisms has a major influence on the final design of the flood defence. Figure 3.5 shows an example of two flood defences with an equal probability of failure. However, the different designs are because the flood defences both have a different dominant failure mechanism. On the left is the dominant failure mechanism height and on the right stability (Knoeff, 2016).

Figure 3.5: An overview of two different designs with an equal probability of failure. The design with height as dominant failure mechanism results in a lower and wider dike, while a design with stability as dominant failure mechanisms results in a higher and smaller dike (Knoeff, 2016).

The idea of a distribution over the failure mechanisms is that if all failure mechanisms meet the failure probability requirements derived from the standards and the relative distributions, a distribution over the failure mechanisms can never lead to an unsafe design. However, an incorrectly defined distribution over the failure mechanisms can lead to an inefficient design (Knoeff, 2016).

The most economic (efficient) design is when a large percentage of the distribution over the failure mechanisms is allocated to the dominant failure mechanism and a small percentage to the irrelevant failure mechanisms. This economic distribution over the failure mechanisms is usually equal to the actual failure probability distribution of the flood defence.

The 'actual' distribution over the failure mechanisms is influenced by various factors within a dike section. A dike section is a part of a flood defence with more or less equal strength properties and hydraulic load. Trajectories, part of primary flood defences that is separately standardised, is divided in several dike sections. A standard failure probability distribution has been included in the WBI derived from VNK2. For the WBI it was decided not to include regional distributions over the failure mechanisms because they would not deviate significantly (Knoeff, 2016). In this standard distribution over the failure mechanisms, 24 percent is reserved for height, i.e. the failure mechanism overflow and overtopping. An overview of the standard distribution over the failure mechanisms is shown in the Figure 3.6.
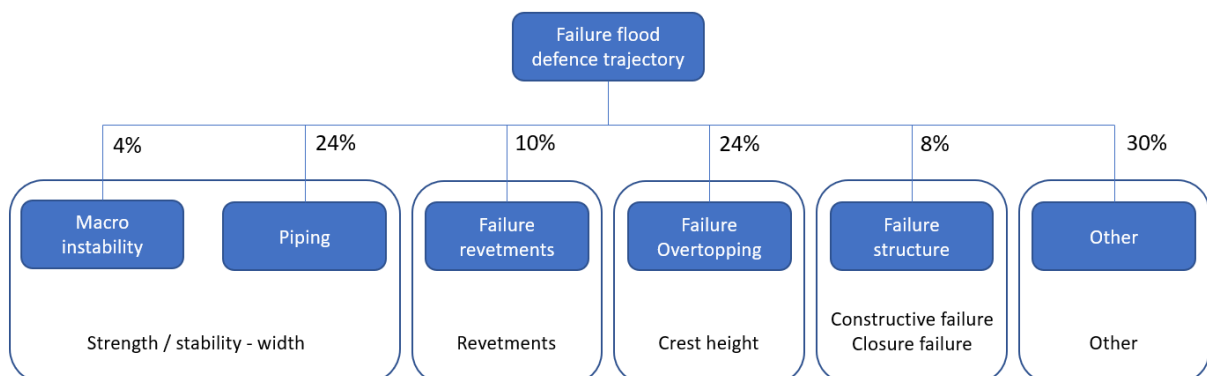
Figure 3.6: Standard distribution over the different failure mechanisms (Knoeff, 2016).

However, for future designs, this distribution over the failure mechanisms is a degree of freedom. The conditions for a flood defence are different at different locations in the Netherlands and therefore the standard distribution over the failure mechanisms can sometimes be somewhat conservative. Without an analysis

of the distribution over the failure mechanisms, the final design can lead to high and wide flood defences. Therefore, a method that will be used for the rest of this study, in which the standard distribution over the failure mechanisms will be used as a starting value, will be briefly presented. It must be determined which starting value is too conservative for the area of dike ring 14 and why there will be any deviation from these starting values. It is not recommended to adjust a distribution over the failure mechanisms if this will have little effect on the total investment for strengthening the flood defence. This is the case, for example, when replacing revetments, where the initial costs are so high that optimizing the distribution over the failure mechanisms is hardly useful (Knoeff, 2016). In most situations, adjusting the distribution over the failure mechanisms only makes sense once the uncertainties of the basic schematic have been reduced by means of an expensive study (Knoeff, 2016). This adjustment is made through an iterative process in the design process. In this process, after an analysis of the results of the calculations with the starting value, a decision is made whether the failure probability estimate needs to be adjusted.

Distribution over failure mechanisms: VNK2

Recently available probabilities are reported in VNK2 (Jongejan, 2010). It is interesting to examine the relative contribution of height, the failure by overtopping and overflow, to the distribution over the failure mechanisms. The area assessed in VNK2 for dikering 14 includes the flood defences along the Nieuwe Maas and Nieuwe Waterweg. Failure probabilities have been calculated for all failure mechanisms and by comparing these probabilities to the combined probability of failure, the relative contribution of each failure mechanism can be assessed at section level. This report (Jongejan, 2010) deviates from the previously described standard distribution over the failure mechanisms. For almost all sections from 1 to 30, height has a relative contribution of 100 percent to the combined failure probability. Exceptions are sections 3 and 18, where the dominant failure mechanism is failure of the revetments. For section 6, height has a relative contribution of 60 percent. However, from section 33 onwards, the contribution of height to the distribution over the failure mechanisms starts to change drastically. In many of the sections along the Nieuwe Waterweg, the contribution of height according to VNK2 is negligible (approximately 0 percent) and piping or failure of the revetments is the dominant failure mechanism. Since this study only includes the failure mechanism overtopping and overflow, it is important to mention that this may lead to an underestimation of the failure probability for sections 33-49. An overview of the dike sections of dike ring 14 is given in Figure 3.7. An overview of the relative contribution of the height per section is shown in Appendix A. In the VNK2 report, the entire distribution over the failure mechanisms for the dunes is allocated to the failure mechanism dune erosion. This applies to all dune sections 52 through 73. However, there are engineering structures in these dunes that are assessed differently. For the purposes of this study, it is assumed that the probability of structures is negligible compared to the dunes for all scenarios. At ring level, the failure mechanisms dune erosion and height contribute most to the total failure probability, 36 percent and 46 percent respectively. Piping follows with 17 percent and approximately 1 percent is spent on other failure mechanisms, such as failure of the revetments.
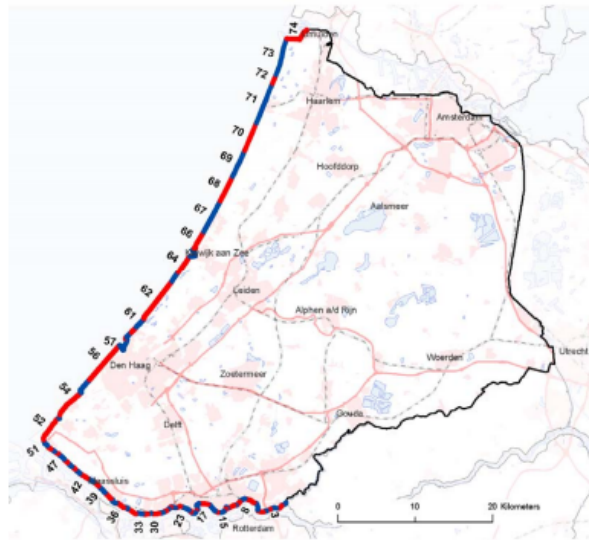
Figuur 62: Vakindeling dijkring 14.

Figure 3.7: Overview of the dike sections of dikering 14 from VNK2 (Jongejan, 2010). As this study is from 2010, the present numbering of the dike sections may differ. In this figure trajectories 14-2 and 14-3 are divided in dike sections in 1 to 25 and 26 to 45 respectively. Trajectory 14-1, along the river Hollandse IJssel, is not included in this figure.

Distribution of failure mechanisms used in this study
A decision must be made on how much of the distribution over the failure mechanisms is allocated to height for the dikes and how much to dune erosion for the dunes. Adopting the standard distribution over the failure mechanisms for the river dikes of dike ring 14 seems somewhat conservative, since it can already be concluded from the VNK2 report that height contributes almost 100 percent to the combined failure probability for most of the dike sections. However, the aim of this study is not to develop a new distribution of over the failure mechanisms. The ideal method would be to calculate the failure probability for the different failure mechanisms separately and add them up to obtain the total failure probability. Here, it should be assumed that the failure mechanisms are independent to sum these probabilities. Because there is a limited amount of time available for this study, the probability of flooding is calculated using two hydraulic load levels (one where 24 percent is allocated to height and one where 100 percent is allocated to height). This creates a lower and upper limit which can be used for a sensitivity analysis later in this study. This applies to both the assessment of current profiles and possible reinforced profiles for future scenarios. For the dunes, the failure probability is 100 percent dependent on the failure mechanism dune erosion.

Length effect
Besides the relative contribution of the failure mechanism, the length effect must also be considered. The length effect means that the failure probability increases with the length of the assessed dike trajectory. A dike trajectory can be considered as a series system, both in term of failure mechanisms as in terms of dike sections within the trajectory (S. N. Jonkman et al., 2018). The length effect is based on both the hydraulic load and the strength of the flood defence. For example, wave overtopping depends on the revetments of the flood defence, the wind direction and wind strength, the orientation and cross section of the flood defence and the wave direction. For other failure mechanisms such as instability, the parameters of the soil are important and may vary in space. The length effect is small for failure mechanisms with a high degree of dependency or correlation. The length effect for height could be assumed to be 1, as there is a strong dependency between the different dike sections (Jongejan, 2010). Also, the height of a dike is often about the same along a dike trajectory, so the length effect is small, i.e. in the order of 1 - 3 (S. N. Jonkman et al., 2018). The length effect will be larger for failure mechanisms that are more independent between sections, which is the case for piping and stability. The order of magnitude for the length effect of these failure mechanisms is 10 - 100 (S. N. Jonkman et al., 2018). In most recent assessment reports (Hoogheemraadschap van Schieland en de Krimpenerwaard, 2019) a length effect of 2 is assumed for the failure mechanism erosion crest and inner slope (height) for trajectory 14-2. This length effect will be adopted in this study for the assessment of the current profiles and for possible future designs. This length effect of 2 is also in line with the range proposed by S. N. Jonkman et al. (2018).

Finally, the relative contribution of the failure mechanism height, the length effect and the standards of the dike trajectory are used to calculate the required failure probability for each dike trajectory, see Table 1. These required failure probabilities are equal to the recurrence times of the hydraulic load levels from Hydra-NL, which are finally used to calculate the failure probability of the 8 different cross-sections. The failure probability requirement for overflow and wave overtopping is determined according Equation 3.1 (Hoogheemraadschap van Schieland en de Krimpenerwaard, 2019). P_{req} is the signaling value of the dike trajectory, Table 3.1, and ω is the maximum contribution of the failure mechanism to the system failure probability. Two cases are considered in this study: a relative contribution of overflow and overtopping of 24 and 100 percent. For this study 24 percent is chosen but the effect of this assumption will be discussed later. N_{cross} is the length effect factor. In the assessment of Hoogheemraadschap van Schieland en de Krimpenerwaard (2019), a length effect of 2 was used for the dike sections and therefore this will also be used in this study. $P_{req;cross}$ is the required annual failure probability for the cross-section and failure mechanism (in this case overflow and overtopping).

$$P_{req;cross} = \frac{P_{req} * \omega}{N_{cross}} \qquad (3.1)$$

Signal value [1/... per year]	Relative contribution [-]	Preq [1/... per year]	
14-1 30.000 30.000	0,24 1	250.000 60.000	
14-2 100.000 100.000	0,24 1	833.333 200.000	
14-3 10.000 10.000	0,24 1	83.333 20.000	

Table 3.1: Overview of the required failure probabilities for height per dike trajectory for the standard distribution of the failure mechanisms (24 percent) and the distribution used in this study (100 percent). In this study a length effect of 2 is chosen for all trajectories (N=2).

3.4. Methodology failure probability river dikes

In this section, the methodology for determining the flooding probabilities of the river dikes is explained. Eight different locations and their dike profiles were considered. These include 2 cross sections in the dike trajectory 14-1, 4 cross sections in the dike trajectory 14-2 and 2 cross sections in the dike trajectory 14-3. A distinction was made between parts of the trajectories with or without a foreland and different dike heights. Foreland is land outside the dikes, which makes the flood defence more robust and has a positive influence on the water safety. This is explained in more detail later in this section.

3.4.1. Cross-sections

The dike heights were all determined using the AHN, which is an actual elevation database of the Netherlands (AHN Viewer, n.d.). A distinction was made between these parts with the aim of being able to say something useful later in the study about possible costs for reinforcements. Raising an entire Maasboulevard will be more expensive than raising a normal river dike. If the costs of reinforcing the Maasboulevard are taken as normative for the entire dike trajectory, the total costs of possible reinforcements are expected to be significantly overestimated. In addition, the division into parts makes it possible to distinguish in detail which parts of the trajectory may need reinforcement and which may not. An overview of the selected locations location of the Maeslantbarrier and the Hollandse IJssel barrier can be found in the Figure 3.8, Figure 3.9 and Figure 3.10.

Figure 3.8: An overview of the locations of the two assessed cross sections (1 and 2) and the location of the Hollandse IJssel barrier (A) in dike trajectory 14-1. Both locations do not have foreland.

Figure 3.9: An overview of the locations of the four assessed cross sections in trajectory 14-2. All locations do have foreland except for location 3.

Figure 3.10: An overview of the locations of the two assessed cross sections (7 and 8) in trajectory 14-3 and the location of the Maeslantbarrier (B) in dike trajectory 14-3. Location 8 does not have foreland and location 7 does.

3.4.2. Probability of failure

On January 1, 2017, the first round of assessments started, all of which must be completed within 6 years. The assessment is already available from the Waterveiligheidsportaal (n.d.) for dike trajectory 14-2. The assessments for trajectories 14-1 and 14-3 are still in progress or have yet to be carried out. Since this

study only examine the overflow and wave overtopping of the dikes, the calculation for erosion of the dike crest and the inner slope is important. The most critical section for which the failure probability is available for this section of dike is the Maasboulevard. The analysis of this failure mechanism are included in the background reports and were made available by the Schieland and Krimpenerwaard Water Board (Hoogheemraadschap van Schieland en de Krimpenerwaard, 2019). In this background report, the Maasboulevard is divided into subsections, see Figure 3.11, and the failure probability is determined for each subsection. A relationship can be obtained between the height shortage of the dike and the probability of failure. This relationship will also be used to make an initial estimate of the failure probabilities for other cross sections. An overview of the height shortages with their corresponding failure probabilities of the Maasboulevard are shown Table 3.2 and Figure 3.12.

Figure 3.11: An overview the subsections of the Maasboulevard in dike trajectory 14-2 (Hoogheemraadschap van Schieland en de Krimpenerwaard, 2019)

Dike section	Height shortage at signaling value [m]	Probability of failure due to erosion of crest and inner slope [1/... per year]
15a	0,11	414.000
15b	0,30	267.000
15c	0,18	436.000
15d	0,36	202.000
15e	0,44	145.000
15f	0,26	322.000
15g	0,10	572.000
15h	0,12	537.000

Table 3.2: Height shortage and corresponding calculated probability of failure for the failure mechanism erosion crest and inner slope for the Maasboulevard (Hoogheemraadschap van Schieland en de Krimpenerwaard, 2019). The hydraulic loads used for this calculation did correspond to a constant length effect (N =2) and a relative contribution of height of 24 percent.
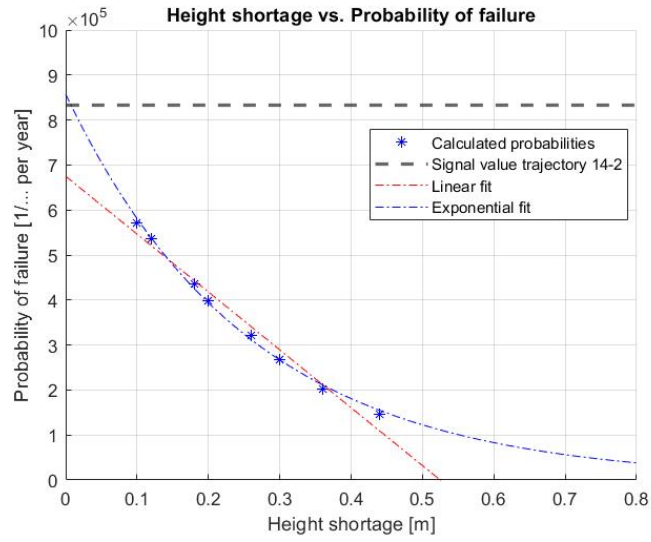
Figure 3.12: An overview of the height shortage vs. the probability of failure with an exponential fit and a linear fit.
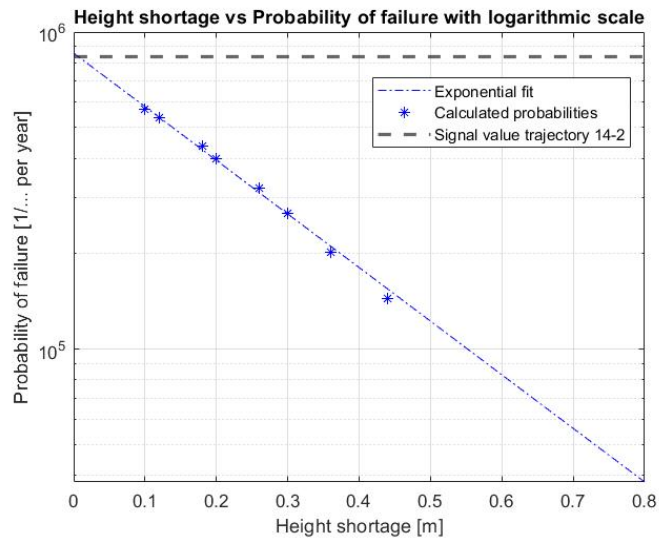
Figure 3.13: An overview of the height shortage vs. the probability of failure on a logarithmic scale on the y-axis.
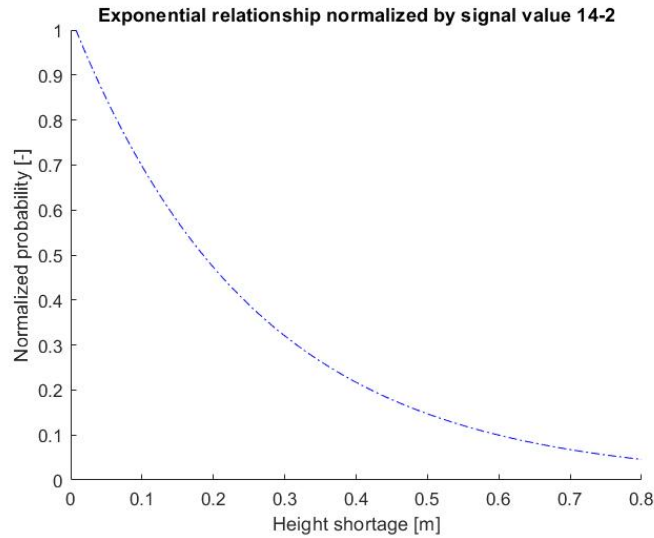
Figure 3.14: Relationship height shortage vs. the probability of failure normalized by the signal value of trajectory 14-2.

To determine which of the two fits should be chosen, the signal value is plotted. As can be concluded from the graph is that the exponential fit intersects the y-axis at the signal value of the trajectory 14-2. Figure 3.13 shows that the calculated probabilities are positioned on a straight line when an exponential relationship is chosen. And it become more clear that this exponential relationship intesects the y-axis at the signal value when the function from Figure 3.12 is normalized by the signal value of 1/833.333 per year. In this new graph, see Figure 3.14, it can be concluded that the exponential relationship intersects the y-axis around 1. In this way the probability of failure of dikes with neither a height shortage nor a height surplus, is equal to the signal value.

Because this study only looks at the failure mechanism at height, the water levels are important. Recent research from the Waal-Eemhaven is evaluated. If the water levels from Table 2.1 are plotted with the recurrence time it can be concluded that there is an exponential relationship, see Figure 3.15. As these water levels have a direct influence on the failure mechanism of wave overtopping and flooding.
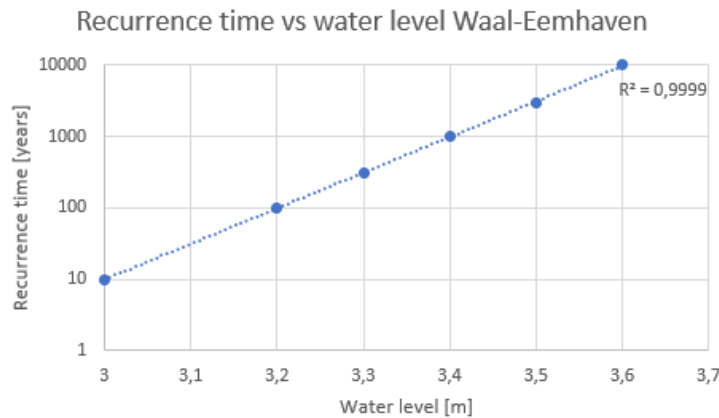
Figure 3.15: Recurrence time vs. water levels for the Waal-Eemhaven.

This can also be seen in the relationship between the probability of flooding and the water level used to determine the risk of flooding. An exponential distribution is used, which is relatively simple but sufficiently reliable (Royal HaskoningDHV, 2017), in which p is the probability of exceedance per year, h is the water level [m compared to NAP] and A and B are coefficients of the exponential distribution.

$$p = e^{\frac{-(h-A)}{B}} \tag{3.2}$$

36

In addition, it is not plausible that the relationship is shown by means of a linear relationship, because with increased water levels and therefore higher height shortages, there would be negative failure probabilities according to Figure 3.12.

Because of the intersection at the y-axis at the signal value, recent research and that it is unlikely to have a linear relationship, it will be assumed that the exponential relationship shown in Figure 3.12 is sufficient to determine the probability of flooding due to the failure mechanism due to overflow and overtopping. This relationship will be used for the determination of probabilities of failure for all scenario's and cross-sections. The ideal method to determine the probability of failure of a cross-section is described in Section 3.3. But due to time constraints above described method is used for this study.

3.4.3. Effect foreland

An additional positive effect is the presence or absence of foreland. Buildings or vegetation can be present on these lands, but also harbour dams, a clay layer cover and salt marshes. These elements outside the dikes can make a positive contribution to water safety and reduce the risk of flooding (Rijksoverheid, 2017) by reducing the hydraulic loads and increasing the strength of the flood defence. The possible positive effects of foreland are buffer against collisions, breaking and dampening of waves in shallow water and by building and vegetation, reducing ground waterlevel in the dike, adding extra seepage path length and residual strength and forming of a support berm (Boorn et al., 2018). For an overview of the possible positive effects of foreland, see Figure 3.16. These positive effects on the water safety are often not taken into account in the assessment and reinforcement project due to technical, policy and/or legal obstacles. By doing so, this can lead to incorrect rejections of flood defences and unnecessary investments (Rijksoverheid, 2017).
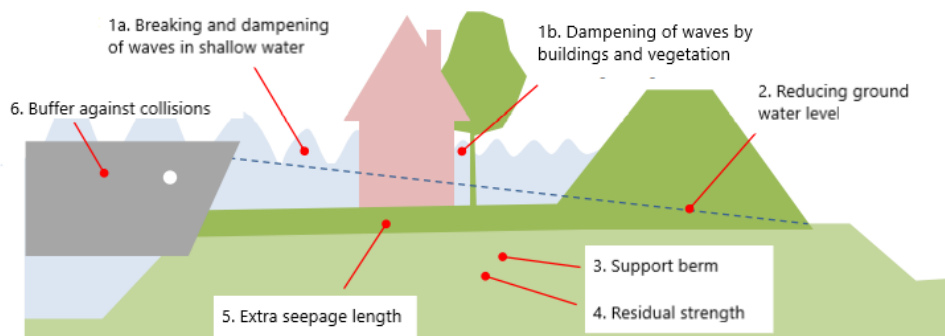
Figure 3.16: Overview of the possible poisitive effects of the presence of foreland (Boorn et al., 2018).

For large stretches along the section 14-2 and for a part of section 14-3 foreland is present. This effect will be taken into account in the reduction of the failure probability by a factor of 28,33. This factor comes from an analysis of the Maasboulevard in which a fault tree was made, see Figure 3.17. In this fault tree, a distinction was made between the presence or absence of foreland. The difference is the failure probability by a factor of 28,33 pMaaskant et al. (2019). This factor is also used in this study and will be assumed constant in the different sea level rise scenarios. This factor will also be used for the failure probabilities for the Maasboulevard, making the failure probabilities significantly lower than those determined by the Water Board HHSK.
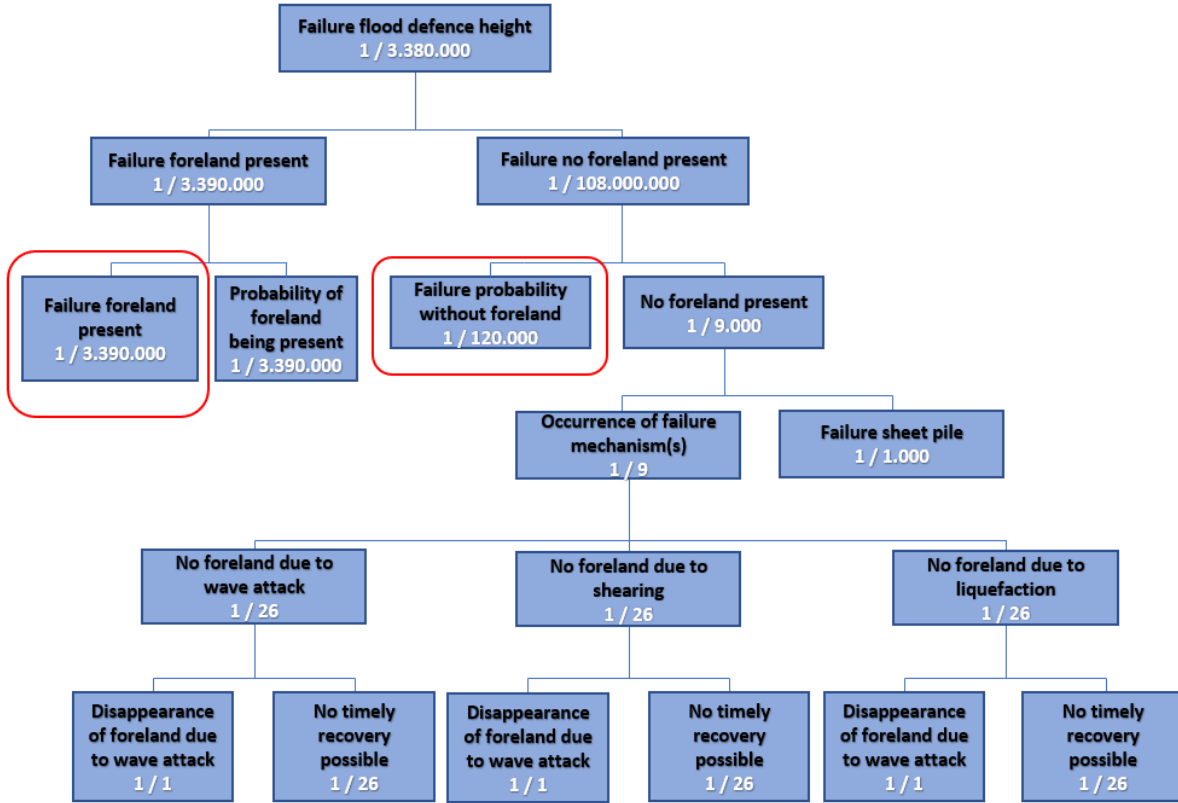
Figure 3.17: Fault tree foreland Tropicana (Maasboulevard) (Maaskant et al., 2019).

3.4.4. Hydraulic load levels

Now that the relationship between height shortage and probability of failure is determined, and how the presence of foreland is included in this probability of failure, the failure probability for the different scenarios can be determined. First the hydraulic load levels will be determined using Hydra-NL. The hydraulic load level is a measure for the required crest height of a dike for a certain load level. To determine the hydraulic load level, a dike profile and a critical overflow flow rate are used as input for Hydra-NL. In this thesis we assume for all dikes a critical overflow flow rate of 10 l/s/m. The dike profiles are obtained from the AHN data (AHN Viewer, n.d.). With these hydraulic load levels and the crest heights obtained from the AHN data, the height shortage can be determined and with this height shortage and aforementioned relationship, the probability of failure can be calculated for all different scenario's.

To determine the hydraulic load level for all different scenario's, various statistical datasets are needed for the model input. The input consists of a file with exceedance probabilities for the peak discharge at Lobith, sea level and wind speed. It is assumed that the wind speed does not change with climate change, so only the data sets for peak discharge and sea level need to be adjusted for each scenario. For the exceedance probability of the sea level at the Maasmond estuary, datasets are available for the years 2015, 2050 and 2085 in Hydra-NL with 0, 35 and 85 cm sea level rise respectively. Linear extrapolation was applied to these datasets to obtain datasets for the years 2065, 2115, 2165 and 2215 with 50, 100, 150 and 200 cm sea level rise respectively. For the exceedance probability of the peak discharge at Lobith, datasets were only available for the years 1985 and 2017. These two datasets were also used to obtain the final required datasets using extrapolation. The Maeslant and the Hollandse IJssel barriers are included in the model as a stochastic variable. The failure probabilities of these barriers are set at 0,01 and 0,005 per demand. These are also the failure probabilities used in the reports of VNK2 (Jongejan, 2010).

The hydraulic loads corresponding to the target failure probability with a relative contribution of 24 percent will be used in this study, see Table 3.1. Finally, subtraction of the hydraulic load level from the crest height results in a height shortage of surplus . The crest heights were obtained using AHN data and a deduction of 10 cm was then made for possible settlement, because this was also done for the assessment for dike trajectory 14-2. The Delfland Water Board (trajectory 14-3) uses the AHN data in the same way

as the Schieland and Krimpenerwaard Water Board (Mieke Huisman (HHSK), 2021). The profiles and orientations of the eight different dike cross-sections are used as input for Hydra-NL. The orientations are estimated from the top views in AHN. Finally, the hydraulic load levels are calculated per dike profile and per scenario. By doing so, all probabilities of failures can be calculated using the exponential relationship from the groph in Figure 3.12.

3.5.   Results failure probabilities river dikes

A total overview of the failure probabilities per location is given in the Appendix in Table A.1 to Table A.8. The failure probabilities are also given for the case that the failure mechanism overflow and overtopping contribute 100 percent to the failure probability. The relative contribution of height to the total failure probability is a degree of freedom in future designs. In section 3.3 is explained how the probability of failure should be calculated in an ideal situation. For this study a relative contribution of 24 percent was chosen, but the effect of this choice will be discussed in the discussion at the end of this study.

Because only the height shortage is evaluated, it is assumed that the lowest failure probability of a cross section in a dike trajectory is equal to the failure probability of the entire dike trajectory. For trajectory 14-1 the highest failure probability of profile 1 and 2 is normative for the probability of failure of the entire trajectory 14-1. Profile 3,4,5, and 6 determine the failure probability of trajectory 14-2 in a same way and profile 6 and 7 are normative for trajectory 14-3. These failure probabilities will be used to determine the flood risks in the further chapters. An overview of the calculated probabilities of failure for trajectories 14-1 to 14-3 for each scenario can be found in Table 3.3, Table 3.4 and Table 3.5. An overview of the failure probabilities per scenario for each cross-section are given in Appendix A.2. The locations of the assessed dike profiles are given in Appendix A.1.

Trajectory 14-1	
Scenario sea level rise [m]	Probability of failure [1/... per year]
0,0	370.000
0,5	140.000
1,0	46.000
1,5	3.500
2,0	170

Table 3.3: Overview of the probabilities of failure which will be used for the loss of life estimation and economic analysis per scenario for trajectory 14-1.

Trajectory 14-2	
Scenario sea level rise [m]	Probability of failure [1/... per year]
0,0	2.200.000
0,5	500.000
1,0	90.000
1,5	17.000
2,0	3.500

Table 3.4: Overview of the probabilities of failure which will be used for the loss of life estimation and economic analysis per scenario for trajectory 14-2.

Trajectory 14-3	
Scenario sea level rise [m]	Probability of failure [1/... per year]
0,0	86.000.000
0,5	14.000.000
1,0	2.000.000
1,5	290.000
2,0	44.000

Table 3.5: Overview of the probabilities of failure which will be used for the loss of life estimation and economic analysis per scenario for trajectory 14-3.

3.6.   Dune erosion

The main failure mechanism is dune erosion for dunes, 70 percent, and 30 percent of the standard failure probability distribution is reserved for other (S. N. Jonkman et al., 2018). Due to time constraints and the scope of the study, only the failure mechanism dune erosion is considered for the dunes. The other failure mechanisms are not considered. Dune failure can be determined according to the Technical Report Dune Failure 2006 (Van de Graaff et al., 2006). The difference with the 1984 report is that storm surge conditions are now included with long wave periods, Tp = 16 - 20 s instead of 12 s.

The main purpose of a dune is to act as a (primary) flood defence (Van de Graaff et al., 2006). Storms at sea will result in much higher waves than under normal conditions. Another additional effect of the storm is that the water is pushed up against the Dutch coast. The storm surge level is highest for storms coming from the north. The storm surge level and the higher waves ensure that the seawater and the waves reach the dunes, in contrast to the 'normal' situation, where the dunes (landward of the dune base) do not participate in coastal processes. The dune foot is the transition between the gentle beach, with a slope of approximately 1:20, and the steep dune slope (slope of approximately 1:3). This transition is not abrupt, but gradual. This makes it difficult to determine the actual location of the dune foot. In the Netherlands it is assumed that the dune foot is present at the level of NAP + 3m.

The waves and storm surge level during a storm, combined with the astronomical tide, can cause the seawater to rise well above the dune foot, damaging the dunes. The sand is transported back with the seawater to the deeper waters and as a result, the dune front will move more and more inland. This is the dune erosion process. When the water level has dropped sufficiently again, this process stops. What remains is a steeply sloping dune front (often with a slope steeper than 1:1) with an abrupt transition to the flatter part of the beach. Where this transition point lies depends mainly on the maximum sea level reached. The distance that the dune front is pushed back further inland depends on the storm conditions. The definition of a safe dune is that there is just no dune breach at the design conditions. Therefore, a point can be defined to which the maximum dune front may retreat before a dune breach occurs. This point is the normative dune erosion. In this thesis it is assumed that a breach results in flooding of the area behind. The dune erosion process also offers help in determining the part of the dune that will erode. This information can be used by coastal managers.

The dune erosion process is very complex, but can be well approximated with a relatively simple balance model, called the DUROS-plus model. In this model, the height and shape of the erosion profile after the storm can be determined with some storm surge properties (the maximum sea level, the significant wave height and wave period at deep water) and the grain diameter of the dune sand. This DUROS-plus model is also integrated into the MorphAn application, so that ultimately the normative erosion points per dune profile can be determined. The results of this relatively simple calculation method were compared with the results of the complex probabilistic method. The results hardly differed (by a few percent). The calculation concept prescribed in TRDA2006 (Van de Graaff et al., 2006) will therefore be used to assess the safety of the dunes and this method has also been included in the MorphAn application. For background information about the Duros-plus model see Appendix B.

3.7.   Methodology failure probability dunes

MorphAn will be used to assess the effect of sea level rise. MorphAn can be used to produce dune erosion calculations for the Dutch dunes according to the Duros-plus model. In this way, the safety of the dunes can be assessed. In addition to dune safety, trends in shoreline position and sand volumes can also be determined. For this study, however, only the dune safety model is important, because the probability

of failures need to be determined. Three different dune profiles will be investigated. The locations of these dune profiles are chosen at Katwijk, Noordwijk and Ter Heijde. It was decided to look at these three profiles because Katwijk and Noordwijk are among the normative dune profiles (Joost Veer, 2021) for the Rijnland Water Board and because recent assessment (Arcadis, 2018) shows that Ter Heijde is the normative point between the Hoek van Holland and Kijkduin. The probability of failure of the cross-section at Ter Heijde will be used in combination with the hydrodynamic models for Kijkduin and Monster. The highest probability of failure of the cross-sections Noordwijk and Katwijk will be used for the hydraulic model Noordwijk. Foor the locations of the three different cross-section, see Figure 3.19.

A number of assumptions will be made in this study. The dune profiles will not grow with sea level rise. The minimum profile that could be expected in recent years is taken into account and this profile is assessed and kept constant for all scenario's. In reality, however, the dune profiles will grow along with sea level rise and will be continuously maintained by the depositing of sand on the Dutch coast (suppletion). This dune growth and maintenance of the dune profiles are called dynamic dune profiles. Furthermore, the dunes will be assessed according to the method recommended by Joost Veer, who is responsible for assessing the dunes of the Rijnland Water Board. The normative year after the BKL (base coastline) control has been determined for each stretch (in Dutch: raai). An overview was given by Joost Veer. These years will be used for the dune profiles of Noordwijk and Katwijk. If these profiles are sufficient, the dune can be considered safe (Joost Veer, 2021). The Delfland Water Board performs the assessment in the same way. The normative years for the dune profiles are 1991 and 1994 for Kijkduin and Noordwijk respectively.

It will be examined at which design water level in combination with the significant wave height, Hs, wave period, Tp, a boundary profile can no longer be formed. For an explanation of how the boundary profile is formed, see Appendix B. The wave period and wave height increase with the rise of the sea level. For this study, the Noordwijk measuring station is used for these differences. This measuring station has shown that for each meter rise in sea level there is an increase of about 3.7 percent in significant wave height and 0.9 percent in wave period (HKV, 2018). One meter sea level rise results in a one meter rise of the water level along the coast of dike ring 14. The change in wave direction remains almost the same and is therefore negligible.

3.7.1. Locations Katwijk and Noordwijk

The assessment will start with the hydraulic boundary conditions that have been calculated for a signaling value of 1/30.000 per year for Noordwijk and Katwijk. All dunes currently meet this signaling value (Joost Veer, 2021). This has also been confirmed in the method used in this study. For the erosion profiles with the boundary profiles for dune profiles of the location Noordwijk and Katwijk, see Figure 3.18.
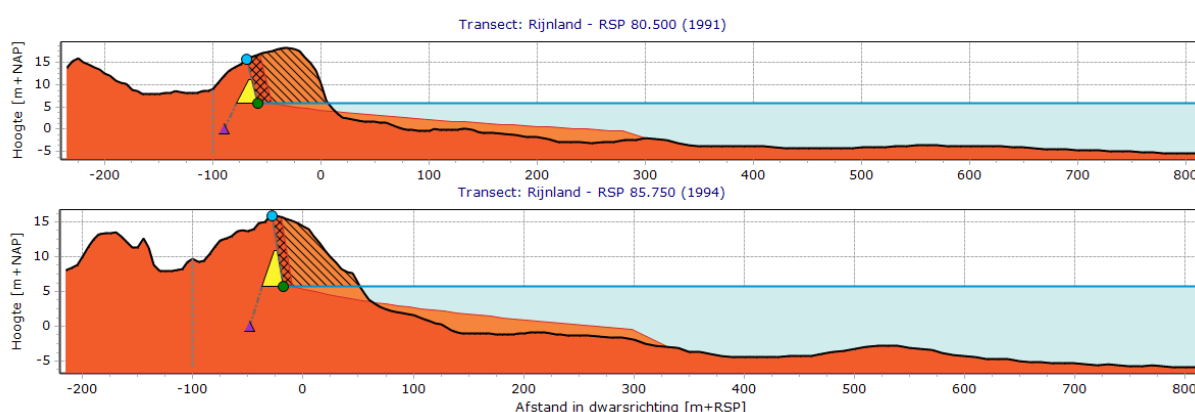
Figure 3.18: Overview of the normative dune profiles of Noordwijk (below) and Katwijk (above) from MorphAn. The normative profile was chosen according to the method by Joost Veer. In this case, under the hydraulic boundary conditions associated with the signaling value, it can be concluded that the dune is safe, because the boundary profile (yellow) can easily be fitted landwards of the erosion profile.

From this signaling value, the hydraulic load was increased for the sea level, wave height and wave period. If for a certain hydraulic load no boundary profile could be shown anymore, the recurrence time was

calculated for this design water level/seawater level with the Hydra-NL program. Hydra-NL also includes a number of locations along the coast where the recurrence times of the sea water levels can be determined. In this study it is assumed that the recurrence time for a certain sea level is the same for the coast between Hoek van Holland and IJmuiden. The location at Katwijk/Noordwijk is used in this study. For an overview of the locations in Hydra-NL see Figure 3.19.

Figure 3.19: Overview of the locations available in Hydra-NL for the coast in green and the locations of the used cross sections in red

The hydraulic boundary conditions for different combinations of sea level, wave height and wave period are shown in the Appendix. It also shows in red for which combination the dune profile is not longer able to retrieve a boundary profile and therefore no longer meets the safety requirements. The recurrence time is determined for this seawater level. This is done for different scenario's of sea level rise. Since the dune is not considered dynamic in this study, the sea water level at which the dune fails remains constant in all scenarios. The sea water level for which the profile fails is NAP + 7,38m and NAP + 8,21m for the locations Noordwijk and Katwijk respectively. The probability of recurrence of this water level and therefore the probability of failure increases with each step of sea level rise and can be determined using Hydra-NL. For the location Noordwijk, this increasing failure probability is shown in Figure 3.20. The results of the failure probabilities are shown in Table 3.8 and Table 3.7.
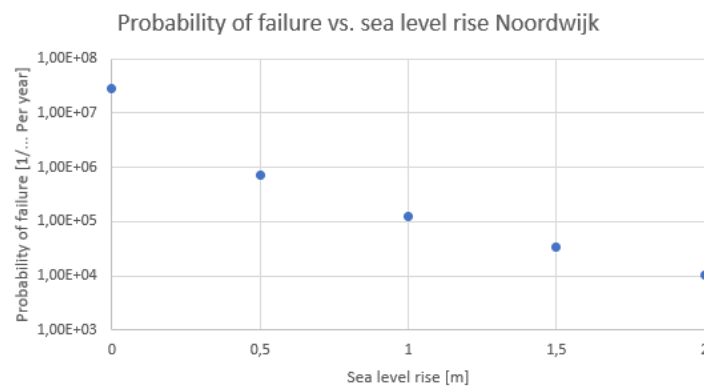
Figure 3.20: Results Noordwijk shown in a graph per scenario of sea level rise.

3.7.2. Location Ter Heijde

Unfortunately, at the time of writing the method of determining the probability of failure described in the previous subsection cannot be used for the cross-section at Ter Heijde. This is because MorphAn is not able to return boundary profiles while there is more than enough room to fit a boundary profile for a situation with a sea water level of NAP + 6,32m, see Figure 3.21. This is unlikely and also results in a much higher probability of failure than the signaling value. This is not true according to the most recent assessments by the Water Board Delfland. According to Joost Veer, this is also not correct and error messages appear that have not been seen before. At the moment of writing, this question is being dealt with by the makers of MorphAn.
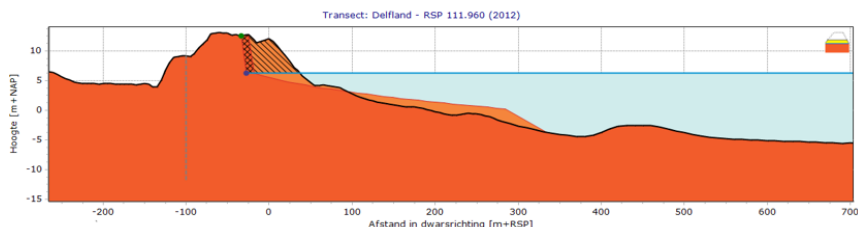
Figure 3.21: Error output MorphAn location Ter Heijde.

Therefore, another simplified method has to be used in this study to arrive at the probabilities of failures for this cross-section. Recently (2009-2010) the Delfland coast was reinforced by widening the beach (Arcadis, 2018). From The Hague to Hoek van Holland, the beach has been heightened by one metre. A new row of dunes has been added for the location at Ter Heijde, see Figure 3.22. The failure probabilities for the reinforced and unreinforced situation have recently been determined and are shown in Table 3.6. The reinforced situation has been taken as the starting point for this study because these failure probabilities are now also used to determine the risk of flooding (Arcadis, 2018). For this study the failure probability of Ter Heijde for the reinforced situation will be used for the hydrodynamic model Monster and Kijkduin.
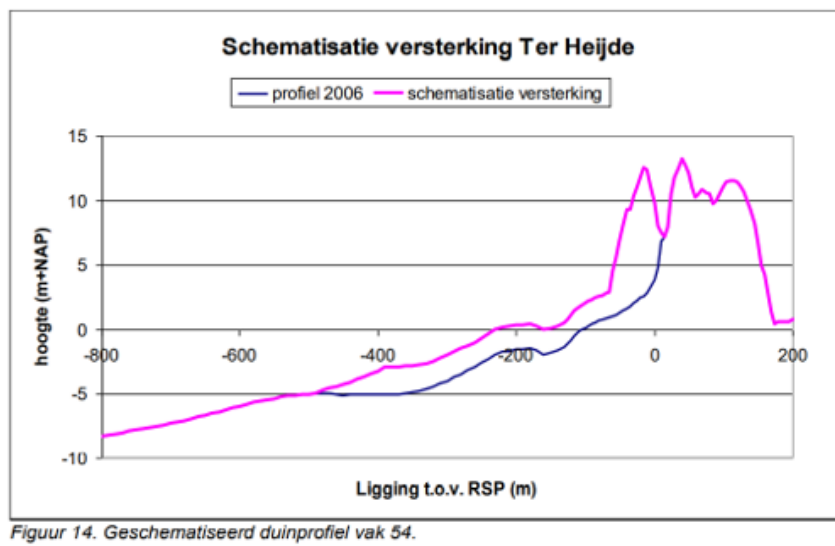
Figure 3.22: Schematic representation of the Ter Heijde reinforcement. The profile in blue is the profile in 2006 and the pink is the reinforced profile (Arcadis (2018))

Location	Unreinforced [1/... per year]	Reinforced [1/... per year]
Hoek van Holland	8,85E6	2,95E8
The Hague	1,76E6	2,47E7
Ter Heijde	1,72E6	1,89E7
Solleveld	7,14E6	2,51E7
Kijkduin	8,55E9	2,16E10

Table 3.6: Probabilities of failure per year for dike trajectory 14-5 (Arcadis, 2018).

The failure probability from Table 3.6 for Ter Heijde corresponds approximately to a return time of 1/1.89E+07 per year. From Hydra-NL this recurrence level corresponds approximately with a sea water level of NAP + 7.33m. It is assumed that the dune will fail with at sea water level. This sea water level will be held constant for all scenarios. The recurrence time of this sea level and therefore the probability of failure is calculated for the different sea level rise scenarios using Hydra-NL. The results are shown in Table 3.9.

3.8.   Results failure probability dunes

The results of the calculated failure probabilities are shown in Table 3.7, Table 3.8 and Table 3.9 for the cross-sections at Noordwijk, Katwijk and Ter Heijde respectively. As can be concluded from these results, the dunes are quite safe. The factors by which the probability of failure increases vary a lot. This is because Hydra-NL is not very accurate for the high return periods (above 1/100.000 per year). Finally, factors in this order of magnitude are not important for this study because it is expected that in this case no reinforcements will have to be realised at these locations. The signaling value of 1/30.000 per year will then be comfortably met and it will not be profitable to invest in these locations. Therefore, the scenarios with a probability around or below the signaling value only become interesting, because according to Water Act, the requirements are just met or not satisfactory anymore. The factors per half meter sea level rise with associated failure probabilities around or below 1/100.000 per year are already more constant and lie between 3.38 and 5.89. This confirms that Hydra-NL is more accurate for the lower return levels.

Sea level rise [m]	Probability of failure [1/... per year]	Factor
0	2.8E+07	-
0,5	710.000	39
1,0	120.000	5,89
1,5	34.000	3,54
2,0	10.000	3,38

Table 3.7: Results Noordwijk (RSP 80.500 (1991)) using MorphAn and Hydra-NL.

Sea level rise [m]	Probability of failure [1/... per year]	Factor
0	1.3E+10	-
0,5	3.2E+08	41
1,0	7.9E+06	41
1,5	340.000	23,5
2,0	77.000	4,4

Table 3.8: Results Katwijk (RSP 85.750 (1994)) using MorphAn and Hydra-NL.

Sea level rise [m]	Probability of failure [1/... per year]	Factor
0	1,9E+07	-
0,5	560.000	35
1,0	110.000	5,27
1,5	30.000	3,50
2,0	9.000	3.40

Table 3.9: Results Ter Heijde using Hydra-NL

For the risk analysis, the flood scenario's simulated hydrodynamic models need to be linked with this failure probabilities. The flood simulation at Noordwijk will be linked to the normative failure probabilities between the profiles at Katwijk and Noordwijk. As can be concluded from the results, the Noordwijk profile is normative and therefore the failure probabillites of Table 3.7 will be used for the analysis. For the flood scenario's as a result of a breach at Monster or Kijkduin, the failure probabilities of the cross-section at Ter Heijde will be used, see Table 3.9. For an overview of the locations of the dune breaches used in the hydrodynamic models, see Figure 3.23, and for the locations of the assessed cross-sections, see Figure 3.19.
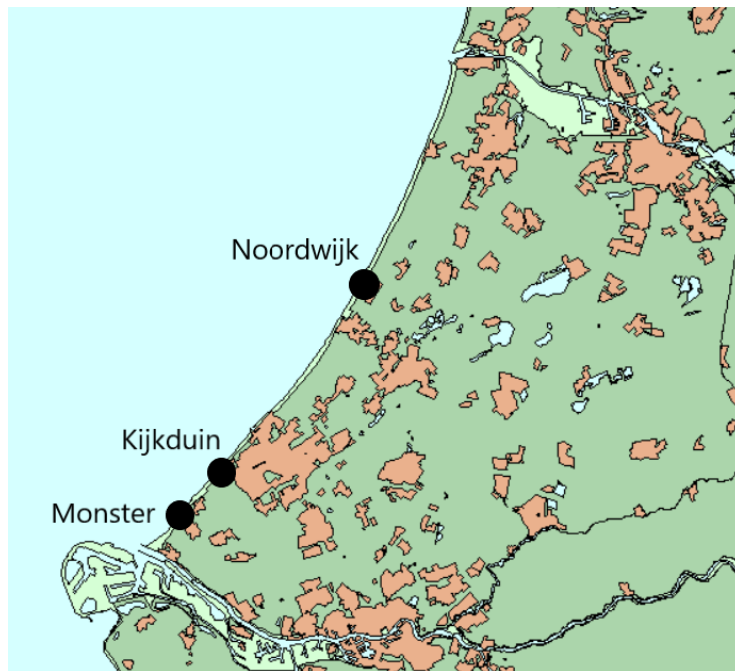
Figure 3.23: Overview of the locations of the dune breaches.

4. Economic damages

In the previous chapter, the failure probabilities used as input for the economic risk analysis and loss of life estimation were determined. The economic damages are determined using flood depth maps, damage curves in the Global Flood Risk Tool and the created land use map, see Figure 1.8, whereby the map is divided into several categories. The estimated damages per category that are used are shown in Table 2.4.

4.1. Economic damages riverside

For the riverside, the maps with flood depth are created using the LIWO database. In LIWO, flood simulations with different exceedance probabilities for the river water levels are available. These different recurrence times in LIWO were compared with the calculated failure probabilities for the scenario with 0 meter sea level rise (present situation) determined in the previous chapter, see Table 3.3, Table 3.4 and Table 3.5. The LIWO scenario's with exceeding probabilities that comes closest to the calculated flood probability in the previous chapter are chosen to perform the risk analyses. In Table 4.1 it is shown how the calculated probabilities are linked to the LIWO scenario's.

Dike trajectory	Probability of failure 0m sea level rise [1/.. per year]	LIWO scenario [1/... per year]
14-1	370.000	10.000
14-2	2.200.000	1.000.000
14-3	86.000.000	1.000.000

Table 4.1: Chosen LIWO scenarios with their exceedance probabilities compared to the calculated probabilities of failures per trajectory.

All available breach locations along the trajectories are combined to create the total extent of the possible floods. The maximum value for the waterdepth per grid cell is determined using ArcMap. Three maps are created with floods corresponding to a trajectory. This three floods will be used to perform both the economic risk analysis as the loss of life estimation. An overview of the three floods corresponding to the trajectories is given in Figure 4.2. The flood depths maps are compared to elevated positions according to AHN Viewer (n.d.), see Figure 4.1. The combination of these figures shows that the greatest flood depths occur in the deep polder along section 14-1. The area along 14-2, including the city of Rotterdam, has a higher elevated position and therefore the flood depths are lower. Along the route 14-3 high flood depths can also occur at Maassluis.

Figure 4.1: Map which shows the elevation along the trajectories 14-1 to 14-3 (AHN Viewer, n.d.). In blue are the lower-lying areas and in green the elevated areas.
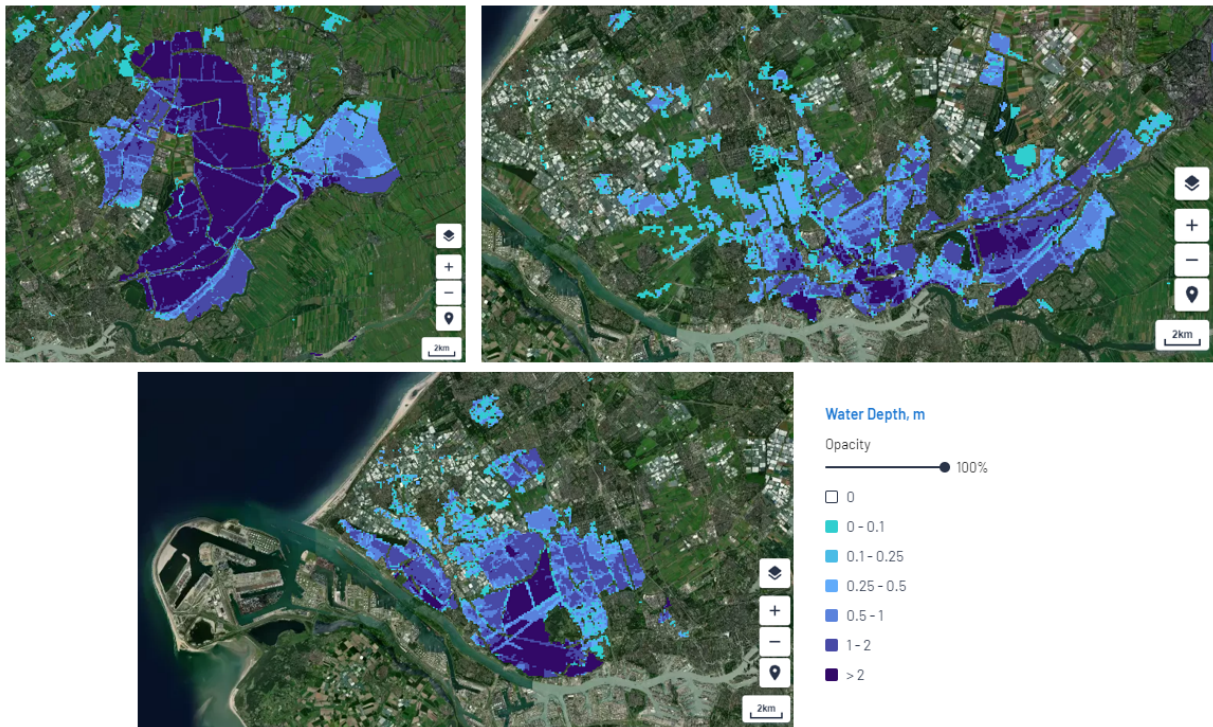
Figure 4.2: Created flood scenarios for the three different trajectories using LIWO data: 14-1 (upper left), 14-2 (upper right) and 14-3 (below).

To analyze the effect of sea level rise and increase of river discharge, the extent of these floods are kept constant, but the calculated failure probabilities will increase in future scenario's, see Chapter 3.5. Because the extent of the floods are kept constant, the calculation is based on damages remaining the same in the future, which is not the case in reality. It is likely that the potential damage in the area will increase due to an increase in flood depths and the extent of the floods as a result of higher river water levels in the future. Unfortunately, there are not hydrodynamic models available which include this increasing in river water levels. And therefore in this study, the floods and their characteristics as a result of a breach at the river dikes are kept constant for all scenario's. At the coast the influence of the rising sea water level on the extent of floods is included, as hydrodynamic models designed by Ranneft (2020) are available.

With the water depths for the floods in Figure 4.2, the damage curves in the Global Flood Risk Tool and the land use map, the direct economic damage can be calculated for each trajectory. This direct economic damage is defined as a damage per grid cell and visualized with the Global Flood Risk tool of Royal HaskoningDHV. The maps with damages per grid cell are shown in Figure 4.3.

Figure 4.3: Damages per grid cell (100x100m) for the three different trajectories along the rivers.

4.2. Economic damages seaside

The direct economic damages on the sea side have already been determined for the three breaching locations in study of Ranneft (2020). This is done in a similar way as for the riverside as explained in the previous section. The important thing to understand is that the difference between the seaside and the riverside is that the effect of the sea level rise on the flood extent is included in the hydrodynamic models at the seaside. Figure REF shows that with each step of sea level rise, the size of the flood increases and so does the total direct economic damage. An overview of the other two breach locations is shown in Appendix D.
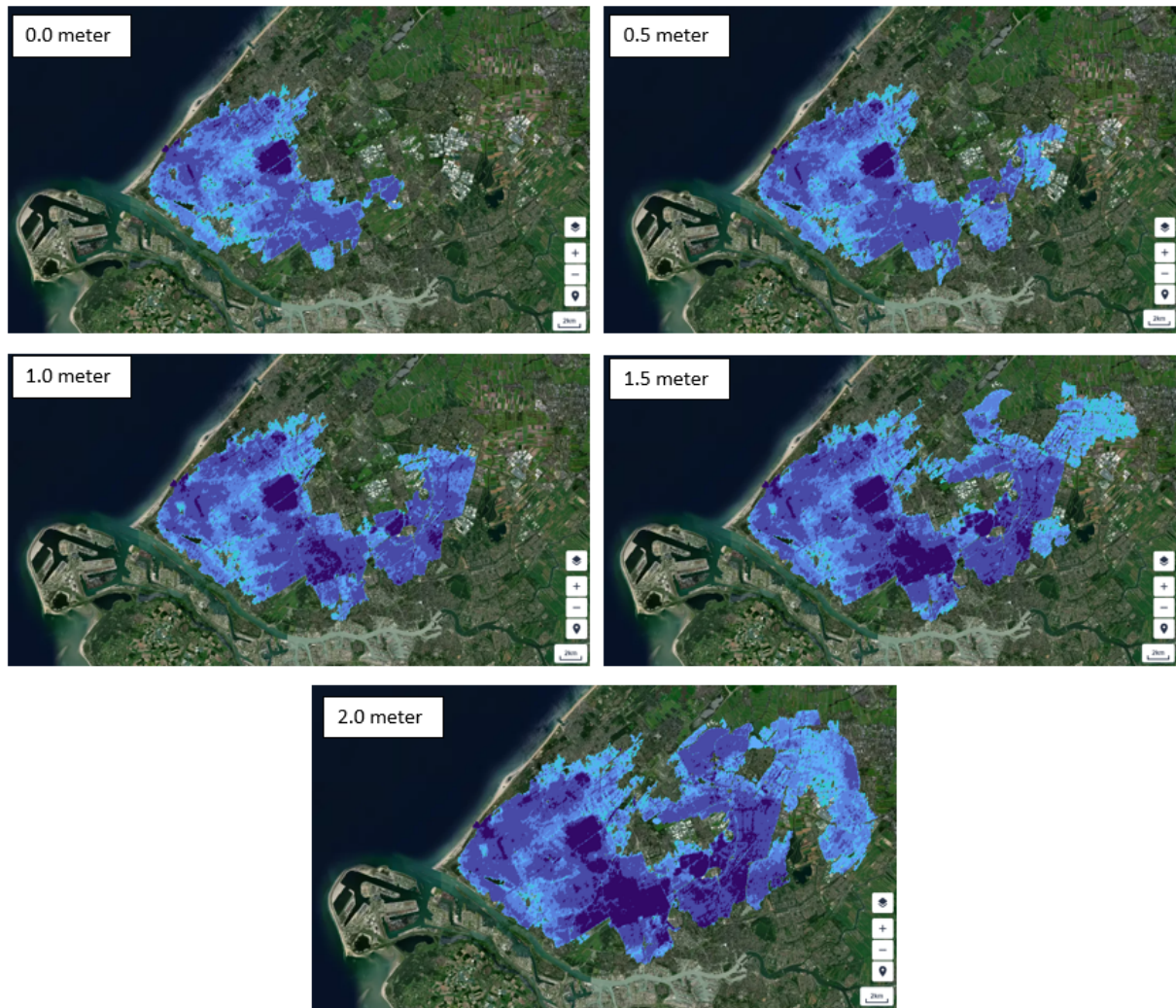
Figure 4.4: Hydrodynamic models for the breach location at Monster (Ranneft, 2020).

4.3. Results

The total economic damages are shown in Table 4.2. These total economic damages are constant for all scenario's at the riverside, but increase at the seaside for every step of sea level rise. It can be concluded that that the total economic damages as a result of a breach along trajectory 14-1 are the highest for the riverside. This can be due to the potential high flood depths due to low-lying polders, see Figure 4.2. A dune breach at Monster will result in the highest economic damages at the seaside. This is a result of potential flooding of the large cities The Hague and Rotterdam. The hydrodynamic models are based on a simulation time of 5 days where the damage estimation in VNK2 are based on a flood simulation of two weeks. A conservative calibration factor of 1,2 is applied to compensate for these longer flood simulation time (Ranneft, 2020). Besides the direct economic damages, the indirect economic damages will be taken into account. Indirect damages are the interruption of production and therefore result in a decrease in production capacity. It is assumed that the indirect economic damages are 50 percent of the direct economic damages (Kind, 2011). The total economic damages will be combined with the damages as a result of the loss of life estimation, which are calculated in the next chapter.

Flood scenario	Direct economic damages [million euros]	Indirect economic damages [million euros]	Total economic damages [million euros]
14-1	9.600	4.800	14.300
14-2	5.800	2.900	8.800
14-3	4.100	2.000	6.100
Noordwijk [m sea level rise]			
0,0	1.600	800	2.500
0,5	2.300	1.100	3.400
1,0	3.200	1.600	4.700
1,5	4.300	2.100	6.400
2,0	5.700	2.800	8.500
Kijkduin [m sea level rise]			
0,0	2.600	1.300	3.900
0,5	3.300	1.700	5.000
1,0	4.300	2.200	6.500
1,5	5.700	2.900	8.600
2,0	8.100	4.000	12.200
Monster [m sea level rise]			
0,0	4.000	2.000	6.000
0,5	5.400	2.700	8.100
1,0	7.800	3.900	11.700
1,5	10.200	5.100	15.300
2,0	13.000	6.500	19.500

Table 4.2: Total calculated economic direct damages for each different flood scenario and location.

5. Loss of life estimation

5.1. Input loss of life estimation

The total amount of fatalities and affected persons can be calculated using the method of S. Jonkman (2007), explained in Chapter 2.2. For the loss of life estimation the same LIWO flood scenarios have been used as for the economic damage, see Figure 4.2. Apart from water depths, maps of the flow velocity and rise rate in the flooded area are required. These parameters are also available in the LIWO data based (Rijkswaterstaat, n.d.-a). The maps were created using Arcmap, where maximum values per grid cell were determined for the combined breach locations, see Figure 5.1 and Figure 5.2. The highest velocities and rise rates occur close to the river breach locations with high potential flood depths. The maps of the rise rates have a smaller extent, because of grid cells with negligible rise rates (zero m/hr), are not displayed in these maps.
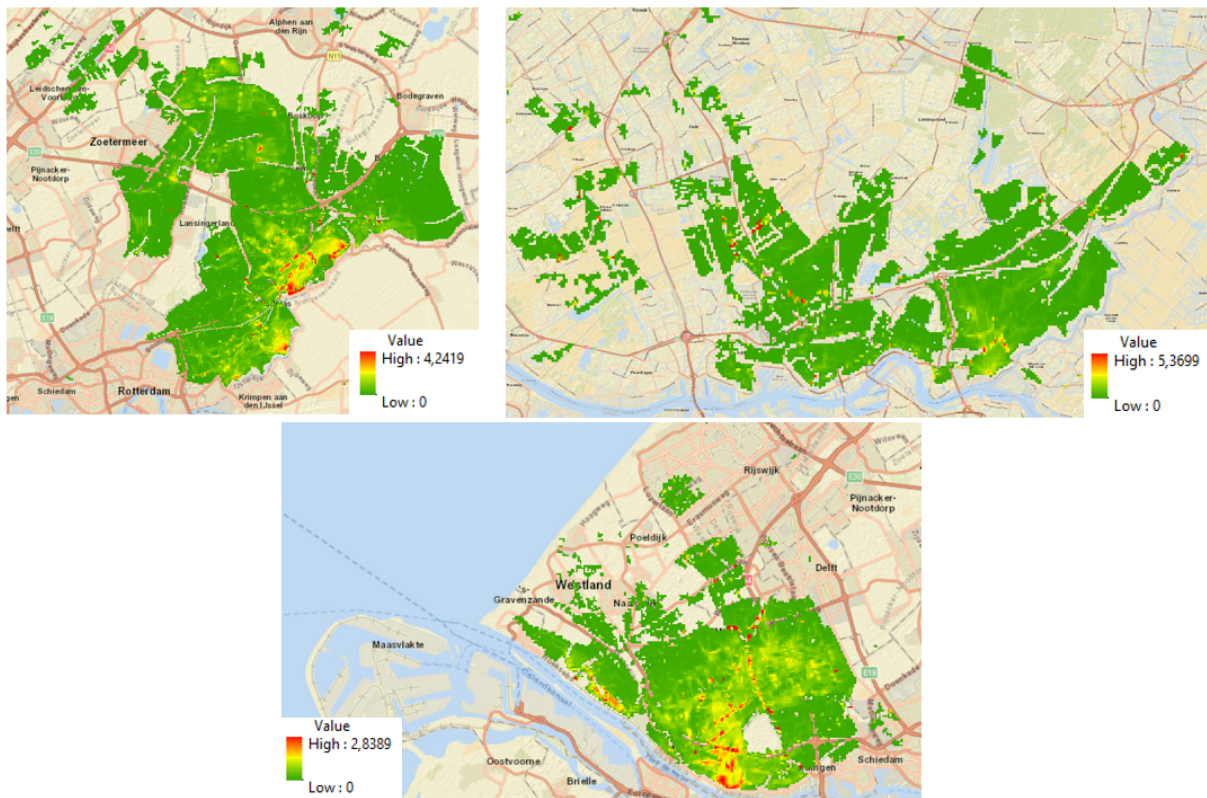
Figure 5.1: Maps with maximum velocities [m/s] per grid cell for the three different trajectories using LIWO data: 14-1 (upper left), 14-2 (upper right) and 14-3 (below).
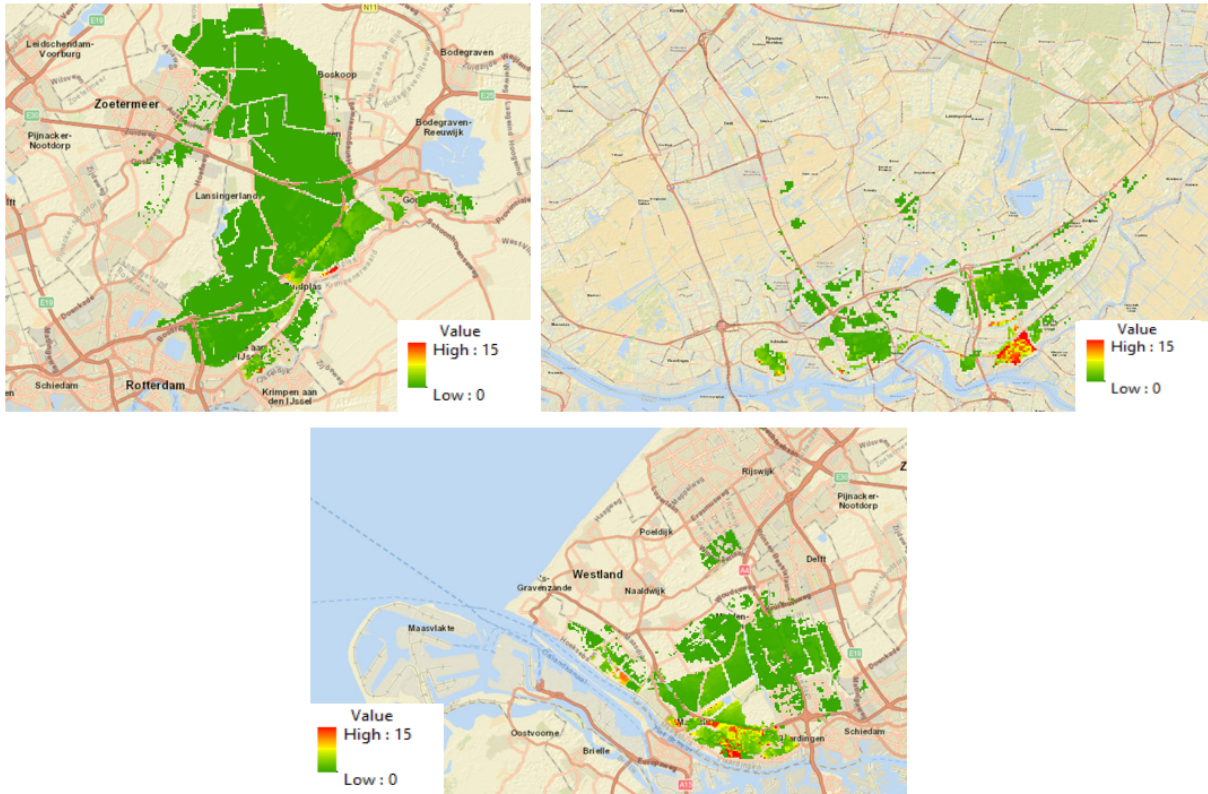
Figure 5.2: Maps with maximum rise rates [m/hr] per grid cell for the three different trajectories using LIWO data: 14-1 (upper left), 14-2 (upper right) and 14-3 (below).

Eventually, these parameters are combined into a mortality rate per grid cell in the areas. This is done using the different log-normal distributions corresponding to three different zones (breach zone, zone with rapidly rising water and the remaining zone) explained in Chapter 2.2. These log-normal distributions and the flood characteristics (maximum flood depth, flow velocity and rise rate) are combined in a in tool in Arcmap designed by Royal HaskoningDHV and with this tool the mortality per grid cell is calculated. For the methodology of the tool, see Figure 5.3. The created mortality maps for the different floods at the riverside are shown in Figure 5.4. From this figure it can be concluded that the highest mortality rates occur in the areas close to the breach locations with high potential flood depths, velocities and rise rates, see Figure 4.2, Figure 5.1 and Figure 5.2. Because the flood characteristics do not change in future scenarios, the mortality per grid cell will be the same in each scenario.
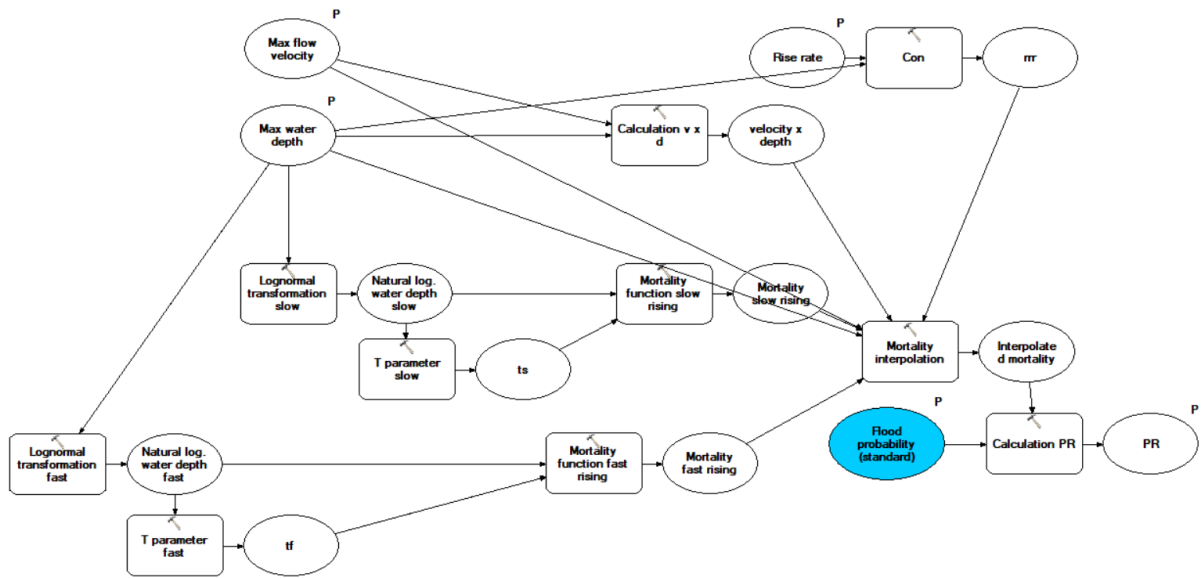
Figure 5.3: Overview of methodology of the tool used to obtain the mortality values per grid cell (designed by Royal HaskoningDHV)
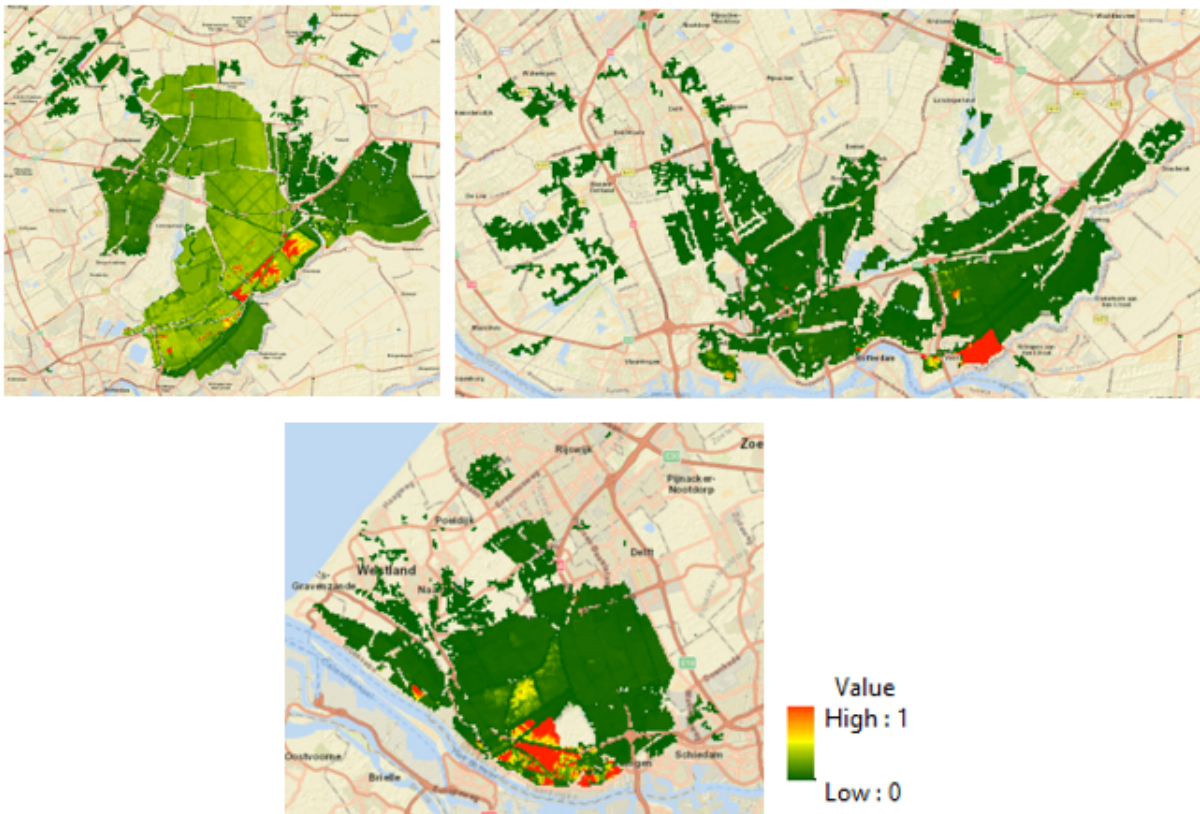
Figure 5.4: Mortality maps created for the trajectories 14-1 to 14-3 with the tool in Arcmap.

Above mortality maps are combined with the probability of failure of the flood defence and the evacuation factor to calculate the potential number of fatalities and affected persons. Affected persons are defined as the the number of people living permanently in the area that has been flooded. No threshold is applied for the depth of the flooding, which means that a person is already a affected if there is a small amount of water. A fatality is defined as a person who dies as a result of the flood.

The number of fatalities and affected persons are determined by combining a population data base and the flood characteristics using ArcMap. For this, the 2020 population data set made available by 'Centraal Bureau van de Statistiek (CBS) is used. The number of fatalities can be determined by taking the sum of all grid cells of the product of the mortality, the number of people living permanently in this area and (1 - evacuation fraction). To arrive at the number of affected persons, the number of fatalities is subtracted from the number of persons living permanently in the flooded area. This is to avoid double counting. Two situations have been considered. A situation in which there is no evacuation and therefore the evacuation fraction is 0, and a lower limit in which an organised evacuation is included. For dikering 14, this evacuation fraction is 0,15. This 15 percent is obtained by multiplying and adding up all evacuation fractions with their corresponding conditional probability, see Table 5.1. This constant evacuation fraction is conservative, because not every area will have the same evacuation fraction. In reality, locations close to the breach will have a much lower evacuation fraction compared to locations where the water arrives much later (couple of days). It is likely that people will not wait for the water to arrive in a few days, but will evacuate as a precaution. However, for this study a constant evacuation fraction is assumed for the entire dikering.

Flood scenario		Evacuation fraction [-]	Conditional probability [-]
Flooding predicted shortly before or unexpectedly	No evacuation	0	0,55
	Organised evacuation	0,23	0,24
Flood predicted well in advance	No evacuation	0,30	0,06
	Organised evacuation	0,50	0,15

Table 5.1: Conditional probabilities of evacuation for dikering 14 (Rijkswaterstaat VNK Project (2012)).

The amount of potential affected persons and fatalities due to the floods at the seaside are determined in the same way explained as above. Instead of using LIWO databases, the hydrodynamic models are used, Appendix D, in which the flood depths and flow velocities can be simulated for every scenario of sea level rise. Unfortunately, the rise rates are not included in this model and therefore some assumptions are made based on the method of the loss of life estimation (S. Jonkman, 2007). Three different zones are estimated: breach zone, zone with rapidly rising water and a remaining zone. A breach zone is estimated close to the breach with the highest velocities and a zone with low rising water is estimated at the last part of the flood. The remaining zone is defined as the zone with high rising water. A rise rate of 2 m/hr, 0.5 m/hr and 0.05 m/hr is assigned to the breach zone, zone with rapidly rising water and low rising water respectively. These values are based on the characteristics of each zone, see Chapter 2.2, where the zone with rapidly rising water has rise rates equal or higher than 0,5 m/hr and the zone with low rising water has rise rates smaller than 0,5 m/hr. The breach zone is not defined by the rise rate, but only by the velocity, higher or equal than 2 m/s and the depth-velocity product, higher or equal than 7 m^2/s. Therefore the breach zone is already defined by the tool in ArcMap without information about the rise rate. In Figure 5.5 is shown how the three different zones are determined. This is done for every flood scenario for the three different breach location at the seaside.
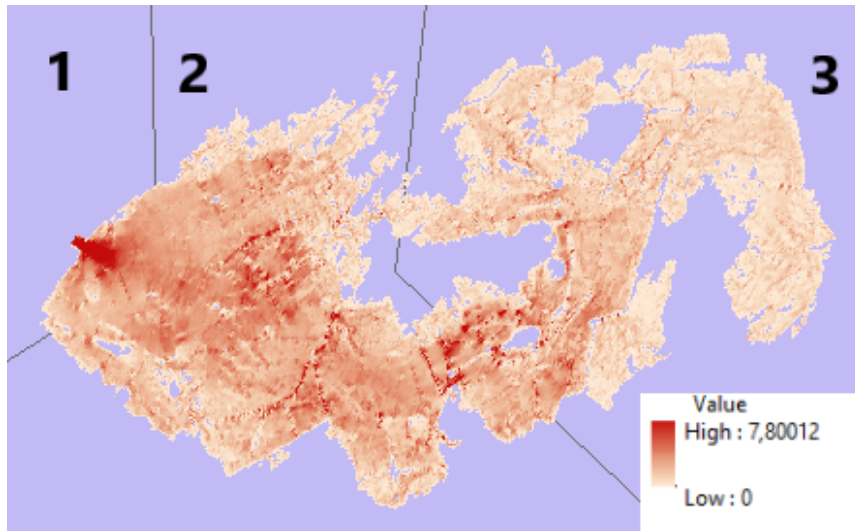
Figure 5.5: Indication of the three zones based on the flow velocities [m/s]. This flood scenario at the location Monster with 2m sea level rise with a recurrence time of 1/10.000 per year.)

5.2. Results

An overview of the total calculated affected persons and fatalities for scenarios with and without evacuation can be found in Table 5.2 for the riverside and Table 5.3. From this tables can be concluded that the threats from flooding due to river dike breaches are higher than for dune breaches. This is because of a higher amount of fatalities is expected when a flood occurs due to a river dike breach. This can be explained that the flood depths as a result of a river flood are higher compared to the flood depths as a result of a dune breach. Besides this, the river floods will result in floodings of populated cities like Rotterdam and Gouda. By far the greatest number of potential fatalities occur as a result of a river dike breach in trajectory 14-2, due to the fact that the major city Rotterdam is flooded. Noordwijk is the location at the seaside with the highest potential fatalities. This is due to the fact that the breach location is exactly at Noordwijk and therefore the breach zone with the highest mortality rates is in Noordwijk as well. For the breach locations Kijkduin and Monster is the breach zone located in a less populated area. The difference between the scenario's with and without evacuation are also shown in Table 5.2 and Table 5.3. For the total damages, determined in next chapter, and the optimisation problems, the scenario with a evacuation fraction of 15 percent is used.

Trajectory	Scenario	Affected persons /victims	Fatalities
14-1	no evacuation	370.816	2.609
	evacuation	371.207	2.218
14-2	no evacuation	424.985	9.260
	evacuation	426.374	7.871
14-3	no evacuation	229.837	4.343
	evacuation	230.488	3.692

Table 5.2: Results loss of life estimation riverside.

Breach location	Scenario	Affected persons /victims	Fatalities
Noordwijk [m sea level rise]	-	-	-
0,0	no evacuation	124.063	1.132
	evacuation	124.233	962
0,5	no evacuation	174.881	1.344
	evacuation	175.083	1.142
1,0	no evacuation	232.183	1.672
	evacuation	232.434	1.421
1,5	no evacuation	274.451	2.094
	evacuation	274.765	1.780
2,0	no evacuation	301.321	2.434
	evacuation	302.686	2.069
Monster [m sea level rise]	-	-	-
0,0	no evacuation	350.940	590
	evacuation	351.029	502
0,5	no evacuation	434.325	815
	evacuation	434.447	693
1,0	no evacuation	546.378	1.217
	evacuation	546.561	1.034
1,5	no evacuation	683.202	1.633
	evacuation	683.447	1.388
2,0	no evacuation	807.886	2.074
	evacuation	808.197	1.763
Kijkduin [m sea level rise]	-	-	-
0,0	no evacuation	289.310	670
	evacuation	289.411	570
0,5	no evacuation	371.520	785
	evacuation	371.638	667
1,0	no evacuation	463.355	1.105
	evacuation	463.521	939
1,5	no evacuation	536.088	1.572
	evacuation	536.321	1.336
2,0	no evacuation	739.622	2.263
	evacuation	739.961	1.924

Table 5.3: Results loss of life estimation seaside.

The results of the loss of life estimation can be compared with underlying calculations of previous research (Slootjes & Wagenaar, 2016). This has been done for the scenario with evacuation, see Table 5.4. For trajectory 14-1, it becomes clear that the difference is a factor 1,8. This is due to the fact that Gouda is flooded in the flood simulation used in this study and not in the other study. Besides this, a population database of 2020 is used in this study instead of a population database of 2011. The greater flood extent and population growth could explain this factor of 1,8. Nowadays, more flood simulations are available in LIWO compared to the year 2011 and therefore the extent of the total floods is greater in this study. The comparison of trajectory 14-3 is not very useful, since few flood scenario's were used in 2011 and therefore the extent of the floods differ very much. For a comparison of the used flood scenario's in this study and in Slootjes & Wagenaar (2016), see Figure 5.6.

Trajectory	This study	Slootjes & Wagenaar, 2016	Factor difference
14-1			
Fatalities	2.218	1.242	1,8
Affected persons	371.207	206.704	1,79
14-2			
Fatalities	7.871	2.926	3,61
Affected persons	426.374	118.143	2,69
14-3			
Fatalities	3.692	511	20,21
Affected persons	230.488	11.404	7,22

Table 5.4: Comparison results loss of life estimation
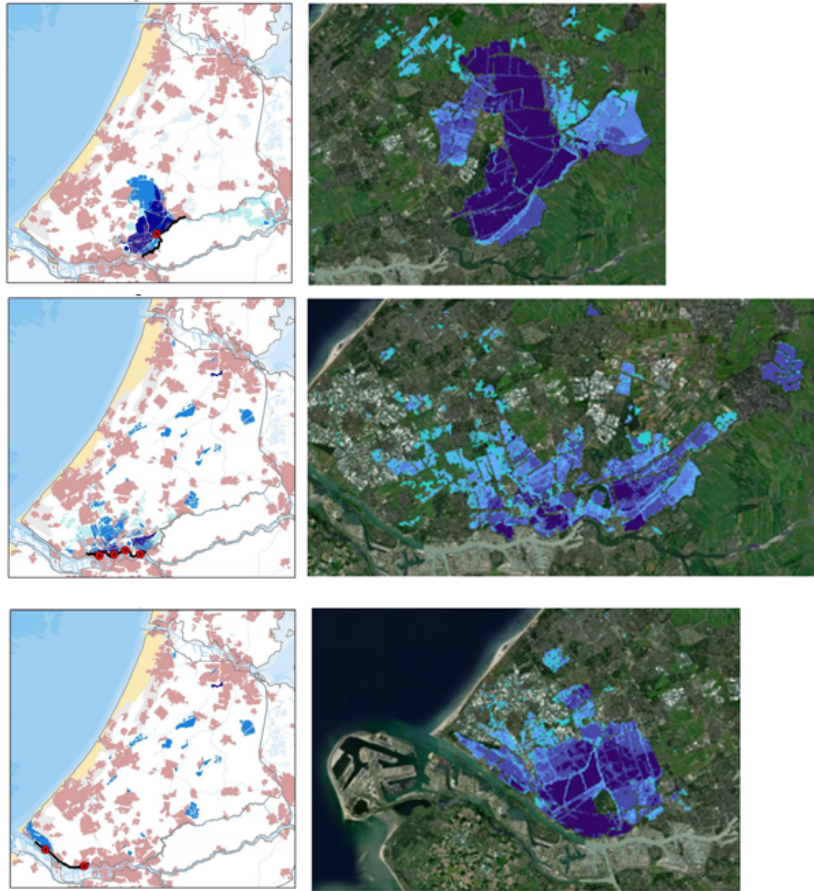
Figure 5.6: Comparison between the flood simulations at the riverside used in this study (right) and Slootjes & Wagenaar (2016) (left).

Besides the amount of affected persons and fatalities, the LIR requirement should also be considered, which is introduced in Chapter 1.2. This means that the loss of life estimation is actually taken into account twice, both in finding the optimum and in meeting a separate requirement. This shows that the loss of life estimation is taken into account very heavily. The LIR for the trajectory 14-1 for the different sea level rise scenarios is shown in Figure 5.7. For all trajectories an evacuation factor of 15 percent is included. Because the distinction between the maps with and without evacuation cannot be seen, only the LIR requirement in case of organised evacuation is shown here. The LIR requirement is 1/100.000 (10e-6) per year and therefore the orange and red cells do not meet the requirement. The maps show that the LIR is increasing with each step of sea level rise. The LIR is the highest for the around around trajectory 14-1, because the probabilities of failure of the river dikes are the highest for this trajectory. Chapter 8 examines whether the LIR requirement is met after the economic optimisation has been carried out.
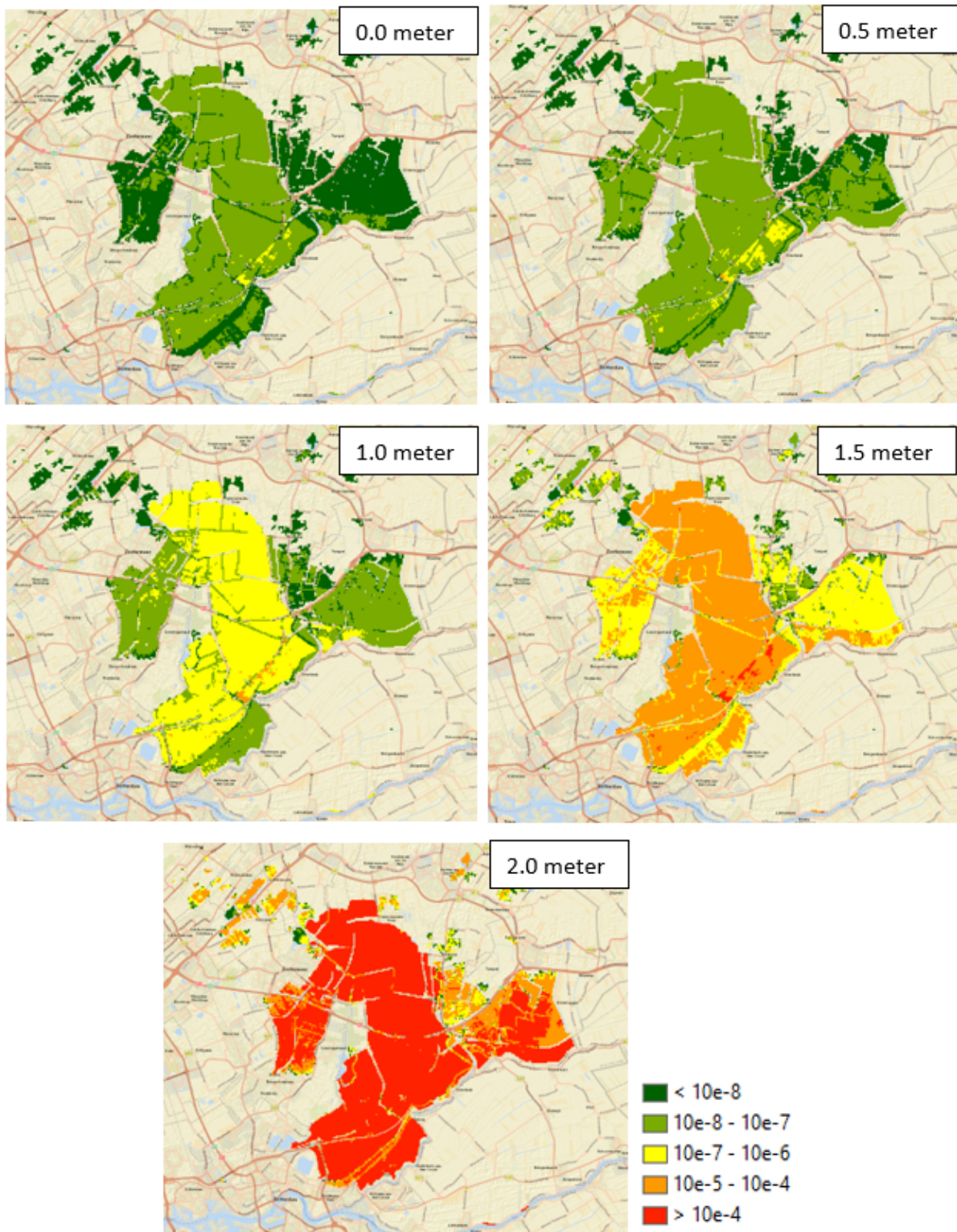
Figure 5.7: Overview of the Local Individual Risk (LIR) per year for all scenarios for trajectory 14-1.
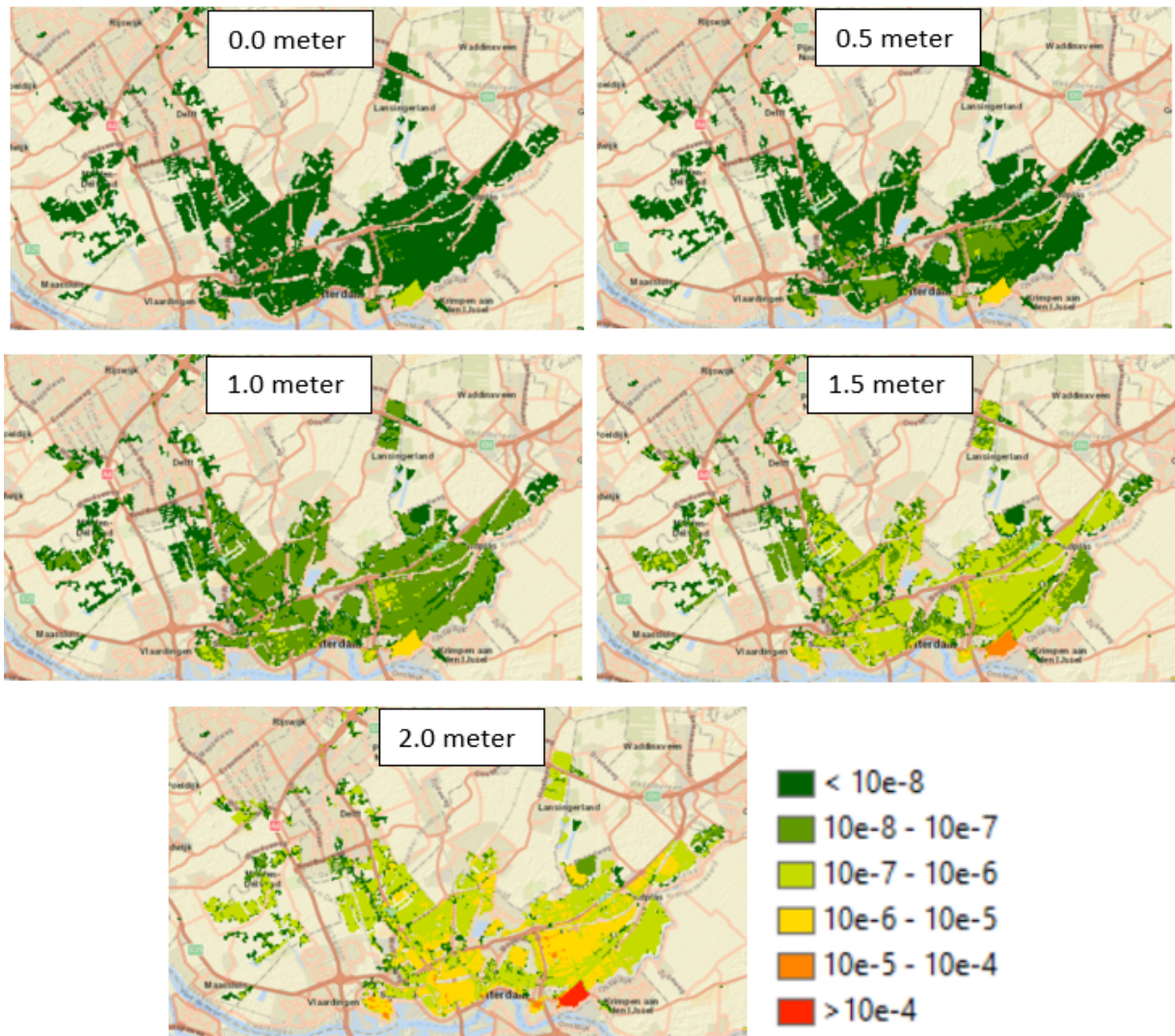
Figure 5.8: Overview of the Local Individual Risk (LIR) per year for all scenarios for trajectory 14-2.
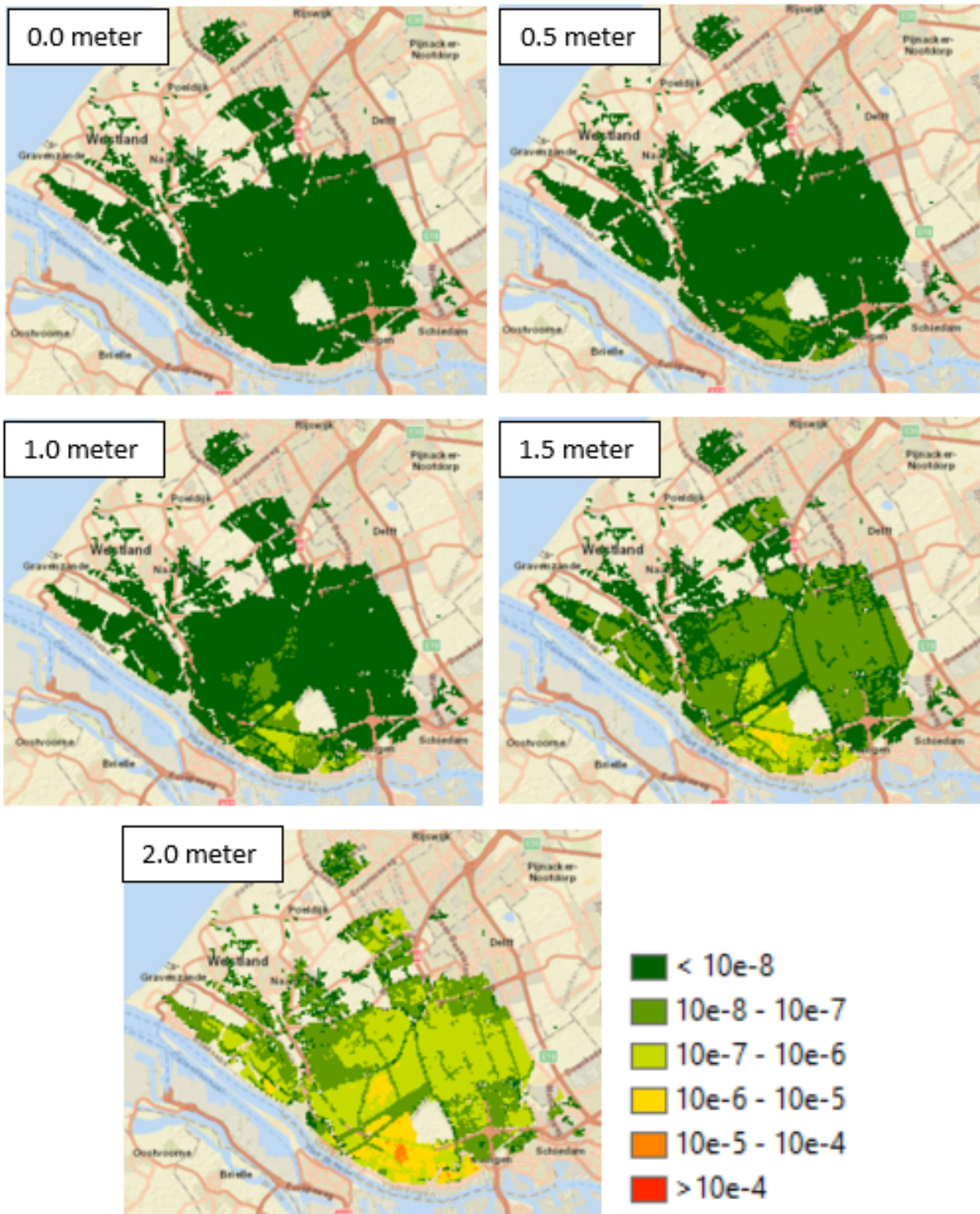
Figure 5.9: Overview of the Local Individual Risk (LIR) per year for all scenarios for trajectory 14-3.

6. Total damages

The last step of the analysis before starting with determination of the costs of reinforcement projects used in the optimisation problem is to combine the results from the loss of life estimation and economic damages. Here, monetary values are assigned to an affected person and a fatality according to Rijkswaterstaat VNK Project (2012). The calculations are based on 12.000 euros per affected person and 6,7 million euros per fatality. The total economic damages are shown in detail for the riverside in Table 6.1 for the riverside. From this table it can be concluded that the trajectory 14-2 has the highest potential damages. This is mainly due to the fact that there are many potential fatalities in case of a dike breach along trajectory 14-2. Because this trajectory has the most potential damage, it is also why the safety standards for this trajectory are the most strict, Figure 1.5. It becomes clear that the largest part of the total possible damage is caused by the results of the loss of life estimation with a contribution between 57 and 87 percent. The contribution of the damages resulting from the loss of life estimation on the total damage from previous studies (Slootjes & Wagenaar, 2016) was also the highest with 65 and 69 percent for the trajectories 14-2 and 14-3 respectively. The contribution for the 14-1 trajectory was a lot smaller, 31 percent. The results in Table 6.1 show a higher contribution of the loss of life estimation on the total damages. The difference is because more available and more recent flood simulations from the LIWO database have been used as input for the loss of life estimation and more recent population statistics from the year 2020 have been used to determine the number of affected persons and fatalities.

Parameter	14-1	14-2	14-3
Direct economic damages [million euros]	9.600	5.800	4.100
Indirect economic damages [million euros]	4.800	2.900	2.000
Total economic damages [million euros]	14.300	8.800	6.100
Affected persons	371.207	426.374	230.488
Price [euros]	12.000	12.000	12.000
Fatalities	2.218	7.871	3.692
Price [million euros]	6,7	6,7	6,7
Damages loss of life estimation [million euros]	19.300	57.800	27.500
Total damages [million euros]	**33.700**	**66.600**	**33.600**
Relative contribution loss of life estimation to total damages[%]	57,4	86,9	81,8

Table 6.1: Total damages for the trajectories 14-1 to 14-3 determined by combining the economic damages and the damages from the loss of life estimation. In these results, organised evacuation is included.

Breach location	Total economic damages [million euros]	Damages loss of life estimation [million euros]	Total damages [million euros]	Relative contribution loss of life estimation to total damages [%]
Noordwijk [m sea level rise]				
0,0	2.500	7.900	**10.400**	76,0
0,5	3.400	9.800	**13.200**	74,2
1,0	4.700	12.300	**17.000**	72,4
1,5	6.400	15.200	**21.700**	70,0
2,0	8.500	17.500	**26.000**	67,3
Monster [m sea level rise]				
0,0	6.100	7.600	**13.600**	55,9
0,5	8.100	9.900	**18.000**	55,0
1,0	11.700	13.500	**25.100**	53,8
1,5	15.300	17.500	**32.800**	53,3
2,0	19.500	21.500	**41.000**	52,4
Kijkduin [m sea level rise]				
0,0	3.900	7.300	**11.200**	65,2
0,5	5.000	8.900	**14.000**	63,6
1,0	6.500	11.900	**18.300**	65,0
1,5	8.600	15.400	**24.000**	64,2
2,0	12.200	21.800	**33.900**	64,3

Table 6.2: Total damages for the seaside determined by combining the economic damages and the damages from the loss of life estimation. In these results, organised evacuation is included.

Finally, the above mentioned damages can also be visualised with Arcmap, which is done for the riverside. The damages from the loss of life estimation per grid cell of 1 ha (100x100m) are added to the economic damages per grid cell. These visualisations can be seen in Figure 6.1 to Figure 6.3. These figures show that the highest expected damage occurs in cities with many people and many buildings. For trajectory 14-1, it is clear that Gouda, a part of Rotterdam and Zoetermeer are the high risk areas. For trajectory 14-2, this is entire city of Rotterdam and Schiedam, and for trajectory 14-3, this is Vlaardingen and Maassluis.
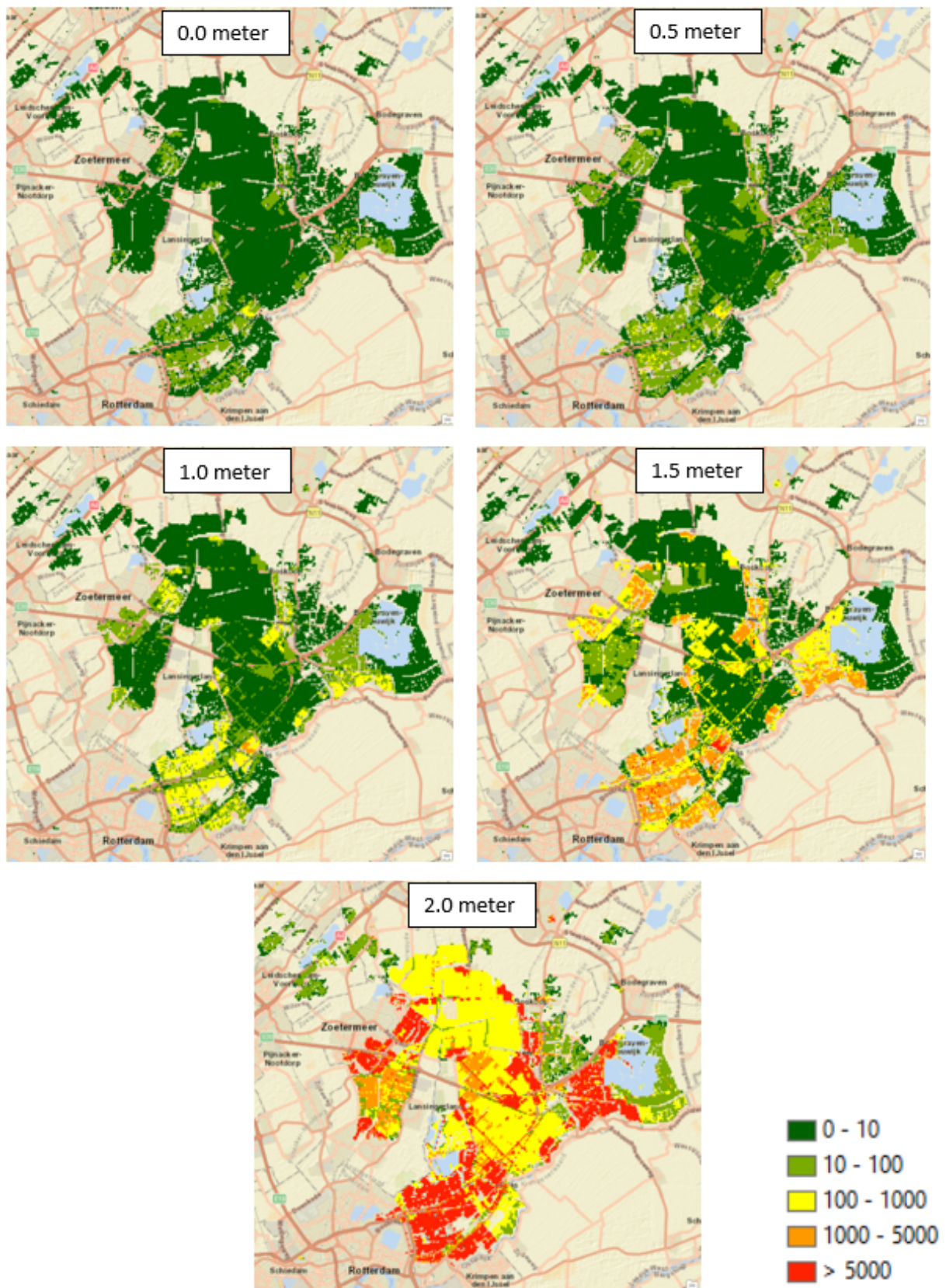
Figure 6.1: Total expected damages for trajectory 14-1 for the 5 different scenarios (0 - 2m sea level rise) per ha [EUR/ha/year].
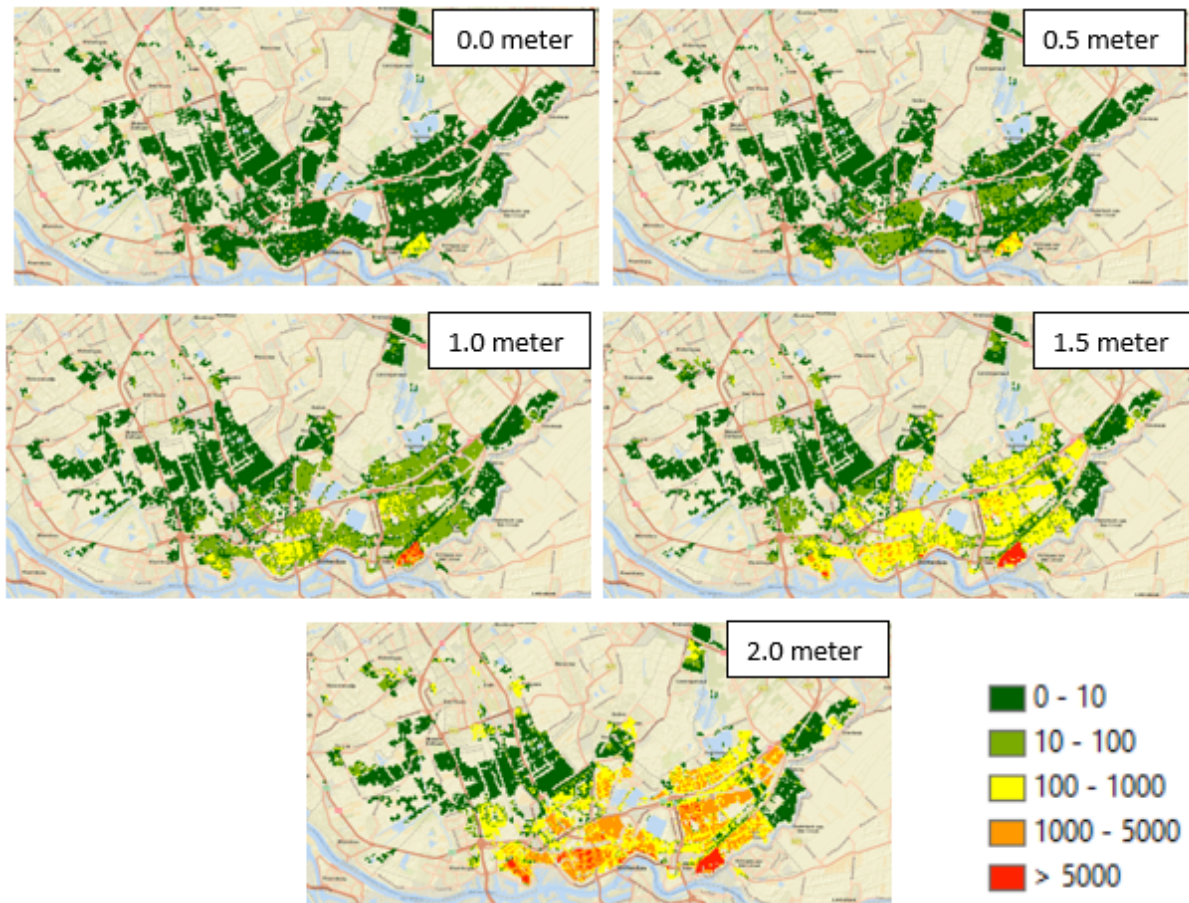
Figure 6.2: Total expected damages for trajectory 14-2 for the 5 different scenarios (0 - 2m sea level rise) per ha [EUR/ha/year].
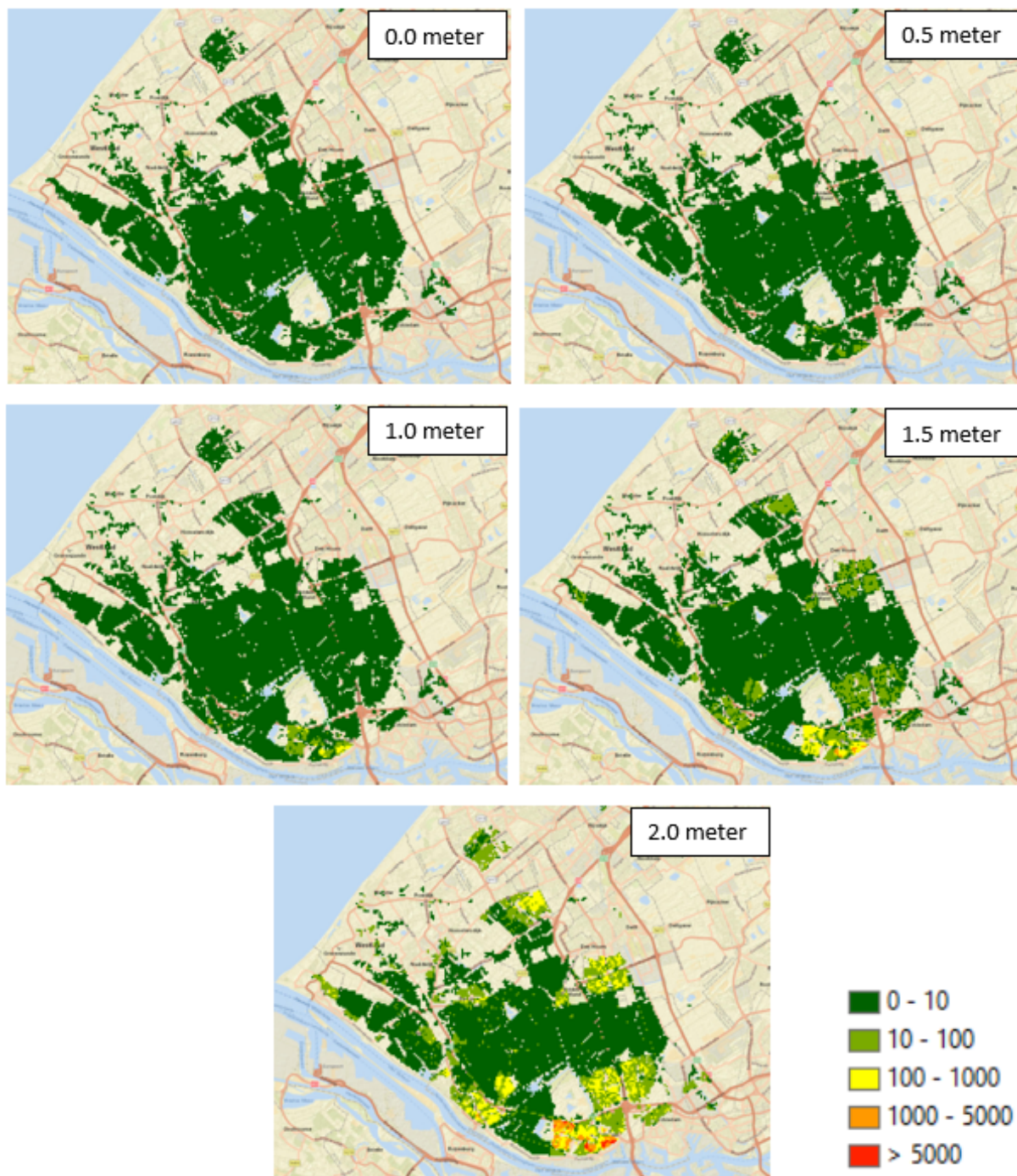
Figure 6.3: Total expected damages for trajectory 14-3 for the 5 different scenarios (0 - 2m sea level rise) per ha [EUR/ha/year].

7. Costs of reinforcements

In this chapter, an estimate will be made for various reinforcement projects for the river dikes and the dunes. The KOSWAT programme will be used for the river dikes and an estimate will be made for the extra volume of sand required for the dunes to reach different safety levels. For a background on the KOSWAT program, see Chapter 2.4.

7.1. Costs river dike reinforcements

For the river side, 8 different river dike profiles were assessed in Chapter 3, see Appendix A.2 for an overview of all cross sections. First, it has to be determined which profile is normative for which length along a trajectory. Trajectory 14-1, 14-2 and 14-3 are divided into 2, 4 and 2 lengths respectively, corresponding to the amount of assessed profiles in a trajectory. An overview of this division, which is included in KOSWAT, is shown in Figure 7.1, Figure 7.2 and Figure 7.3.
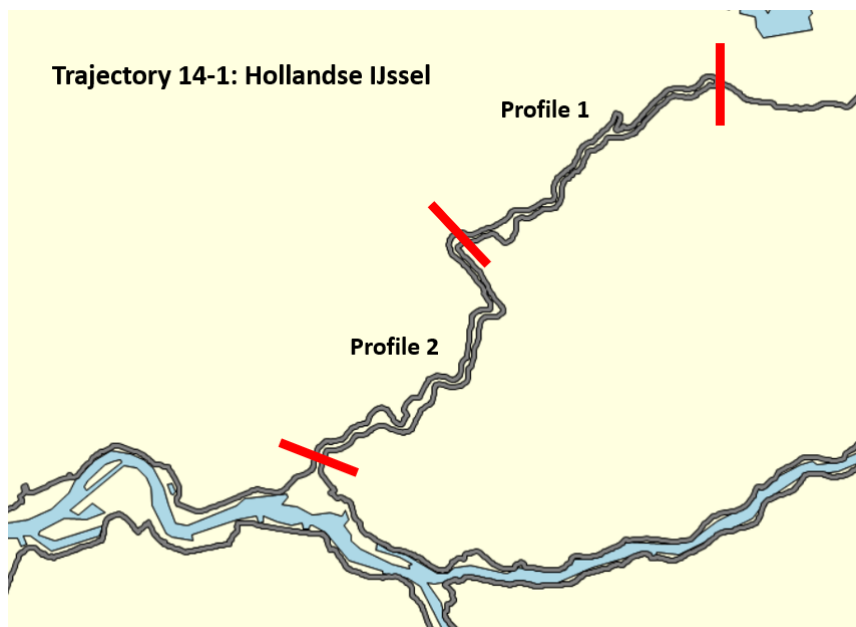
Figure 7.1: Overview of which profile is normative for which part of trajectory 14-1.
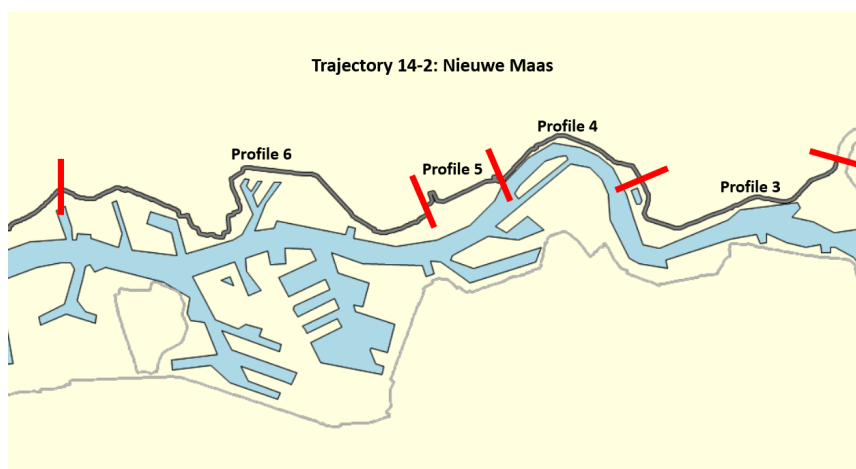
Figure 7.2: Overview of which profile is normative for which part of trajectory 14-2.
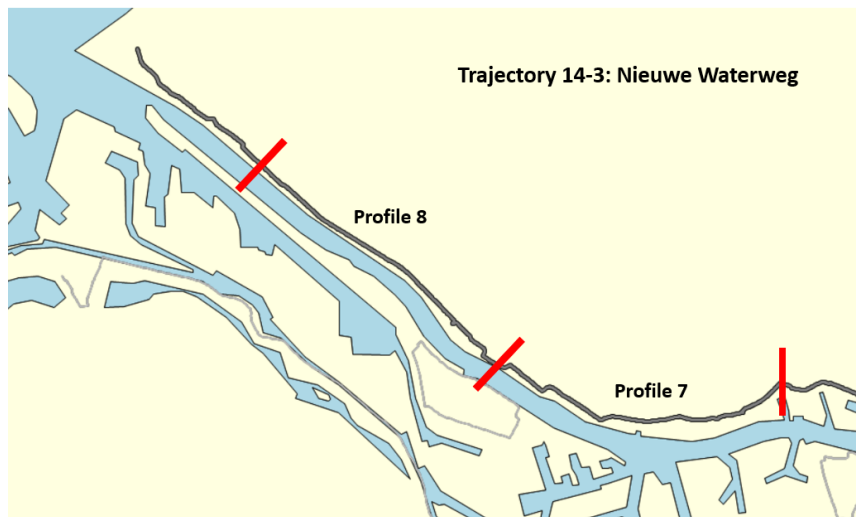
Figure 7.3: Overview of which profile is normative for which part of trajectory 14-3.

The profiles from Appendix A.2 are used as input for the KOSWAT program. Because this study only assesses failure due to a height deficit, the crest height is important. For each profile, an analysis of the necessary costs versus the increase in crest level is made. Unit prices and various reinforcement measures were used, which are based on the presence of buildings, (rail)roads and large water bodies. The locations of these objects are known in the KOSWAT programme. The costs determined by KOSWAT are the total project costs instead of the direct construction costs. For a more detailed explained about the methodology used in KOSWAT and an overview of the different reinforcement measures, see Chapter 2.4.

The costs in KOSWAT use a price level based on prices from 2016. As a result, this price level have to be converted to today's price level. This is done by means of the Consumer Price Index (CPI) which serves as the main inflation indicator in most countries (Inflation.eu, n.d.). The annual inflation rate for the Netherlands is used in this study, which is compared to the previous year in December each year. By multiplying the different inflation rates, a 7,1 percent price increase has to be included compared to the costs determined in KOSWAT to determine the today's costs.

The total project costs for different crest levels are shown in Figure 7.4, Figure 7.5 and Figure 7.6. From these figures, it can be concluded that the project costs are mainly determined by the start and the execution of the reinforcement project. The difference between increase in crest level of 20 centimetres and 1.4 metres is relatively small, 107,1 million versus 120 million. For all profiles, the initial costs are relatively high and the incremental costs for additional dike heightening are relatively low. In addition, it can be seen that, for example, raising the river dike, profile 3, is much cheaper than raising the Maasboulevard, profile 4, see Figure 7.5. Raising the Maasboulevard (profile 4) between 0,20m and 1,4m will cost between 38.000 EUR/m and 42.000 EUR/m. Raising profile 3 between 0,24m and 1,34m will cost between 6500 EUR/m and 14.000 EUR/m. This indicates that it was a good choice to divide the trajectories into parts instead of taking one profile as normative for the entire trajectory, which would have resulted in a serious underestimation or overestimation of the total project costs. The range of the costs for the different reinforcements for profile 5 is between the 36.000 EUR/m and 39.000 EUR/m and for profile 6 between the 29.000 EUR/m and 34.000 EUR/m. Raising the river dikes along the Hollandse IJssel and Nieuwe Waterweg is cheaper. Raising the river dikes along the Hollandse IJssel cost between 8000 and 22.000 EUR/m depending on the profile and the increase in crest level. Raising the river dikes upstream in the Hollandse IJssel is cheaper than downstream. For the Nieuwe Waterweg the costs are between 10.000 and 27.000 EUR/m depending on the increase in crest level. An overview of some cross-sections of reinforcement projects are included in Appendix E. The calculated costs will be used for economic optimisation in the Chapter 8.
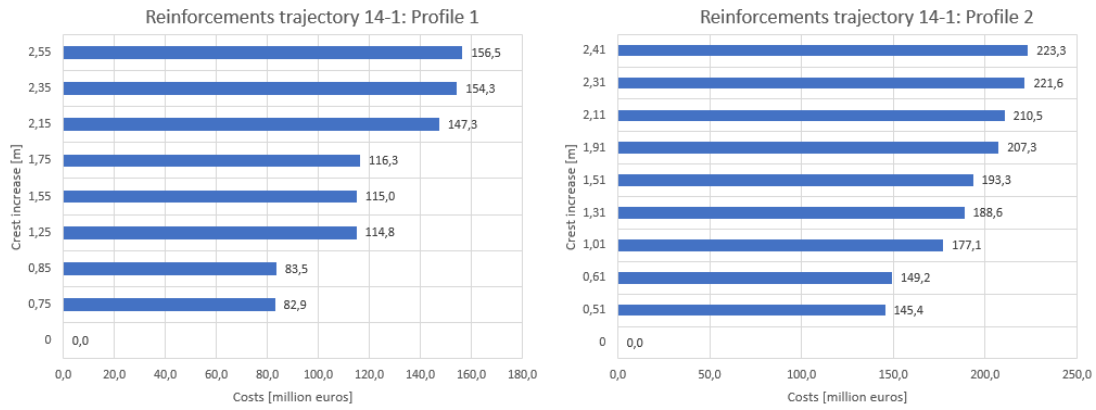
Figure 7.4: Overview of the costs of different reinforcement projects for trajectory 14-1.
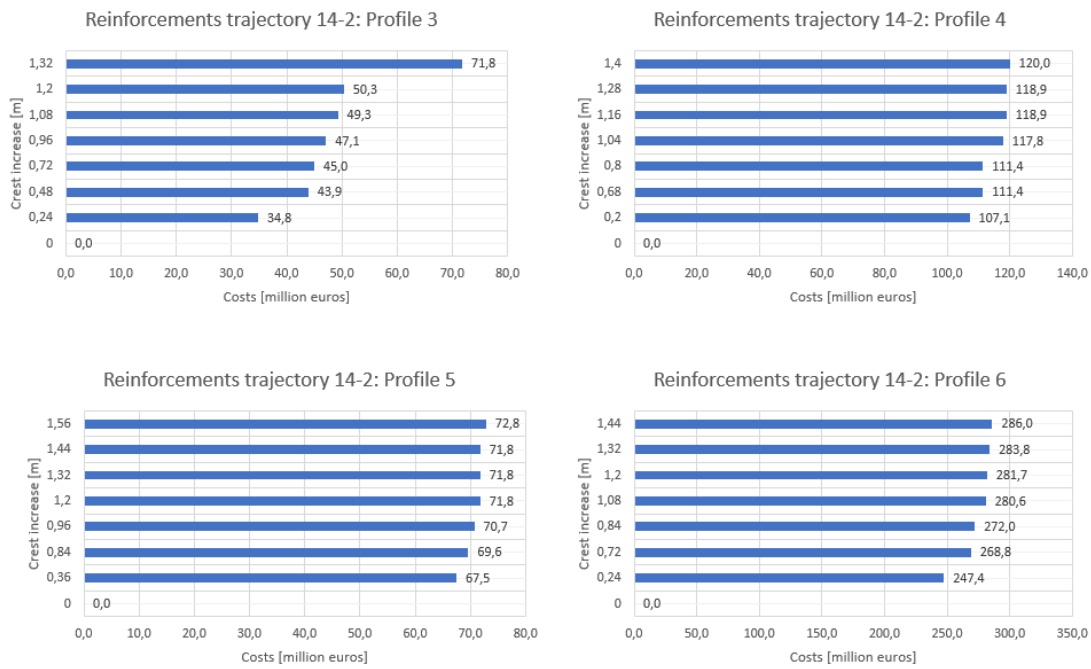
Figure 7.5: Overview of the costs of different reinforcement projects for trajectory 14-2.
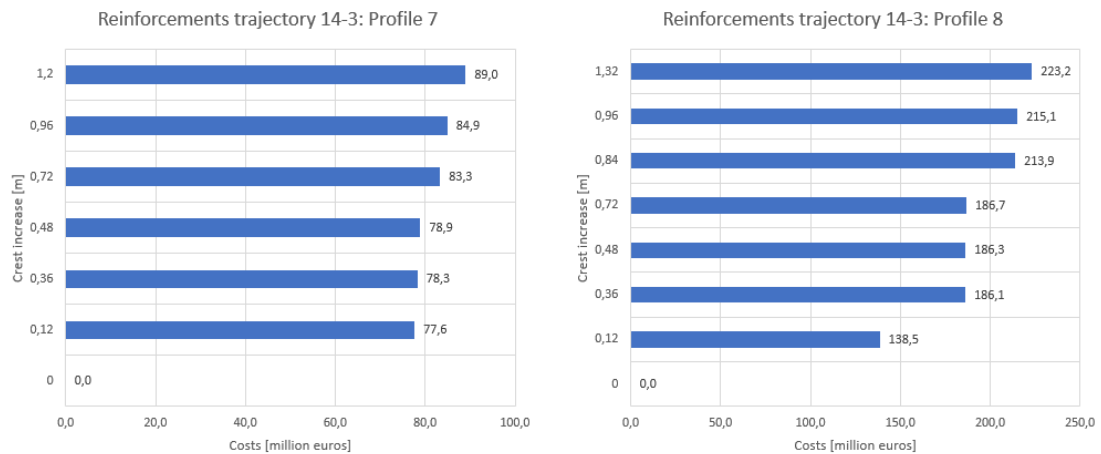
Figure 7.6: Overview of the costs of different reinforcement projects for trajectory 14-3.

Now that the costs for various reinforcement projects are known, the next step is to see how these projects can be combined to achieve a higher safety level expressed in a lower probability of failure. The probability of failure of a trajectory is determined by the highest probability of failure of a profile in a trajectory. For example, from the results in Table 3.3, it can be concluded that profile 1 is normative for the probabilities of failure of trajectory 14-1 in the original situation. This profile will therefore have to be reinforced first in order to reduce the probability of failure for the entire trajectory 14-1. Once this profile has been reinforced/increased in height, it will be determined which profile is normative in the new reinforced situation. This is done for each trajectory for all scenarios of sea level rise. The new height of the reinforced profiles result in a lower probability of failure determined with the relationship explained in Figure 3.12 to Figure 3.14. In this way, it is possible to determine which total project costs correspond to which safety level. The results of this analysis for trajectory 14-1 are shown in Table 7.1 for the scenario with 2m sea level rise. In this table it can be seen that profile 1 is normative for trajectory 14-1 until the crest level is increased by 0,75 m. In that new situation profile 2 is normative and the next step is to increase that height by 0,51 m. The total costs corresponding to probabilities of failure for the other scenarios and trajectories are in Appendix E.2.

Increasing crest height[m]		Consequences	
Profile 1	Profile 2	Costs [million euros]	Probability of failure [1/... year]
0	0	0	170
0,75	0	82,9	1.600
0,75	0,51	228,3	3.100
0,85	0,51	228,9	3.600
1,25	0,51	260,2	11.000
1,25	0,61	264,1	17.000
1,25	1,01	291,9	22.000
1,55	1,01	292,1	70.000
1,75	1,01	293,4	79.000
1,75	1,31	304,8	150.000
2,15	1,31	335,9	250.000
2,15	1,51	340,6	550.000
2,15	1,91	354,6	720.000
2,35	1,91	361,6	1.600.000
2,55	1,91	363,8	2.600.000
2,55	2,11	367,0	3.400.000

Table 7.1: Total costs, inflation included, corresponding to different probability of failures for trajectory 14-1 in case of the scenario with 2m sea level rise.

7.2. Costs dune reinforcements

As explained in Chapter 2.4, the volumes of sand required to reach different safety levels will be considered to determine the costs of dune reinforcements. The volumes of sand and the price per m^3 of sand will be used to determine the costs of the reinforcement projects. The price per m^3 of sand used for beach nourishment is 7,5 EUR per m^3 and this price, which dates from 2009 (S. N. Jonkman et al., 2013), has been converted to today's price level using the Consumer Price Index (Inflation.eu, n.d.). If this annual CPI is converted, it appears that a price increase of 21 percent must be included. Therefore, the price per m^3 of sand used in this study is 9 Euros.

As with the riverside, the coast will again be divided into sections for which a particular dune profile is normative, see Figure 7.7. This is done with the lengths of the trajectories according to Slootjes & Wagenaar (2016). Only the lengths of dunes are included in the cost calculation. Hard flood defences along the coast, such as the underground dike in the dunes at Katwijk (Berkers, 2016) and the boulevard at Scheveningen, are not included in these lengths. These hard flood defences are considered safe under all scenarios and are therefore not relevant for determining the costs in the economic optimisation in Chapter 8. In addition, the dune breaches of Monster, Kijkduin and Noordwijk will all be treated independently. In reality there will be a degree of dependency between the dune breaches as the sea water levels are approximately equal for all three breach locations. From Figure 7.7 it is clear that the hydrodynamic flood simulation at Noordwijk, see Figure D.2, corresponds to the greatest length of dunes, followed by Kijkduin and Monster, which can are shown in Figure D.1 and Figure 4.4 respectively. The profile from

Figure C.1 is normative for the north of the coast, Noordwijk, and the reinforced profile from Figure 3.21 for the south of the coast.
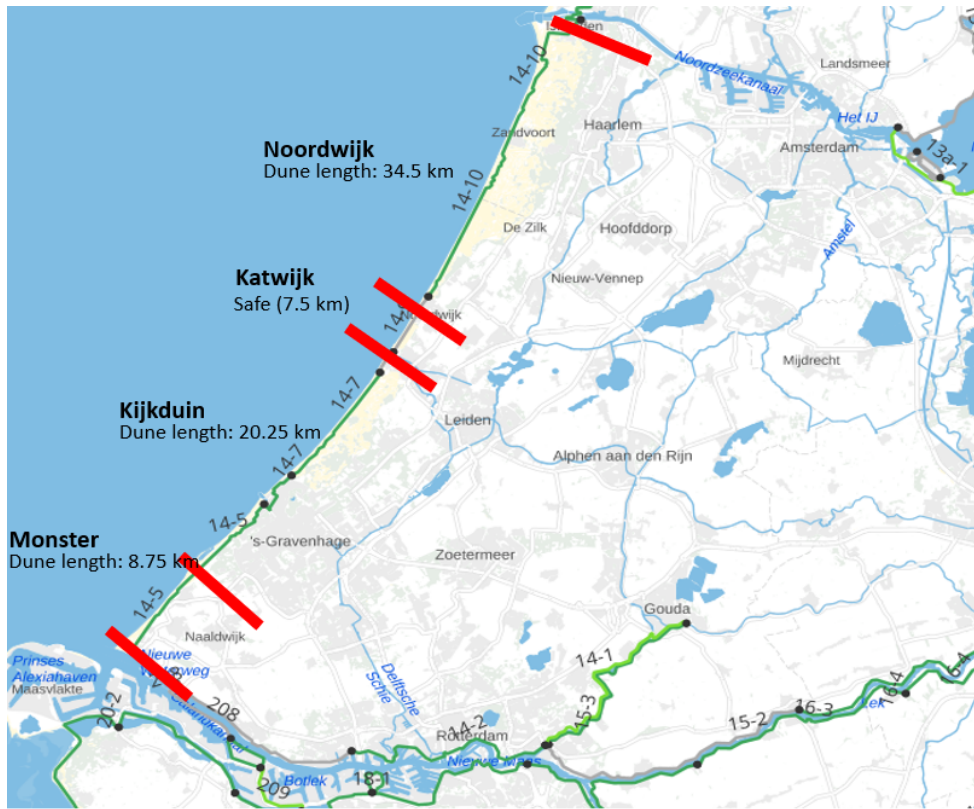
Figure 7.7: Overview of division of the coast. The profile at Noordwijk and Ter Heijde are normative for the north and the south of the coast respectively.

Now that the lengths over which a particular profile has to be reinforced are known, the actual reinforcement of the profiles can be examined. These is done by adding sand volume to the original profiles. From the construction method, it is more realistic to reinforce the dune on the seaside, which will also be assumed in this study. In addition, there is a greater impact on the landscape if the dune is reinforced on the landward side. Three different reinforced profiles are considered in which 150 m^3/m, 400 m^3/m and 750 m^3/m sand are added to the original dune profile, see Figure 7.8.
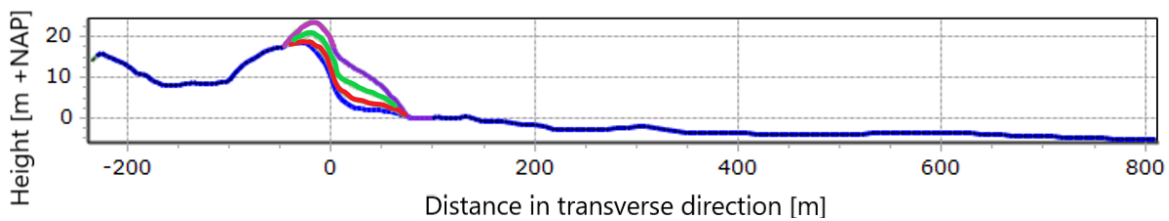
Figure 7.8: Different volumes added to the original profile of Noordwijk (blue): 150 m^3/m (red), 400 m^3/m (green) and 750 m^3/m (purple).

These quantities of sand are multiplied by the costs per m^2 of 9 Euros and the length over which the dune profile of Noordwijk is normative, 34,5 kilometres. The costs of 9 EUR per m^2 for beach nourishment are relatively high compared to shore nourishment. With shore nourishment, the sand is applied more seaward instead of on the dune profile itself. As a result the placed volumes of sand form a reinforced dune profile in a natural way instead of actually placing the sand on the dune itself. The costs of shore nourishment are lower, in the order of 3 - 6 EUR per m^2 (S. N. Jonkman et al., 2013).

In this way, the total costs can be determined for the three different reinforcement projects. For the new reinforced profiles the probabilities of failure are determined using the method explained in Chapter 3.7.1

which looks at the sea water levels at which the dune profile is no longer able to fit a boundary profile. This is done using the program Morphan. The recurrence times of the corresponding sea levels are then determined using Hydra-NL, as explained in Chapter 3.7.1. The results are shown in Table 7.2, which are used for the economic optimisation in Chpater 8. For an overview of the costs corresponding to the probability of failure for all scenarios, see Appendix E.3.

Volume reinforcement [m^3/m]	Costs [million euros]	Sea water level dune breach [m+NAP]	Probability of failure [1/... year]
0	0	7,38	10.000
150	47,0	7,63	19.000
400	125,3	7,88	34.000
750	234,9	8,38	120.000

Table 7.2: Total costs, inflation included, corresponding to different probability of failures for the Noordwijk profile in case of the scenario with 2m sea level rise.

At the time of writing the MorphAn program is not able to make calculations of the dune profile that would be normative for a flood caused by a dune breach at Monster and Kijkduin. The probabilities of failure for the profiles normative for Monster, Kijkduin and Noordwijk are approximately equal for the scenarios with sea level rise of 1 to 2 metres, see Table 3.7 and Table 3.9. The scenarios with 1,5 and 2 m sea level rise are those for which it is expected that dune reinforcements may be necessary. Since it is not possible to calculate with the dune profile which is normative for the south of the coast and since these probabilities of failure are almost equal to those of Noordwijk, it is assumed in this study that the same amounts of sand per m^3/m are needed for a similar safety level in a reinforced situation. For a more detailed explanation of the error in MorphAn, see Chapter 3.7.2. An overview of the costs corresponding to the probability of failure for the locations Monster and Kijkduin is given in Appendix E.3. The probabilities of failure for the reinforced situations are the same, but the costs are lower compared to Noordwijk. This is because the length of the coasts corresponding to the hydrodynamic models are shorter than the length of the hydrodynamic model of Noordwijk, see Figure 7.7.

Finally, a comparison will be made with the costs used in the previous thesis (Ranneft, 2020). These costs were based on cost estimates from 2016 (Slootjes & Wagenaar, 2016). Therefore, these costs have been converted to today's price level by means of the Consumer Price Index (Inflation.eu, n.d.). The calculated costs in this study are higher than Slootjes & Wagenaar (2016). The costs per km calculated in this study is based on a decrease of the probability of failure of a factor 12 for Noordwijk, see Table 7.2, and a factor of 13,3 for Kijkduin and Monster. This is the result of an addition of 750 m^3/m sand to the profile. For this study, one profile was used to determine the costs for the entire coast, which may lead to an overestimation of the costs. Further research into the costs of dune reinforcements would be useful to obtain a better estimate of the costs.

Location	Costs (Slootjes & Wagenaar, 2016) [million euros per km]	Calculated costs [million euros per km]
Noordwijk	4,6	6,81
Kijkduin	4,3	6,81
Monster	2,57	6,81

Table 7.3: Comparison costs increasing safety level. The costs per km used in Slootjes & Wagenaar (2016) are based on a decrease of probability of failure with a factor 10.

8. Economic optimisation

8.1. Economic optima

The final step of this research is to find the economic optima for the different scenarios. This is done by combining the total costs, determined in Chapter 6, with the costs for different reinforcement projects, determined in Chapter 7, in an optimisation problem. For the total damages, both the discount rate and the growth rate are taken into account. The growth rate takes into account that the potential flood area will represent more value in the future and therefore the potential damages will increase in the future. By including the discount rate, the devaluation of money in the future is taken into account. The total risk will be determined according to Equation 2.23. In addition, this risk depends on the probability of occurrence: the probability of failure of a certain trajectory or length of coast. In Chapter 7, for different probabilities of failure, the corresponding reinforcements costs have been calculated. By varying the probability of failure, a economically optimal safely level can be determined in the optimisation problems. This economically optimal safety level is the probability of failure that corresponds to the minimum of the total costs. The total costs are calculated by adding the costs necessary for a reinforcement project and its corresponding risk. This will be done for all scenarios for the seaside and riverside. In Figure 8.1 the results of the optimisation for trajectory 14-1 can be seen. It can be seen that the risk curve moves further to the top left for each sea level rise scenario. This indicates that the risk is increasing in the future. It can be concluded that the the economic optima for the scenarios of 0,5 and 1m sea level rise lies on the probability of failure corresponding to the original situation. Both original failure probabilities are above the threshold/lower limit and therefore it can be concluded that from these analysis, reinforcements are not necessary and economically efficient. From the scenario with 1,5 m and 2 m sea level rise, it becomes economically efficient to reinforce. Both original probabilities of failure are below the lower limit. Therefore, reinforcements are necessary to meet the safety requirement. The both economic optima are above the threshold and therefore these safety levels are recommended. The method of Figure 8.1 is used for every dune breach location and trajectory. The economic optimisations for trajectory 14-2 and 14-3 are shown in Appendix F.1.

The economic optimisation of the dune breach location Kijkduin is shown in Figure 8.2. For the scenario of 2m sea level rise the economic optimum of the probability of failure is 1/19.000 per year with a corresponding investment for reinforcement of 27,6 million euros. For the scenario of 1,5m sea level rise it is not economically efficient to reinforce, because the economic optimum is at the original probability of failure, 1/30.000 per year. Because this safety level is above the threshold of 1/10.000 per year for this breach location, reinforcements are not necessary. It became clear that for the scenarios with 0,5 and 1 m sea level rise, it is not economically efficient to reinforce for the seaside. This is due to the low calculated probabilities of failure for the dunes for these scenarios. The economic optimisation of the breach locations Noordwijk and Monster are in Appendix F.1.

In Table 8.1 and Table 8.2 the results are shown for the economic optimisations with the corresponding costs for necessary reinforcements and risk. For all locations it was not economically efficient to reinforce for the scenarios with 0,5 and 1m sea level rise and therefore it is assumed that reinforcements are not necessary.
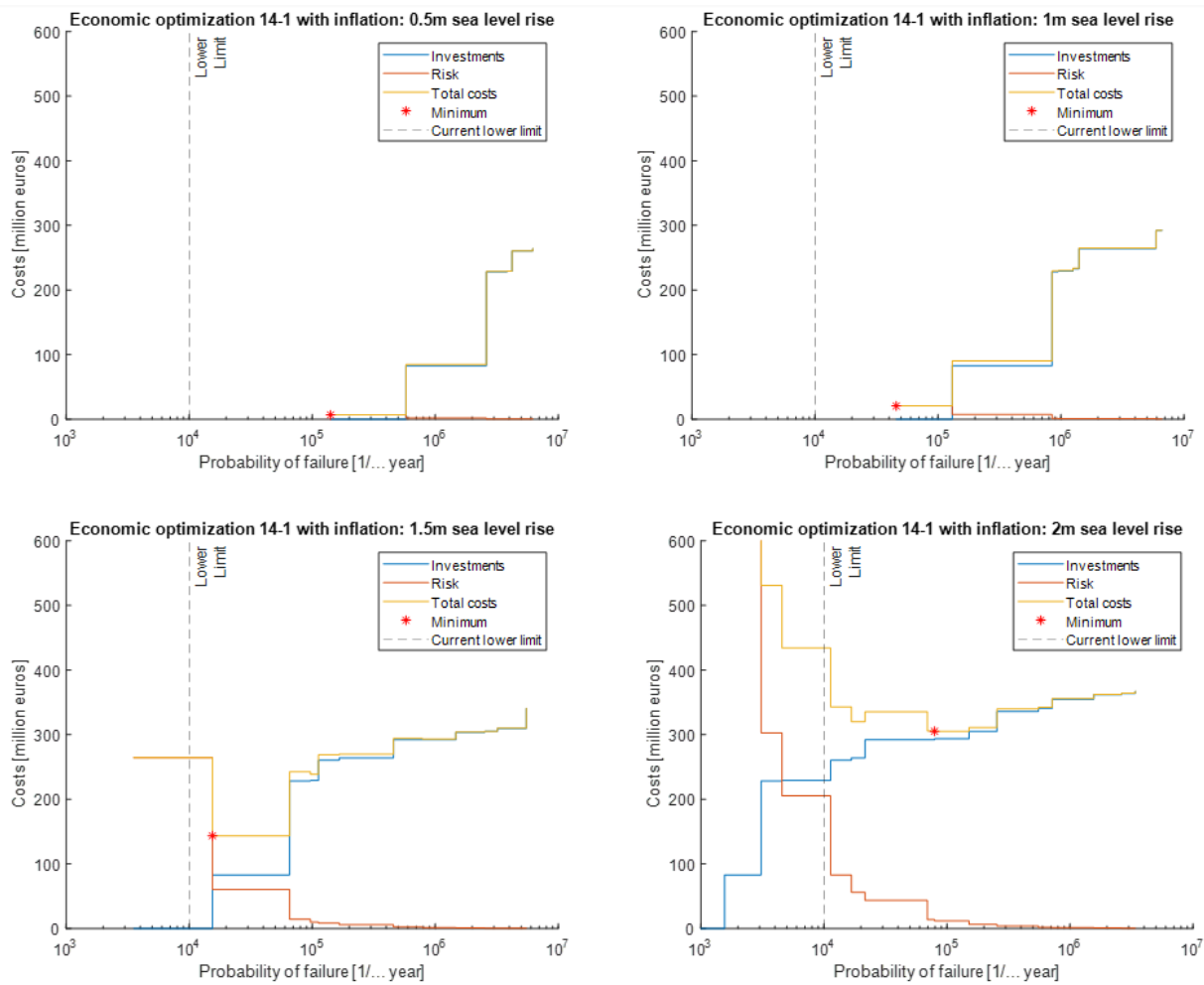
Figure 8.1: Overview of the economic optimization for the scenarios of 0,5 to 2 m sea level rise for trajectory 14-1. The threshold / lower limit of the safety level of trajectory 14-1 is 1/10.000 per year.
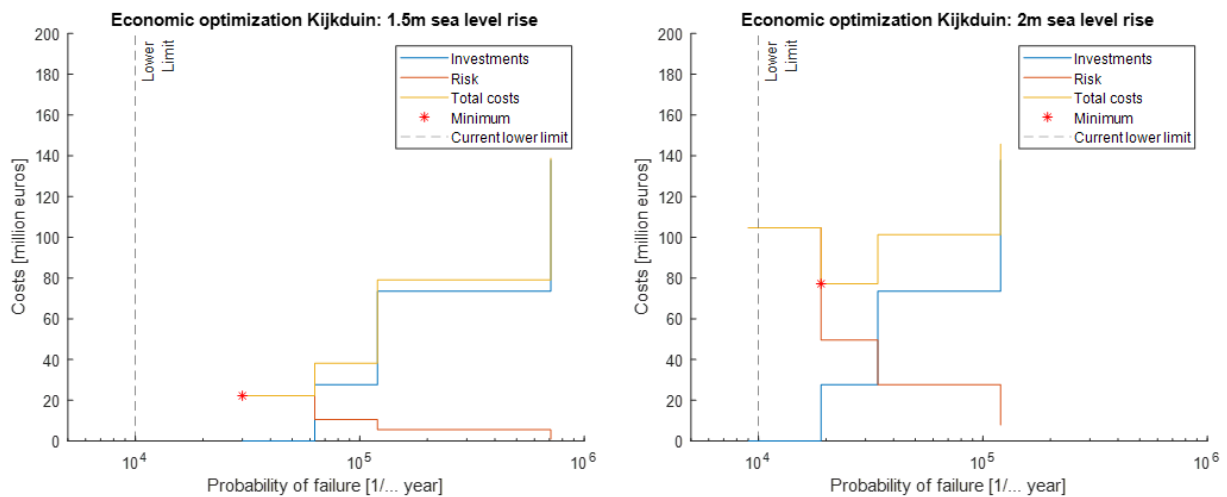
Figure 8.2: Overview of the economic optimization for the scenarios of 1,5 to 2 m sea level rise for Kijkduin. The threshold / lower limit of the breach location Kijkduin is 1/10.000 per year.

Location	Threshold [1/... year]	Signal value [1/... year]	Optimal probability of failure [1/... year]	Costs necessary reinforcents [million euros]	Total costs including risk [million euros]
Noordwijk	30.000	30.000	10.000	0	72,2
Monster	10.000	30.000	34.000	31,7	65,2
Kijkduin	10.000	30.000	19.000	27,6	77,2
Trajectory 14-1	10.000	30.000	79.000	295,4	305,2
Trajectory 14-2	30.000	100.000	15.000	155	278,5
Trajectory 14-3	10.000	10.000	44.000	0	21

Table 8.1: Results of economic optima for every dune breach location and trajectory for a scenario of 2m sea level rise.

Location	Threshold [1/... year]	Signal value [1/... year]	Optimal probability of failure [1/... year]	Costs necessary reinforcents [million euros]	Total costs including risk [million euros]
Noordwijk	30.000	30.000	34.000	0	17,7
Monster	10.000	30.000	63.000	11,9	26,4
Kijkduin	10.000	30.000	30.000	0	22,2
Trajectory 14-1	10.000	30.000	15.000	82,9	143,3
Trajectory 14-2	30.000	100.000	17.000	0	106,3
Trajectory 14-3	10.000	10.000	290.000	0	3,2

Table 8.2: Results of economic optima for every dune breach location and trajectory for a scenario of 1,5m sea level rise.

From the Table 8.1 and Table 8.2 it can be concluded that the dunes and the river dikes will remain safe for a long time under the influence of sea level rise. Only in a scenario of 1,5 m and 2 m rise in sea level does it become economically efficient to reinforce some locations. Another reason to reinforce is that the threshold for the probability of failure is no longer met. This happens for the first time in the scenario with 1,5 m sea level rise for trajectory 14-2. Reinforcement is therefore recommended, even though the economic optimum is a no reinforcement situation. This is also the case for the Noordwijk breach location and trajectory 14-2 in a scenario with 2 m sea level rise. As a result, for these cases, the recommended safety levels are not equal to the economically efficient probability of failure, see Table 8.3. This table shows that the total costs are higher than the total costs from Table 8.1 and Table 8.2, but the threshold is now met. This study recommends a minimum safety level that meets the threshold. Therefore, the economic optima are compared with the threshold. If it was decided that the flood defences should at least meet the signal value, more expensive investments will have to be made to achieve this.

Scenario	Threshold [1/... year]	Recommended probability of failure [1/... year]	Costs necessary reinforcents [million euros]	Total costs including risk [million euros]
Noordwijk 2m SLR	30.000	34.000	125,3	146,5
Trajectory 14-2 2m SLR	30.000	32.000	470	528,7
Trajectory 14-2 1,5m SLR	30.000	38.000	141,9	190,7

Table 8.3: Results of recommended probabilities of failure for locations where the threshold is not met.

The KOSWAT program was used to estimate the costs of dike reinforcements. From the experience of employees of Royal HaskoningDHV, KOSWAT often leads to an underestimate of the total costs and this could also affect the optimisation. Therefore, a sensitivity analysis is needed to the costs determined by KOSWAT. Thre results show what would happen to the economic optima if the costs determined with KOSWAT would be higher by a factor of 2. The conclusion is that the economic optima remains the same for all scenarios except for trajectory 14-1: 2m sea level rise. The economic optimum for this scenario would shift from a failure probability of 1/79.000 per year to 1/17.000 per year. As this is the only scenario for which it changes, the influence of the KOSWAT on the final recommended probability of failure is small

and therefore the recommended probability of failure from Table 8.1 to Table 8.3 are still valid. For an overview of the results of this sensitivity analysis, see Appendix F.2.

8.2. LIR requirements

In this section, the economic optima will be tested against the LIR requirement. The probability of a person dying as a result of flooding must not exceed 1/100.000 per year. For the introduction of the LIR requirement, see Chapter 1.2. The requirement is assessed on the basis of the average LIR of a neighbourhood. Because the average is taken from a neighbourhood, it may be the case that certain places have a greater risk than the LIR requirement. The neighbourhood with the highest local individual risk is normative for the trajectory. In addition, the assessment takes a buffer of 100m around all water bodies which do not have to comply with the LIR requirement. The assessment of the LIR requirement assumes an average and therefore this method is also used in this study. The local individual risk is based on the average mortality of a neighbourhood P_d, the evacuation fraction of 15 percent, F_E, and the probability of failure of of a dune breach location or trajectory, P_f.

$$LIR = (1 - F_E) * P_d * P_f \tag{8.1}$$

The economic optima with the highest probability of failure shown in Table 8.1 to Table 8.3 are used for this analysis. The failure probabilities of the 0 to 1 m sea level rise scenarios are all larger than the economic optima for the 1,5 and 2 m sea level rise scenarios. Therefore, if the economic optima with the highest probability of failure of the 1,5 and 2 m scenarios meet the LIR requirement, all scenarios meet the LIR requirement.

Figure 8.3 shows the local individual risks for the different trajectories. The economic optima corresponding to the highest probabilities of failure are used. From this figure it can be concluded that the economic optima of trajectories 14-1 and 14-3 meet the LIR requirements. This is not the case for trajectory 14-2, where one neighbourhood does not meet the requirement (yellow part). This neighbourhood is normative for testing the LIR requirement. For this trajectory, the LIR requirement is therefore normative instead of the calculated economic optima. In Figure 8.4 is shown for which probability of failure the neighbourhood meets the LIR requirement. This is the case for a probability of failure of 1/100.000 per year. For a scenario with 2 m sea level rise, this probability of failure for trajectory 14-2 is reached by investing a total amount of 503,4 million euros in reinforcement projects, in which profile 3, 4, 5 and 6 are raised with 0,96 m, 1,04 m, 0,84 m and 0,72 m respectively, see Table E.4. The resulting probability of failure is 1/200.000 per year. For the scenario with 1,5m sea level rise, a total amount of investment of 470,2 million euros result in a probability of failure of 1/130.000 per year, Table E.5. These probabilities of failure are recommended to meet the LIR requirement. The economic optima for the coast do meet the LIR requirements, see Appendix F.3.
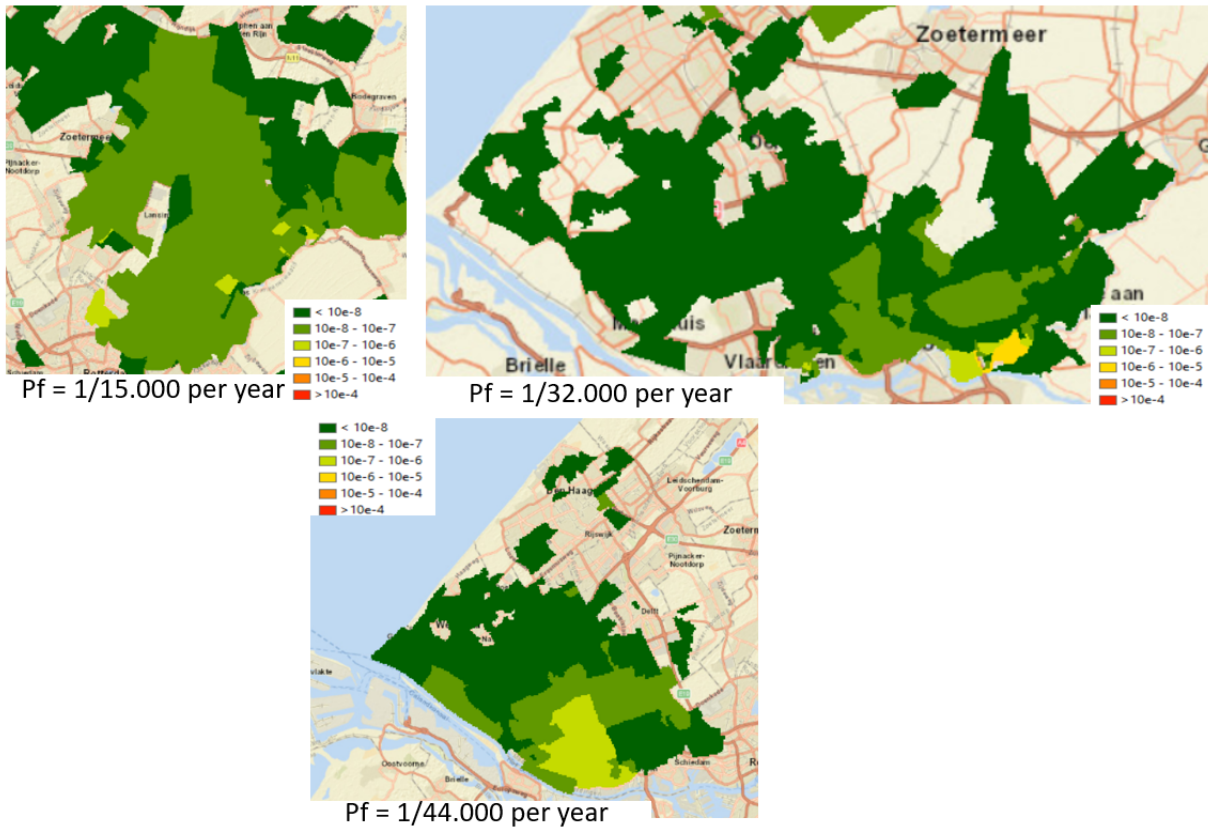
Figure 8.3: Local individual risk corresponding to the highest economic optima for the different trajectories: 14-1 (upper left), 14-2 (upper right) and 14-3 (below).
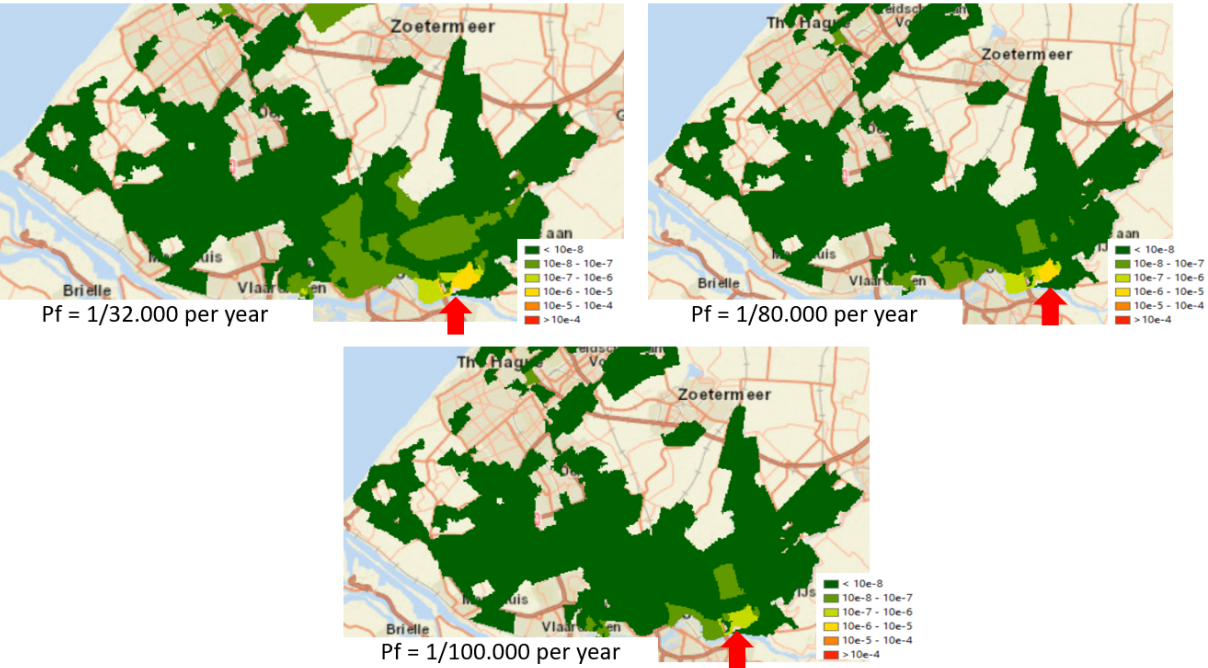
Figure 8.4: Local individual risk for trajectory 14-2 for different probability of failures. Yellow parst do not meet the LIR requirements.

9. Discussion

This chapter will discuss the most important assumptions and their effect on the conclusions. There are assumptions in each model, for which their sensitivity has to be examined. An overview of the most sensitive assumptions discussed is given in a flowchart in which the assumptions are distributed on a three-point scale from least important, 0, to critical assumptions, ++, see Figure 9.1. The sensitivity of these assumptions on the final conclusions, which are the recommended safety levels expressed in a probability of failure and the corresponding total reinforcement costs, is further explained based on the flow chart in Figure 9.1. The purpose of a consideration of the assumptions is to put the conclusions of the next chapter into perspective and to determine the most relevant topics that require further investigation.
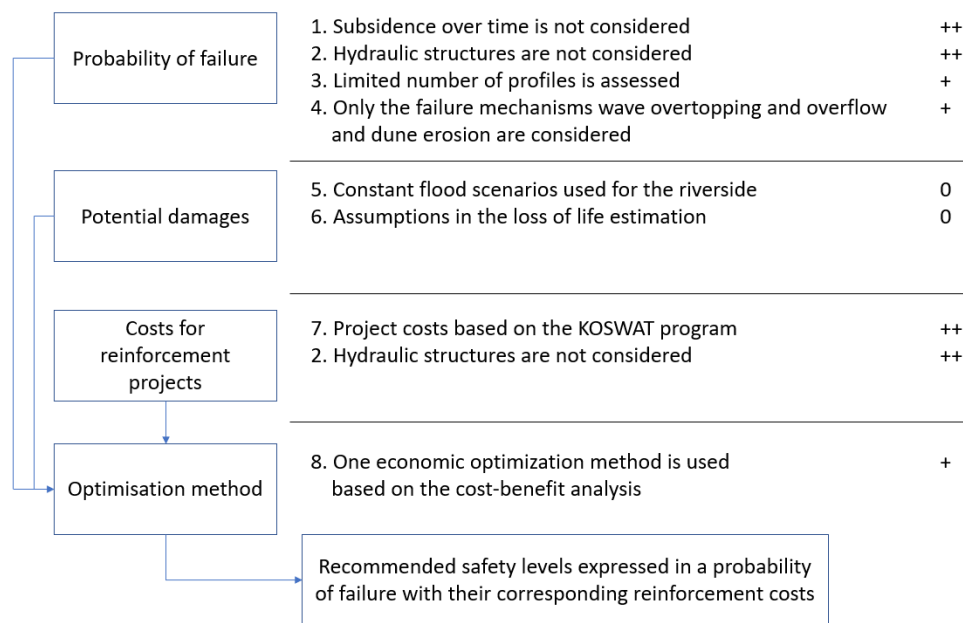
Figure 9.1: Flow chart with assumptions for each step in the calculation method used in this thesis.

1. Subsidence over time is not considered
This study assumes that the height of the dikes and dunes remain the same under all future scenarios. This is not the case, as a time-dependent subsidence must be taken into account. Subsidence results in lower dikes to withstand future sea level rise scenarios, which will increase the calculated probabilities of failure. To assess the effect of not including subsidence, a subsidence scenario is assumed in this evaluation. In the current plans of the Rijkswaterstaat (Kennisprogramma Zeespiegelstijging), a maximum sea level rise of 1 m is assumed for the year 2100. In addition, it is assumed that the sea level will rise by about 1 cm / year from the scenario corresponding to 1m sea level rise, which lies in the range of the two most extreme sea level scenarios for the Dutch coast (KNMI, 2021). A sea level rise of 1 m in the year 2100 and 2 m in the year 2200 is assumed for this sensitivity analysis. In addition, the amount of subsidence per year depends strongly on the location in the area of dikering 14. To determine the subsidence per year, a study from the Delta Programme Rijnmond - Drechtsteden was used in which the expected subsidence over 50 years was estimated, see Figure 9.2. From this figure it can be concluded that there is no subsidence around the dunes and therefore only the river dikes are interesting for this sensitivity analysis. It can also be concluded that the expected subsidence for the river dikes along the Hollandse Ijssel is the highest, followed by the flood defences along the Nieuwe Maas and Nieuwe Waterweg. The expectation is that in 50 years the river dikes of the Hollandse Ijssel will have a subsidence of 45 cm, which corresponds to an average subsidence of 0.9 cm per year. The average subsidence per year are assumed constant in the future and linked to the scenario 1 m sea level rise by 2100 and 2 m sea level rise by 2200. The base year for this sensitivity analysis is 2020. To determine the influence of the subsidence along the Hollandse Ijssel on the conclusions for the scenario 1 and 2m sea level rise, a subsidence scenario is assumed for this sensitivity analysis, shown in Table 9.1.

Scenario	Assumed subsidence Hollandse IJssel
1m sea level rise	72 cm
2m sea level rise	162 cm

Table 9.1: Assumed subsidence scenario in combination with sea level rise.
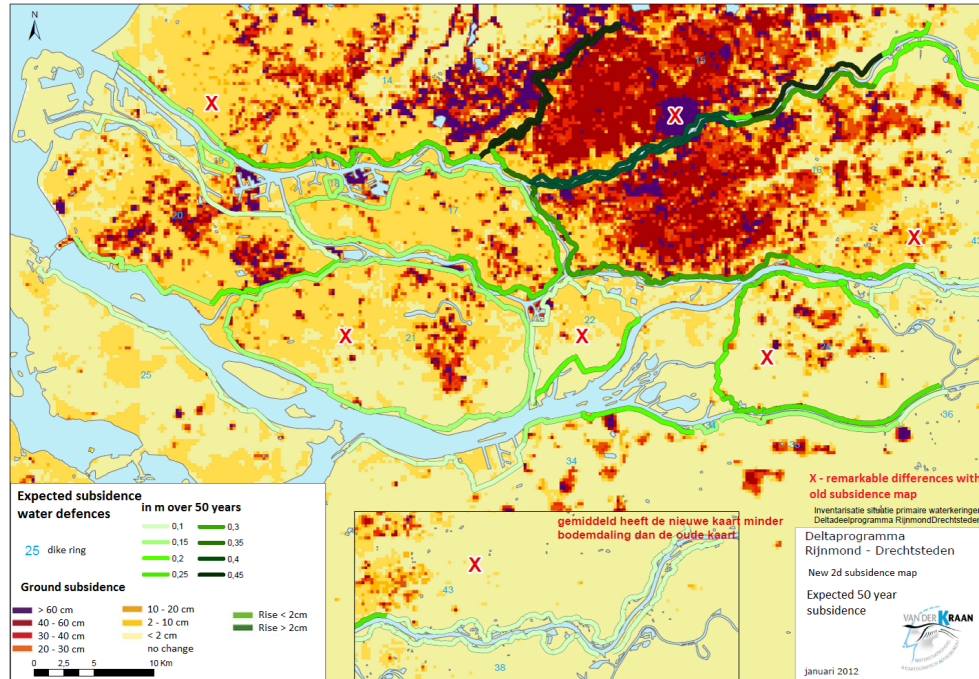
Figure 9.2: Expected subsidence flood defences (der Kraan, 2012).

Another assumption in this sensitivity analysis is that only the river dikes will settle and that the river bed will not. The subsidence of the river dikes will lead to higher probability of failure for the river dikes and therefore the optimisation problem with subsidence will be compared to the original optimisation problem without subsidence. The results are shown in Figure 9.3, from which it can be included that the inclusion of subsidence has a big impact on the results from optimisation problems. The calculated probabilities are higher when taking subsidence into account and therefore the economic optimums change. In the original situation, the economic optimum corresponds to a 300 million investments in combination with a scenario with 2m sea level rise and no investments are recommended in a scenario with 1m sea level rise. In the scenario with subsidence, the economic optimum at 1 m sea level corresponds to investments around 300 million euro and at 2 m sea level rise all designed investments are not enough to reach an economic optimum. It can therefore be concluded that the inclusion of subsidence results in higher recommended investments.
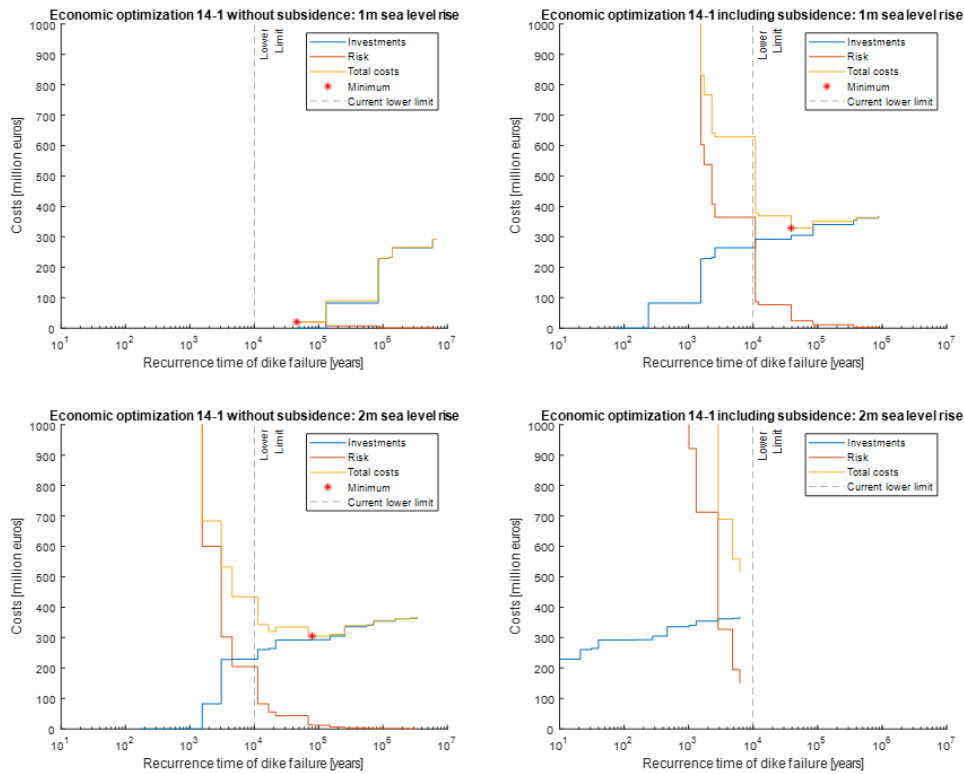
Figure 9.3: Comparison scenario with and without subsidence

2. Hydraulic structures are not included

In this study, the probabilities of failure of the river dike and dunes were evaluated. It is expected that hydraulic structures, such as sluices and other hard water defences like the boulevard at Scheveningen also contribute to a probability of flooding of dikering 14 in future scenarios.

In total there are 17 hydraulic structures in the primary flood defence system for dike ring 14, which include locks, pumping stations and tunnels. In the most recent assessments of VNK2, the probabilities of failure of 10 assessed hydraulic structures (sluices and pumping stations) are negligible compared to the failure probabilities of the dikes and dunes. The probability of failure due to not closing properly is reduced and therefore these probabilities of failure are lower compared to the results of VNK1, when hydraulic structures still contributed significantly to the total probability of failure. Although these hydraulic structures do not contribute much to the probability of failure (smaller than 1/1.000.000 per year) in present-day scenario, the assessment under the influence of a 2m rise in sea level has not yet been done. Therefore, these hydraulic structures will have to be considered under future hydraulic loads to determine their contribution to the probability of failure for each scenario. It is likely that these hydraulic structures will also need to be strengthened in scenarios where the river dikes and dunes need to be reinforced. The same applies to the boulevard at Scheveningen and the outlet structure in Katwijk. A detailed study of the contribution of the hydraulic structures under the influence of sea level rise is therefore a necessity to conclude in which scenario the hydraulic structures need to be reinforced.

Rijkswaterstaat will replace and renovate the hydraulic structures in the years ahead (Rijkswaterstaat, n.d.-b). Built between the 1950s and 1970s, these hydraulic structures will need to be replaced or reinforced. The results of these assessments give a better understanding of the weak spots of dikering 14 and therefore better conclusions can be drawn of which flood defence needs to be reinforced in the future.

3. A limited number of profiles is considered
In this study 8 river dike profiles and 3 dune profiles were assessed. However, to get a better under-
standing of the total flood probability of the dike trajectories, more profiles will have to be considered.
It is assumed that even weaker profiles are present in the trajectories, which increases the total failure
probability. In an ideal scenario, each dike section must be assessed and these individual probabilities of
failure have to be combined to result in a total probability of failure per trajectory. The profiles chosen
in this study have been set as normative for different lengths along the trajectories. Since these lengths
consist of different dike sections, the strength characteristics and loads will not be homogeneous for the
entire length. Normative profiles were chosen for the reinforcement costs of different lengths along the
trajectory. It is possible that the costs of reinforcement will be higher or lower at certain locations because
the reinforcement costs for weaker spots could be higher and for more safe profiles lower reinforcements
costs are necessary. However, it is expected that total cost will be in the same order of magnitude if the
assumption that the cost for the assessed profile will be normative for the particular length is correct. The
costs of reinforcement projects will remain in the same order of magnitude, but the probability of failure
associated with these reinforcement projects will be higher. Because of the higher probabilities of failure,
the total risk will be higher and therefore economic optima are shifted or correspond to higher investments.

**4. Only the failure mechanisms wave overtopping and overflow and dune erosion are consid-
ered**
This study only looked at the failure mechanism due to a height shortage. A relative contribution of the
failure probability due to height of 24 percent is assumed to the total failure probability distribution. In
Appendix A.3 are also the failure probabilities for each profile included in a situation that a 100 percent
relative contribution is assumed. In almost all scenarios, this will lead to a lower probability of failure of
a factor between the 1,5 and 4. However, both calculated failure probabilities remain in the same order of
magnitude. In the ideal scenario, every dike should be tested for all failure mechanisms. Separate failure
probabilities would then be determined for, for example, the failure mechanism due to height shortage,
piping and instability. These failure probabilities can then be summed up if independency between the
failure mechanisms is assumed. In this ideal scenario, where the failure probability is calculated for each
failure mechanism, the relative contribution per failure mechanism to the failure probability distribution
does not have to be taken into account.

However, the order of magnitude of the probabilities of failure is expected to remain the same if the profiles
used are also assessed for the other failure mechanisms. As can be seen from the calculated probabilities of
failures in VNK2, the contribution of the probabilities of failure due to height in the total failure probabil-
ity of the river dikes is about 64 percent. For the various reinforced profiles designed with KOSWAT the
three failure mechanisms overflow and overtopping, macro stability and piping are considered. These three
failure mechanisms are included in the required dike height, the increase of the dike base for macro stability
and the increase of the dike base required for piping. Because the dominant failure mechanism for this
dike ring is failure at height and because the design of reinforced profiles also considers the other failure
mechanisms that affect the dimensions of the dike body, it is expected that the calculated probabilities of
failure will remain in the same order of magnitude when all failure mechanisms are included. Since the
order of magnitude does not change, the recommended safety levels and the corresponding investments
will also hardly change in the optimisation problem.

5. Constant flood scenarios are used for the riverside
Constant LIWO flood scenarios were used for the river side, whereas new hydrodynamic simulations were
used for the seaside. These new hydrodynamic simulations clearly show the increasing damage with each
step of sea level rise because the extent of the flood increases per increment of sea level rise. When looking
at the increase of total damage, the total damage increases by about a factor of 3 from 0 m to 2 m sea level
rise. If hydrodynamic models for the riverside were available, considering any scenario of sea level rise and
increased river discharge, the extent of the floods and thus the damages will increase. To investigate the
effect of these higher damages, the optimisation problem was performed with the total damages multiplied
by a factor of 3. This showed that the increase in investments for section 14-1 due to the climate scenario
with a 2m sea level rise increased by approximately 10 million euros. This is negligible when considering
the total investment costs for the entire diked area. For section 14-2, the economic optimum did shift
from 155 million to around 500 million euros. For the scenario with 1,5 m sea level rise, this optimum
shifted to 0 to 155 million euros in investments. However, the recommended investments for this section

are not based on the economic optimum. The recommended investments are based on meeting the LIR requirement, which was 470 million euros. Therefore, the level of recommended investments will not differ significantly when an increased damage of a factor 3 is considered.

6. Assumptions in the loss of life estimation

The method of S. Jonkman (2007) was used to determine the number of potential casualties and affected persons. During a discussion with experts in the field of river and coastal engineering on 24 September 2021, it was concluded that that the sensitivity to the assumptions had to be examined because they may be conservative since they are based on data from historical floods such as the flood in the Netherlands in 1953 and the flooding of New Orleans after hurricane Katrina in 2005. In addition, it is assumed that all people stay inside and that everyone dies if buildings collapse. For the breach zone, it is assumed that all buildings collapse and therefore everyone present in the breach zone dies. This seems conservative since those who are picked up by the flooding still have a chance of survival. In addition, according to method of S. Jonkman (2007), some buildings outside the breach zone still collapse. Nowadays, this hardly seems to happen anymore due to the improved quality of houses in the Netherlands. The influence of improved house quality on the mortality rate has already been investigated by S. Jonkman (2007), but the old functions are still used to set the safety standards Waterveiligheidsportaal (n.d.). An overview of the effect of this improved building quality is shown in Figure 9.4. It can be concluded that the improved building quality has a positive effect on mortality. A logarithmic fit is plotted through the historical data, but the fit of this function also has uncertainty. The total damages will remain in same order of magnitude when using a different fit and therefore the recommended safety levels and corresponding investments would not change significantly.
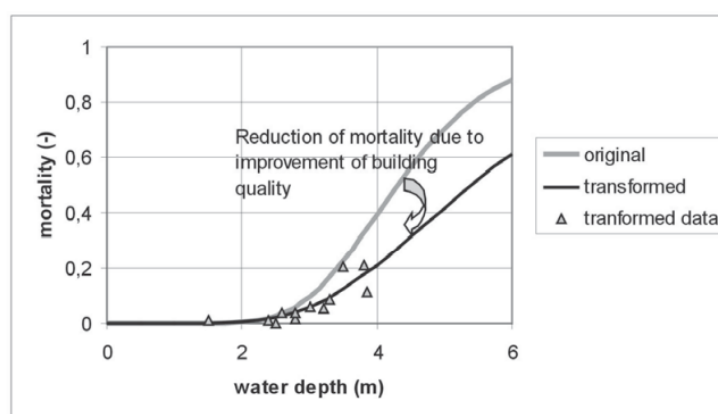
Figure 9.4: Effect of the improved building quality on the mortality functions (S. Jonkman, 2007).

This study uses a constant evacuation fraction for the entire protected area, but a better understanding of this evacuation fraction can improve the results. The proposed approach does not capture individual behavior and the individual causes of loss of life. The evacuation fraction can be better estimated by using a more detailed model, which includes interactive dynamic processes such as the occurrence of traffic jams during evacuation and the behaviour of people, such as whether or not people follow an evacuation order. Although the loss of life estimation may be somewhat conservative and the evacuation fraction is not included in detail in this study, the difference in the final results will not be significantly. If the calculated number of potential casualties is reduced by a factor of 2, it turns out that the economic optima and corresponding investments hardly change, so that the assumptions in loss of life estimation designed by S. Jonkman (2007) do not significantly influence the conclusions of this thesis.

7. The investments costs are based on the results of the program KOSWAT

Using KOSWAT, it was relatively easy to make a first estimate of the costs for various dike reinforcements. The results of KOSWAT have a strong influence on the amount of the total investments. However, the recommended safety levels will not differ much if the costs from KOSWAT are multiplied by a factor of 2, see Appendix F2. A discussion with experts of Royal HaskoningDHV showed that the use of KosWat often gives an estimate of the order of magnitude for the total project costs, but that in reality the costs are often higher by a factor of 2 or 3. Therefore, Royal HaksoningDHV does not use the KOSWAT tool

to estimate the total project costs. Due to time constraints, no other method was used to estimate the total project costs. The recommended safety levels will not change much, but a multiplication of the total project costs by a factor of 2 or 3 must be taken into account. It is therefore recommended to evaluate the costs of these dike and dune reinforcements using other more comprehensive methods before assuming that the investment costs are the same based on the results of the KOSWAT program.

8. Economic optimisation

In this study, a cost-benefit analysis was used, which included both the economic damage and the damage resulting from the loss of life estimations. The calculated optimum failure probabilities could be used for risk-informed decision making by showing the impact of climate change on the flood risk and whether the standards need to be adjusted. Another method to find the optimal investments is based on an analysis of the investments and the associated failure probability reduction of a flood defence, in which different failure mechanisms are considered. In this way, cost-effective analyses can be made that do not take much time compared to the cost benefit analysis. Rijkswaterstaat plans to have regional analyses carried out in the Netherlands from 2022 onwards, based on the this economic optimisation method. Because the increasing damage levels are not determined in this method, the outcome can only be compared to the old standards and no conclusion can be drawn as to whether the standards should be adjusted based on the cost-benefit analysis.

It would also be interesting to think about alternative strategies than raising the river dikes to reduce the flood risk for dikering 14. These alternative strategies are increasing the reliability of the Maeslant and Hollandse IJssel barriers or other future solutions such as Delta21 or the placements of locks in the Nieuwe Waterweg. Delta21 is an idea to create a lake between the coast of Maasvlakte 2 and the island of Goeree Overakkee, which would also reduce the hydraulic load in the Nieuwe Waterweg and Nieuwe Maas (Delta21, n.d.). By considering other strategies for improving water safety, the most cost-effective measures can be determined.

10. Conclusions and recommendations

10.1. Conclusions

This section answers the research questions. The objective of this study was to make an impact assessment as complete as possible for dikering 14 of future flood scenarios considering sea level rise and increased river discharge due to climate change. The river dikes and dunes of the primary flood defences of dikering 14 are assessed in this study. The river side consists of the river dikes along the Hollandse Ijssel, Nieuwe Maas and Nieuwe Waterweg. The seaside consists of the coast between Hoek van Holland and Ijmuiden. First, the 5 sub-questions will be answered and the methodology will be briefly discussed, after which the main question will be answered.

How does climate change affect the probability of failure of the primary flood defences at the seaside and riverside of dikering 14?
To answer this sub-question, 8 dike profiles and 3 dune profiles were assessed under the influence of climate change, considering sea level rise up to 2m and an associated increase in river discharge. A base case scenario of the current situation with 0 m sea level rise and 4 future scenarios of sea level rise of 0,5 m, 1 m, 1,5 m and 2 m were assessed, resulting in a total of 5 scenarios. The 8 dike profiles and 3 dune profiles are representative of different lengths along the flood defence trajectories. The hydraulic load level for the river dikes was determined with a probabilistic model that calculates the statistics of the hydraulic load level. Extrapolation was used to transform the available statistical datasets of the seawater level at the Maasmond and the river discharge at Lobith into datasets which were used as input for the 4 future climate change scenarios. Using the most recent assessment reports for primary flood defences along the Nieuwe Maas, a relationship between height shortage and the probity of failure of a profile was determined. The same relationship was used for all 8 different dike profiles. In an ideal case, the probability of failure would be determined by assessing each dike profile on all failure mechanisms and adding up these individual failure probabilities if independence between the failure mechanisms is assumed. By using this relationship, only the failure mechanism overtopping and overflow is assessed and not piping, instability and revetment failure. However, because the failure probabilities of the assessed profiles are dominated by the failure mechanism overtopping and overflow, the failure probabilities considering all failure mechanisms is assumed to remain in the same order of magnitude as the calculated failure probabilities in this study. By assessing only 8 river dikes, the actual failure probability of a part of flood defence is higher than the calculated failure probabilities in this study, because possible weak spots are not included. To gain better insight into the total failure probability of a trajectory, a larger number of profiles and failure mechanisms will therefore have to be assessed. However, because profiles have been chosen that are ultimately representative for the final reinforcement costs, the conclusions at the end will not differ significantly. By subtracting the hydraulic load level from the crest height of the dike, determined with an current altitude database of the Netherlands, the height shortage or surplus were determined and the corresponding failure probabilities in all scenarios. The probability of failure of the 3 dune profiles at Noordwijk, Kijkduin and Monster, were calculated with an application with which dune erosion calculations can be made using the Duros-plus model. It was examined whether a minimum required profile, the boundary profile, could be fitted behind the erosion profile and it was determined at which sea water level, significant wave height and period the dune profile could no longer fit a boundary profile. The recurrence time of this critical sea level was then determined and equated to the failure probability of the dune profile.

The results clearly show the effect of climate change on the probability of failure of the primary flood defences. Scenarios with higher sea levels and higher river discharge lead to higher probability of failure of the flood defences. The probability of failure of the flood defences along the Hollandse Ijssel is the highest, rising from 1/370.000 per year in the current situation to 1/170 per year in the scenario involving a 2 m sea level rise. The profile located in the upstream Hollandse Ijssel is the weak spot. The probability of failure of the flood defences along the Nieuwe Maas rises from a probability of failure of 1/2.200.000 per year to 1/3.500 per year with a scenario of 2 m sea level rise, whereby the upstream sections along the Maasboulevard and the Nijverheidsstraat are the weak spots. Both the flood defences along the Hollandse Ijssel and the Nieuwe Maas meet the threshold of the safety level stated in the Water Act up to and including the scenario of 1m sea level rise. The failure probabilities for the river dikes along the Nieuwe Waterweg will also increase significantly but will meet the threshold even in a scenario of 2 m sea level rise. However, in this study it is assumed that dike heights remain the same in the future but in reality,

a time-dependent subsidence has to be included. This study does not consider the moment in the future when a certain climate scenario occurs. If subsidence is to be included, a method for this will have to be developed. For a sensitivity analysis a simple subsidence scenario has been included in which the dikes along the Hollandse Ijssel will settle 72 cm and 162 cm in combination with a scenario of 1 and 2 m sea level rise, respectively. It was concluded that in a climate scenario with a sea level rise of 1 m, the dikes no longer meet the threshold, and the failure probabilities are significantly higher than those calculated in this study. Therefore, a method will have to be determined for the rivers whereby the subsidence is linked to the climate scenarios to obtain gain more insight into the actual failure probabilities in the future.

The influence of climate change is also visible in the results of the failure probabilities for the dunes. The current failure probabilities for the dune profiles are very low but become significantly higher as sea level rises. Ultimately, the failure probabilities of the dune profiles are a factor of 2000-3000 higher than in the original situation under the influence of a 2 m rise in sea level. However, up to and including a scenario of 1,5 m sea level rise, the dune profiles meet the safety standards included in the Water Act. Only with a scenario of 2 m sea level rise the dune profiles no longer meet the standards. The failure probabilities of the dunes profiles located at the southern coast, Kijkduin and Monster, have a failure probability of 1/9000 per year in a scenario of 2 m sea level rise, and the dune profile of Noordwijk located on the northern part of the coast has a failure probability of 1/10.000 per year.

The conclusion is that the failure probabilities of the primary flood defences will increase significantly under the influence of climate change. Significantly higher failure probabilities have been calculated for the river dikes than for the dunes. For the primary flood defences along the Hollandse Ijssel and Nieuwe Maas the probabilities of failure no longer meet the thresholds stated in the Water Act, in case of a scenario involving a 1,5 m rise in sea level. For the dunes this is only the case with a scenario of 2m sea level rise. A limitation of these results is that it has been assumed that all hydraulic structures such as locks, pumping stations and hard water defences in the dunes are safe in all scenarios. The most recent VNK2 reports conclude that in the current situation hydraulic structures make only a small contribution to the flood risk of the area, but a detailed assessment will have to be made to see if this is also the case under future scenarios. It was also concluded that the inclusion of time-dependent subsidence has a major influence on the probability of failure of the river dikes. This is not the case for the dunes, as it is assumed that they will not subside in the future.

To what extent does climate change affect the loss of life estimation for the area on both the river side and the seaside?
To answer this question, existing models from the national water and flood information system for the riverside as well as new hydrodynamic models simulated by Ranneft (2020) for the seaside were used. For the river side all available flood scenarios were combined by taking a maximum value per grid cell. In these available models for the river side, the effect of the different climate scenarios could not be considered, as no models are available yet for the future scenarios. The coastal hydrodynamic models show the effect of sea level rise on the flood extent. With each step of sea level rise, the extent of the flooding increases. The flood depth, flow velocity and rise rate and the evacuation fraction are used as input for determining the mortality rates. These mortality rates are determined with the logarithmic functions from the loss of life estimation designed by S. Jonkman (2007). With these mortality rates and the population numbers, the affected persons and casualties could be determined.

The results showed that the number of potential casualties and affected persons are highest for the trajectory along the river Nieuwe Maas with a potential number of 7900 casualties and 430.000 affected persons. This is because the densely populated cities Rotterdam and Schiedam would be flooded in case of failure of a flood defence along the river Nieuwe Maas. The potential casualties are higher in case of a river breach than in case of a dune breach because the flood depths in these deep polders are higher.

Comparing the present-day scenario and the scenario with 2m sea level rise, the potential number of casualties approximately doubles for the breach location Noordwijk to 2100 casualties and 300.000 affected persons and triples for the locations Kijkduin and Monster. A dune breach at Kijkduin will result in 1900 casualties 740.000 affected persons and a dune breach at Monster will result in 1800 casualties and 800.000 affected persons in the scenario corresponding to 2m sea level rise. To assess whether this doubling or tripling effect should also be included for the river side in a follow-up study, the effect of an increasing number of casualties and affected persons on the final results was examined. This showed that the recommended safety levels and associated investment did not change significantly.

To what extent does climate change affect the expected damage for the area on the river side?

The economic damage for the seaside was already determined a previous study (Ranneft, 2020), so only the economic damage for the river side was calculated in this study. By using the created flood depth maps, land use map and damage curves in the Global Flood Risk tool, the expected damages were visualized. The highest economic damage occurs if a dike failure occurs along the Hollandse IJssel. This is because a flood can reach high flood depths in the deep polders. The total economic damage is obtained by the sum of the direct and indirect economic damage. The effect of sea level rise and an increase in river discharge is not investigated for the river side in this analysis. This is because constant flood scenarios were used instead of hydrodynamic models in which the effect of climate change on the extent of the floods was included as is the case for the seaside. A river dike breach in the Hollandse Ijssel leads to the highest economic damage of 14.300 million euros, followed by an economic damage of 8800 million euros due to a dike failure along the Nieuwe Maas and an economic damage of 6100 million euros due to a dike failure along the Nieuwe Waterweg. These results are in the same order of magnitude if the total damage due to all available breach locations in the National Water and Flood Information System (LIWO) is added up.

What are the expected costs for specific dune and dike reinforcements that would increase the safety levels?

The trajectories and the coast are divided into parts for which profiles are normative. These profiles contain the 8 river dike profiles and 3 dune profiles. In this way, a good insight can be gained into which parts need to be reinforced to achieve a higher safety level. For the riverside, the costs of dike reinforcements are determined with a program which, based on the existing infrastructure and the applicable reinforcement measures, estimates the total project costs for achieving different safety levels. The profile with the highest probability of failure is reinforced first. Therefore, for different combinations of dike reinforcements, the total costs and their corresponding probability of failures are determined. For the Hollandse Ijssel, 16 different combinations of reinforcements are considered with the corresponding costs in the scenario of 2m sea level rise. The total cost of these combinations varies between 0 euro in a situation without reinforcements and 370 million euro for a total length of 20,5 km. Various combinations for reinforcing the flood defences along the Nieuwe Maas and Nieuwe Waterweg have been considered, costing up to 510 million euro and 300 million euro respectively. The lengths of flood defence to be reinforced are 20 km along the Nieuwe Maas and 16,5 km along the Nieuwe Waterweg.

For the profiles on the coast, additional sand volumes of 150, 400 and 750 m^3/m were added to the original profiles. With the lengths for which these profiles are normative and the costs per m^3/m for sand, the total costs can be determined. The Noordwijk profile is representative of the longest part of the coast, 34.5 km, which leads to the highest total reinforcement costs varying from 50 million euros at an additional sand volume of 150 m^3/m and 230 million euros at 750 m^3/m.

Inflation has been considered for both the costs of the coastal and the river dike reinforcements, to arrive at today's price levels. The different total project costs and their corresponding probability of failure are used as input for the economic optimisation. In practice, these costs will be higher because the reinforcement of the 17 hydraulic structures, consisting of sluices, pumping stations and hard flood defences in the dunes, such as the boulevard at Scheveningen, were not included in this study. In addition, real reinforcing projects have shown that the total cost of reinforcing the river side, as determined by a program, is often underestimated. In reality, the total costs may be higher by a factor of 2 or 3. However, this has no significant influence on the determination of the economic optima and therefore the recommended safety level.

What are the economic optimums for the safety level expressed as a probability of failure?

The economic optimums were found by means of a cost-benefit analysis. This analysis was also used to determine the current standards included in the Water Act. The economic optima are compared with the threshold stated in the Water Act. In addition, the economic optima are compared with the local individual risk (LIR) requirement, whereby the probability of a person dying as a result of a flood must not exceed 1/100.000 per year. If the economic optima do not meet this requirement, it will be examined at which safety level the LIR requirement is met. The total damages per scenario are obtained by adding the economic damages to the damages from the loss of life estimation, where monetary values of 6,7 million euros and 12.000 euros are assigned to a casualty and affected persons respectively. The total risk is calculated from the damage, probability of failure, growth rate and discount rate. Next, the costs

are plotted against the probability of failure, with economic optimum at the minimum of the total costs curve. The total costs are determined by adding the investments to the risk.

The results show that it only becomes economically efficient to reinforce from scenarios with 1,5 and 2m sea level rise. The economic optima for the 0,5 and 1 m sea level rise scenarios are at the original probability of failure with no reinforcements and therefore no investments are recommended. It can be concluded that the water system performs well up to a scenario corresponding to 1m sea level rise. This is because the probability of failures and associated risks are already low for these scenarios and that it is therefore not efficient to start reinforcing.

The economic optima found for a scenario of 2m sea level rise are all higher than the current threshold in the Water Act. Therefore, it can be concluded that for the Hollandse Ijssel and the coast it is recommended to use stricter standards in the case of climate change from 1,5 m sea level rise. In a scenario of 2m sea level rise the economic optimum changes from 1/10.000 per year to 1/79.000 per year for the Hollandse Ijssel. The recommended safety levels along the Nieuwe Maas are not determined by the economic minimum, but by meeting the LIR requirement, so that the recommended safety level along this trajectory is 1/100.000 per year. However, these economic optima may differ significantly in case subsidence along the river side is included in future scenarios.

The main research question of this study is:

How does climate change affect the flood risk for the area protected by the primary flood defences of dikering 14 and which investments can optimally ensure the future safety of this area?

In this study, a method has been developed from which it can be concluded whether stricter standards should be used for the primary flood defences of dikering 14 in future scenarios. In addition, by calculating the total potential damage, risk areas are visualized, contributing to the public debate as to whether in the future new cities should be built in deep polders in the Randstad or whether alternatives should be considered in which greater focus is on the development of the higher lying eastern parts of the country.

It has become clear from this study that the river dikes and the dunes belonging to the primary flood defences of dikering 14 are able to protect the area up to future climate scenarios corresponding to 1m sea level rise. Economic damage and damage due to casualties and affected persons have been considered. Most of the total potential damage is due to the number of potential casualties and affected persons. This shows that the loss of life estimation has a heavy share in determining the recommended safety levels. Using coastal hydrodynamic models, it was possible to determine the increasing potential damage under the influence of sea level rise. The potential damage increases by a factor of 2,5 - 3 when the current situation is compared to a future scenario of 2m sea level rise. The potential damage in a scenario with 2m sea level rise caused by a dune breach at Noordwijk is 26.000 million euros, which includes 300.000 affected persons and 2100 casualties. A dune breach at Kijkduin and Monster results in a total damage of 34.000 million euros and 41.000 million euros respectively. This higher damage is because the densely populated area near The Hague is flooded. A dune breach at Kijkduin will result in 740.000 affected persons and 1900 casualties. At Monster this would be 810.000 affected persons and 1800 casualties.

For the riverside, constant scenarios were used and therefore the influence of climate change on flood risks was only considered by increasing probabilities of failure in the future. The greatest potential damage for the riverside occurs in case of a dike failure along the Nieuwe Maas with a total damage of about 67.000 million euros. The potential damage in case of a dike failure along the Hollandse Ijssel and Nieuwe Waterweg both are 34.000 million euro. The flood defences along the Hollandse Ijssel, Nieuwe Maas and Nieuwe Waterweg protect around 1 million people in total, with 14.000 potential casualties due to flooding from the rivers.

The dunes and river dikes will all need to be reinforced except for flood defences along the Nieuwe Waterweg in a scenario corresponding to 2m sea level rise. The weak spots at the riverside are formed by the flood defences along the Hollandse Ijssel and the Maasboulevard and the river dikes upstream the Nieuwe Maas. For the Hollandse Ijssel, a safety level is recommended corresponding to an increase in height for profile 1 by 1,75m and profile 2 by 1,01m for a scenario with 2m sea level rise. Profile 3, 4, 5 and 6 needs to be raised by 0,96m, 1,04m, 0,84m and 0,72m respectively to meet the LIR requirement and therefore

reach the recommended safety level. The dunes need to have sand supplements of 400 m3/m, 150 m3/m and 400 m3/m for the breach locations Noordwijk, Kijkduin and Monster respectively to reach the recommended safety levels. The safety levels in terms of probability of failure that are recommended are equal to economic optima, except in case they do not meet the threshold limit or the LIR requirement. With these local reinforcements of the river dikes and dunes, the hinterland will remain safe under the influence of climate change.

Along each trajectory, reinforcements of the flood defences must be carried out in the scenario corresponding to 2m sea level rise, except for the river dikes along the Nieuwe Waterweg and therefore a length of 104 km of flood defences will have to be reinforced. The total cost of these reinforcements and the protection against potential damage is shown in Table 10.1. The results show that reinforcing the river dikes is significantly more expensive than reinforcing the dunes. As explained in the discussion, there are assumptions in this study that influence the total cost significantly, whereby the non-inclusion of subsidence and hydraulic structures and the rough estimate of the costs for reinforcement projects are the most sensitive. In reality, the total costs will therefore probably be around a factor 3 higher than determined in this study.

Paramater	Scenario 2m sea level rise
Total investment costs	1 billion euros
Length reinforcements river dikes	40,5 km
Average costs riverside	20 million euros/km
Length reinforcements dunes	63,5 km
Average costs dunes	3,8 million euros / km
Potential damage	2,5 million affected persons
	20.000 casualties
	70 billion euros economic damage
Potential total damage	230 billion euros

Table 10.1: Recommended reinforcement and potential damages in a scenario corresponding to 2m sea level rise

10.2. Recommendations

This section provides recommendations for follow-up research. These recommendations will enable more detailed conclusions to be drawn about the water safety and corresponding investments in the future.

Recommendation on the substantiation of the total costs for reinforcements

In a discussion with experts from Rijkswaterstaat and Royal HaskoningDHV on 26 October 2021, it was concluded that the reinforcements determined in this study using the program KOWSWAT are an underestimation of the total costs in reality. To get a better idea of how much it will cost to keep the area safe in the future, a detailed cost estimate must be made that also includes the costs of strengthening the 17 hydraulic structures in the area. In addition, it is also interesting to investigate adjustments to the water system, such as closing off the Nieuwe Waterweg and/or Hollandse Ijssel. In this way, better conclusions can be drawn about which measures are the most cost-effective.

Recommendation on including subsidence over time

This study assumes that the river dikes have the same crest height in each scenario of climate change. In the future, the river dikes are likely to settle, with the annual subsidence being highest for the Hollandse Ijssel. This means reinforcements will have to be carried out earlier than determined in this study, as the failure probabilities of the profiles are higher if subsidence is included. To include subsidence in this study, a method must be developed to estimate the amount of subsidence per scenario of sea level rise.

Recommendations on including hydraulic structures

Because the hydraulic structures in the primary flood defenses of dikering 14 are not included in this study, this can lead to an underestimation of the calculated failure probabilities for the flood defences along the rivers and coast. The primary flood defences of dikering 14 have a total of 17 hydraulic structures, which include sluices, pumping stations and hard flood defences in the dunes. These hydraulic structures are assumed safe for all scenarios in this study, so any necessary reinforcements are not included. To determine

the future risk and recommended investments in more detail, the contribution of hydraulic structures in future scenarios and possible reinforcement costs will have to be investigated.

Recommendations on using different optimisation problems and strategies
In this study, the economic optima based on the cost-benefit analysis were calculated. In this way, the safety standards were also determined and included in Waterveiligheidsportaal (n.d.). Another method is to look at the costs per failure probability reduction. It would be interesting to see if the results of the recommended safety levels and investments are similar to this study. Other strategies could also be included in the optimisation problem. Other strategies than raising the dikes are adjustments such as increasing the reliability of the storm surge barriers or other future solutions such as closing off the Nieuwe Waterweg.

References

AHN Viewer. (n.d.). *AHN Viewer — AHN.* Retrieved 2021-07-06, from `https://www.ahn.nl/ahn-viewer`

Arcadis. (2018). *Vertaling VNK naar WBI2017.* doi: 10.1007/978-90-313-8006-0_1

Berkers, M. (2016). *Een 'dijk-in-duin-constructie' voorziet Katwijk van een robuuste zeewering. De meedenkende Katwijkers wilden en kregen een landschappelijke inpassing.*

Boersen, S., Berg, M. V. D., & Bos, M. (2017). *Hydraulisch onderzoek verhoging Tuimelkade* (No. december).

Boorn, M., Lendering, K., Maaskant, B., Roode, N., Den Hengst, W., & De Graaf, E. (2018). *Tussenversie Handreiking Voorland Tussenversie Handreiking Voorland.*

Chbab, H. (2017). Basisstochasten WBI-2017. *Deltares report, 1209433-012-HYE- 0007.*

Chbab, H., & Groeneweg, J. (2017). Modelonzekerhied Hydra-Ring. Wettelijk toetsinstrumentarium WTI-2017. *Deltares report, 1209433-008-HYE- 0007.*

Delta21. (n.d.). *Delta21: Eén idee, 3 oplossingen .* Retrieved 2021-10-13, from `https://www.delta21.nl/het-plan/`

Deltares. (2014). *Kosten voor versterken waterkeringen.*

der Kraan, V. (2012). *Expected subsidence water defences.*

Diermanse, F., Roscoe, K., Lopez de la Cruz, J., Steenbergen, H., & Vrouwenvelder, A. (2013). *Hydra Ring Scientific Documentation.*

ENW. (2017). *Fundamentals of Flood Protection.*

HKV. (2018). *Verandering golfkarakteristieken en hydraulische belastingniveaus bij zeespiegelstijging langs de Nederlandse kust.*

Hoogheemraadschap van Schieland en de Krimpenerwaard. (2019). *Achtergrondrapport Grasbekleding 14-2.*

Inflation.eu. (n.d.). *Historische inflatie Nederland - CPI inflatie.* Retrieved 2021-10-13, from `https://www.inflation.eu/nl/inflatiecijfers/nederland/historische-inflatie/cpi-inflatie-nederland.aspx`

Jongejan, R. (2010). *Veiligheid Nederland in Kaart 2: Overstromingsrisico Dijkring 14 Zuid-Holland* (No. November).

Jonkman, S. (2007). *Loss of life estimation in flood risk assessment.* Retrieved from `https://repository.tudelft.nl/islandora/object/uuid{%}3Abc4fb945-55ef-4079-a606-ac4fa8009426`

Jonkman, S. N., Hillen, M. M., Nicholls, R. J., Kanning, W., & Van Ledden, M. (2013). *Costs of adapting coastal defences to sea-level rise - New estimates and their implications* (Vol. 29) (No. 5). doi: 10.2112/JCOASTRES-D-12-00230.1

Jonkman, S. N., Jorissen, R., Schweckendiek, T., & Van den Bos, J. (2018). *Flood defences: Lecture notes CIE5314.*

Kind, J. (2011). *Maatschappelijke kosten-batenanalyse Waterveiligheid 21e eeuw (Tech.Rep.).*

KNMI. (2019). *Zeespiegelstijging nu en in de toekomst.* Retrieved 2021-03-05, from `https://magazines.rijksoverheid.nl/knmi/knmispecials/2019/03/nu-en-in-de-toekomst`

KNMI. (2021). *Klimaatsingaal'21.*

Knoeff, H. (2016). *Kennisplatform Risicobenadering.*

Maaskant, B., Jonkman, S. N., & Kok, M. (2009). *Analyse slachtofferaantallen VNK-2 en voorstellen voor aanpassingen slachtofferfuncties.*

Maaskant, B., Yska, D., & Kok, M. (2019). Met faalkansbomen waterkeringen beoordelen. *Land en Water*.

Ranneft, M. (2020). *Assessment of changes in flood risk in South Holland due to sea level rise: How can the dunes of dijkring 14 cope with sea level rise ?* (Tech. Rep.). Retrieved from `http://repository.tudelft.nl/`.

Rijksoverheid. (n.d.-a). *Hydra-NL - Helpdesk water.* Retrieved 2021-07-06, from `https://www.helpdeskwater.nl/onderwerpen/applicaties-modellen/applicaties-per/omgevings/omgevings/hydra-nl/`

Rijksoverheid. (n.d.-b). *KosWat - Helpdesk water.* Retrieved 2021-10-13, from `https://www.helpdeskwater.nl/onderwerpen/applicaties-modellen/applicaties-per/aanleg-onderhoud/aanleg-onderhoud/koswat-0/`

Rijksoverheid. (n.d.-c). *MorphAn - Helpdesk water.* Retrieved 2021-07-06, from `https://www.helpdeskwater.nl/onderwerpen/applicaties-modellen/applicaties-per/aanleg-onderhoud/aanleg-onderhoud/morphan/`

Rijksoverheid. (2017). *Voorlanden: wat dragen ze bij en hoe weeg je dat mee?* Retrieved 2021-10-14, from `https://magazines.deltaprogramma.nl/deltanieuws/2017/01/veiligheid`

Rijkswaterstaat. (n.d.-a). *Kaarten — LIWO.* Retrieved 2021-03-26, from `https://basisinformatie-overstromingen.nl/liwo/{#}/maps`

Rijkswaterstaat. (n.d.-b). *Vernieuwen van bruggen, tunnels, sluizen en viaducten.* Retrieved 2021-10-13, from `https://www.rijkswaterstaat.nl/over-ons/onze-organisatie/vervanging-en-renovatie`

Rijkswaterstaat VNK Project. (2012). *Flood risk in the Netherlands, the method in brief.*

Royal HaskoningDHV. (2017). *KBA terrreinhoogte buitendijks - concept.*

Slootjes, N., & Wagenaar, D. (2016). *Factsheets normering primaire waterkeringen.*

Ter Horst, W. (2012). *Overstromingsrisico van dijkringgebieden 14, 15 en 44* (No. November).

Traa, M. (2012). *Wat gebeurt er eigenlijk als de Randstad overstroomt?* Retrieved 2021-10-13, from `https://www.delta21.nl/het-plan/`

Van de Graaff, J., Van Gent, M., Boers, M., Diermanse, F., Walstra, D., & Steetzel, H. (2006). Technisch Rapport Duinafslag: Beoordeling van de veiligheid van duinen als waterkering ten behoeve van Voorschrift Toetsing op Veiligheid 2006. *WL—Delft Hydraulics (H4357)*.

Van de Visch, J., & Bos, M. (2018). *Waterveiligheid Waal-Eemhaven.*

van Balen, W. (2013). *Hydra-Ring: Computational suite for the safety assessment of flood defences.*

Vergouwe, R. (2015). The National Flood Risk Analysis for the Netherlands. *Rijkswaterstaat VNK Project Office*, 119.

Vrijling, JK, & Van Gelder, P. (2000). An analysis of the valuation of a human life. *Esrel*, 197–200.

Vuik, J., & van Balen, W. (2012). *Overstromingskansen voor de Nederlandse kust.*

Waterveiligheidsportaal. (n.d.). *Nationaal Basisbestand Primaire Waterkeringen.* Retrieved 2021-07-06, from `https://waterveiligheidsportaal.nl/#/nss/nss/norm`

Westerhof, S. (2019). *Uncertainties in the derivation of the Dutch flood safety standards* (Unpublished doctoral dissertation). University of Twente.

A. River dikes

A.1. Overview locations dike profiles
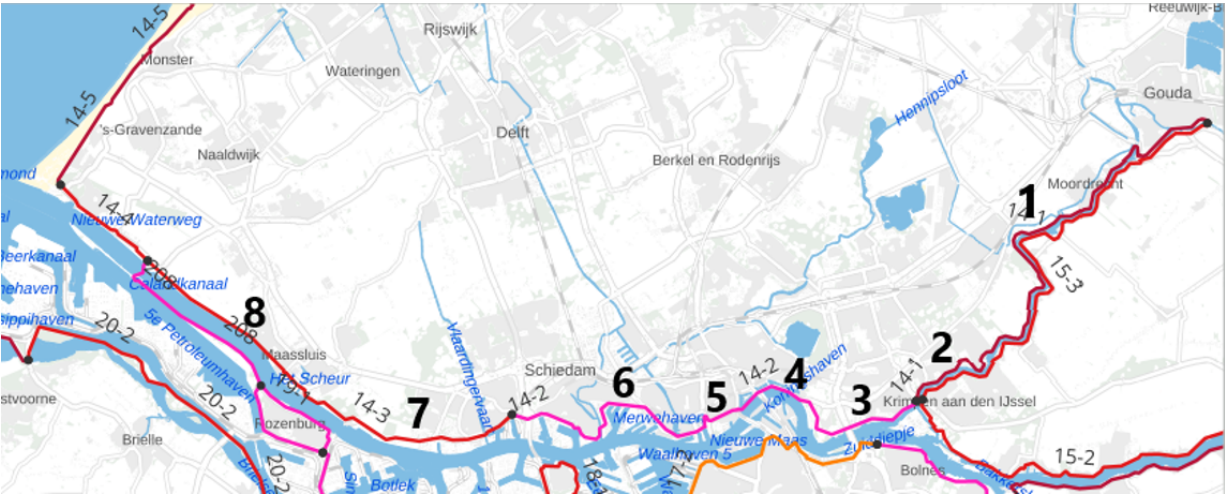
Figure A.1: Overview of the 8 locations for which the cross sections are assessed.

A.2. Cross sections river dikes
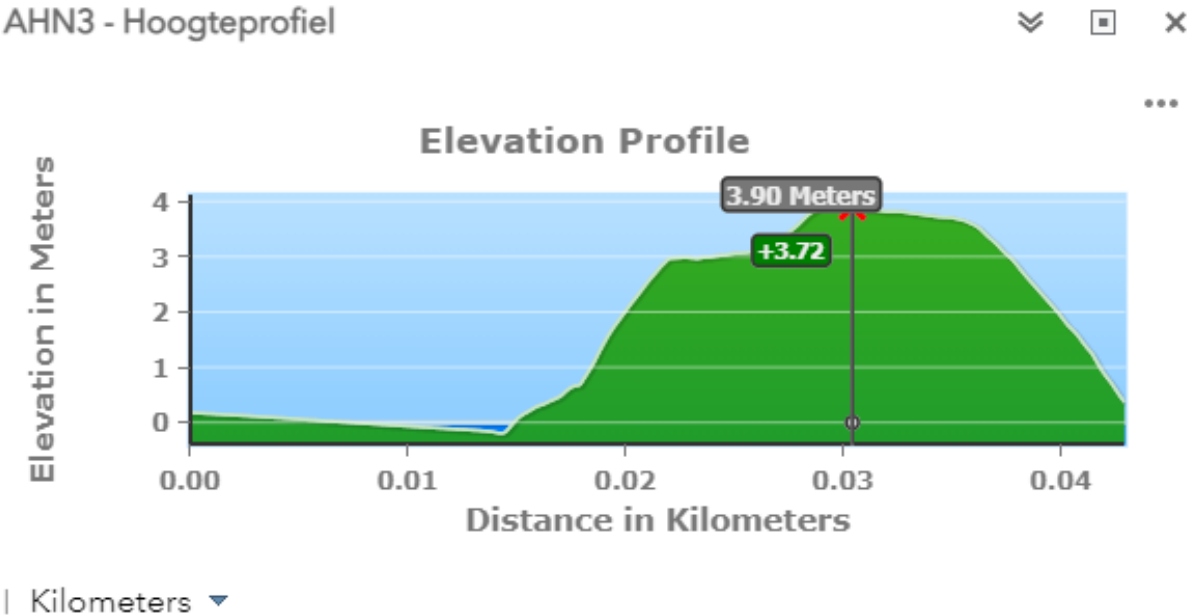
Figure A.2: Cross section of profile 1 along the Hollandse IJssel (Trajectory 14-1) (AHN Viewer, n.d.). On the left side, the river is located.
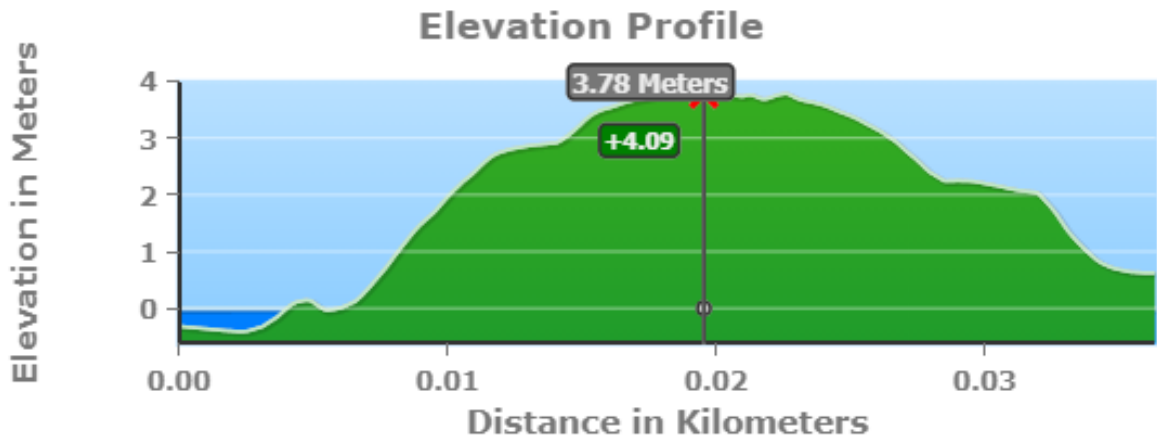
Figure A.3: Cross section of profile 2 along the Hollandse IJssel (Trajectory 14-1) (AHN Viewer, n.d.). On the left side, the river is located.
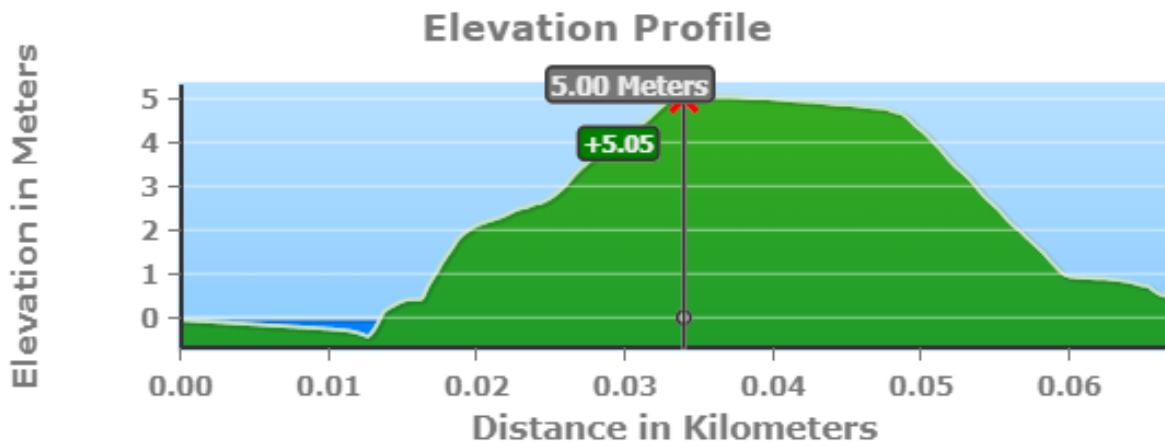
Figure A.4: Cross section of profile 3 along the Nieuwe Maas (Trajectory 14-2) (AHN Viewer, n.d.). On the left side, the river is located.
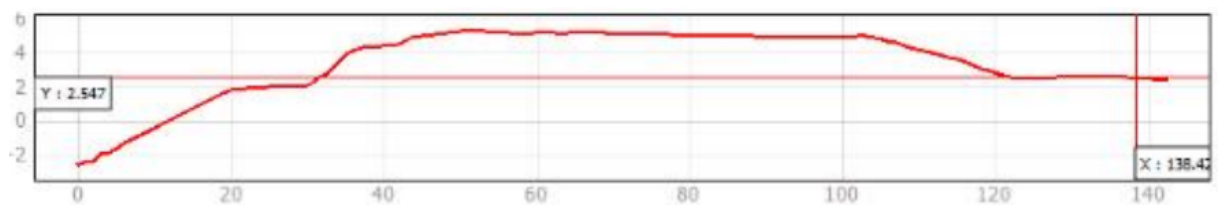
Figure A.5: Cross section of profile 4 along the Nieuwe Maas (Trajectory 14-2). This profile is different from the AHN profiles, because for the Maasboulevard a cross section from recent assessment reports is available (Hoogheemraadschap van Schieland en de Krimpenerwaard, 2019). On the left side, the river is located.
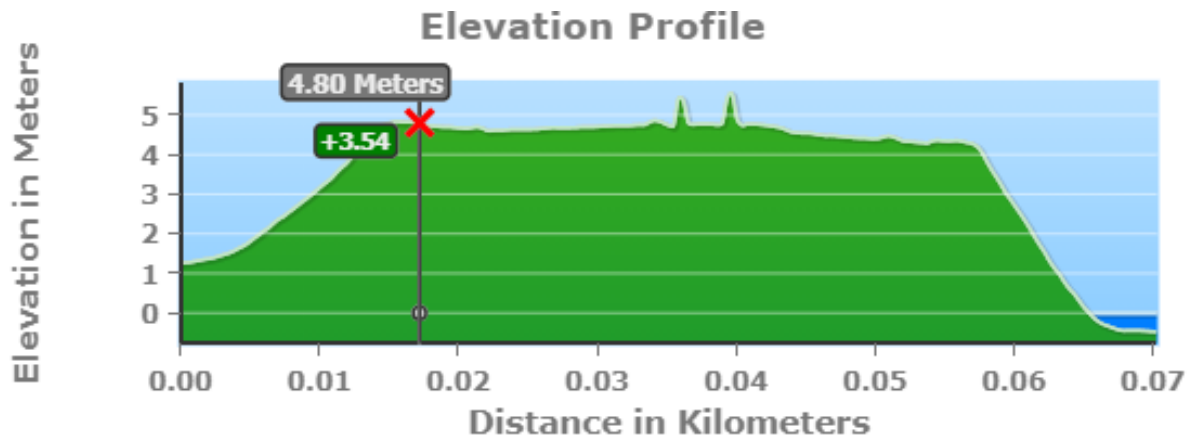
Figure A.6: Cross section of profile 5 along the Nieuwe Maas (Trajectory 14-2) (AHN Viewer, n.d.). On the left side, the river is located.
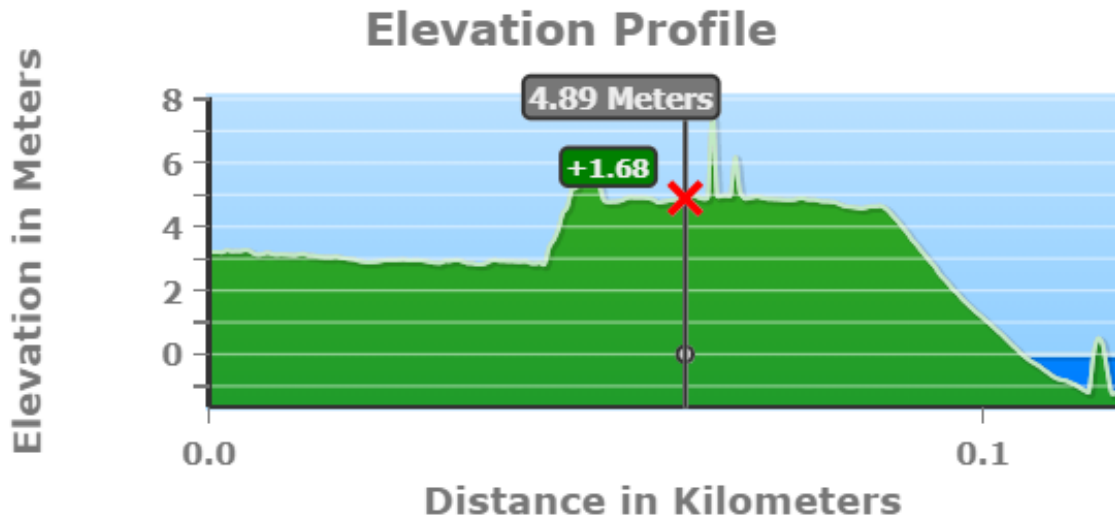
Figure A.7: Cross section of profile 6 along the Nieuwe Maas (Trajectory 14-2) (AHN Viewer, n.d.). On the left side, the river is located.
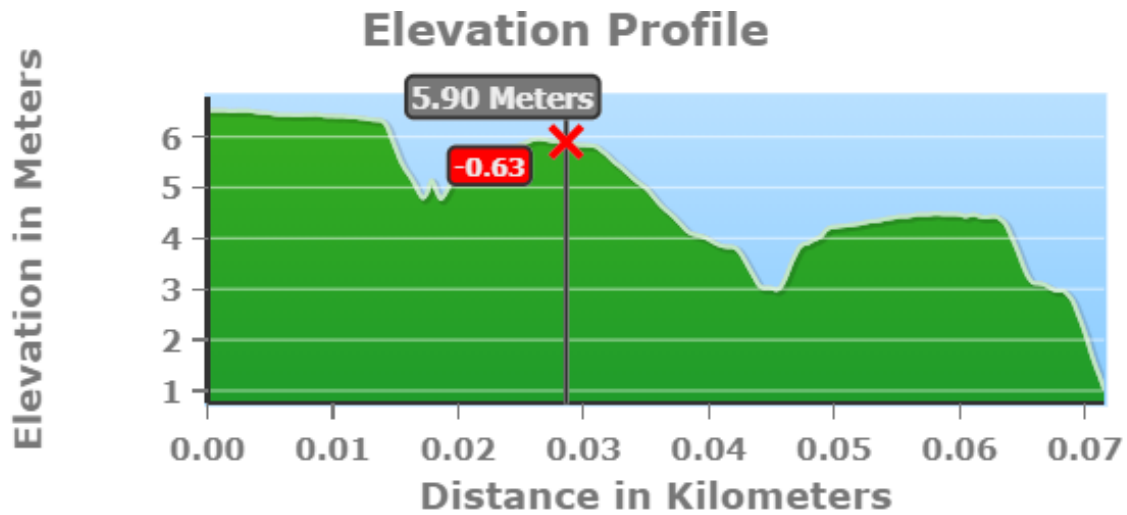
Figure A.8: Cross section of profile 7 along the Nieuwe Waterweg (Trajectory 14-3) (AHN Viewer, n.d.). On the left side, the river is located.
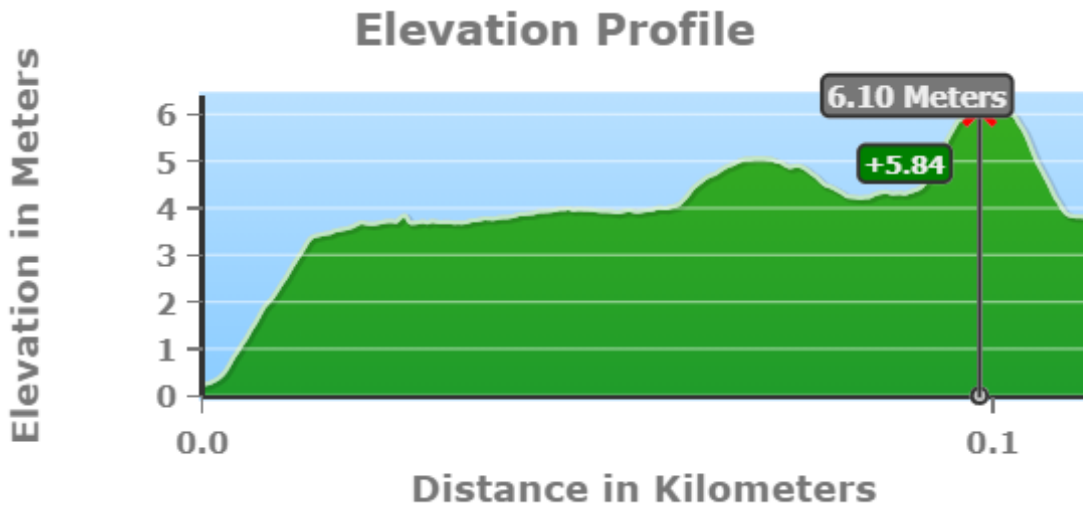
Figure A.9: Cross section of profile 8 along the Nieuwe Waterweg (Trajectory 14-3) (AHN Viewer, n.d.). On the left side, the river is located.

A.3. Probability of failures river dikes

Trajectory 14-1 location 1

Sea level rise [m]	$Pf_{250.000}$ [1/... year]	$Pf_{60.000}$ [1/... year]
0,0	370.000	800.000
0,5	140.000	260.000
1,0	46.000	100.000
1,5	3.500	12.000
2,0	170	600

Table A.1: Overview of the calculated failure probabilities for each scenario for dike trajectory 14-1 location 1. The calculated failure probabilities in column $Pf_{250.000}$ are based on a hydraulic load corresponding to a relative contribution of 24 percent and the failure probabilities in column $Pf_{60.000}$ are based on a hydraulic load corresponding to a relative contribution of 100 percent. The probabilities in column $Pf_{250.000}$ are used in this study. In both cases a length effect of 2 was used (N=2). The target failure probability of trajectory 14-1 is 1/250.000 per year.

Trajectory 14-1 location 2

Sea level rise [m]	$Pf_{250.000}$ [1/... year]	$Pf_{60.000}$ [1/... year]
0,0	1.600.000	2.900.000
0,5	580.000	1.100.000
1,0	130.000	320.000
1,5	15.000	46.000
2,0	1.600	4.800

Table A.2: Overview of the calculated failure probabilities for each scenario for dike trajectory 14-1 location 2. For the explanation of the columns and the target failure probability of 14-1 see the caption of Table A.1.

Trajectory 14-2 location 3

Sea level rise [m]	$Pf_{250.000}$ [1/... year]	$Pf_{60.000}$ [1/... year]
0,0	2.200.000	5.200.000
0,5	510.000	1.800.000
1,0	100.000	400.000
1,5	20.000	80.000
2,0	5.000	17.000

Table A.3: Overview of the calculated failure probabilities for each scenario for dike trajectory 14-2 location 3. The calculated failure probabilities in column $Pf_{833.333}$ are based on a hydraulic load corresponding to a relative contribution of 24 percent and the failure probabilities in column $Pf_{200.000}$ are based on a hydraulic load corresponding to a relative contribution of 100 percent. The probabilities in column $Pf_{833.333}$ are used in this study. In both cases a length effect of 2 was used (N=2). The target failure probability of trajectory 14-2 is 1/833.333 per year.

Trajectory 14-2 location 4

Sea level rise [m]	$Pf_{250.000}$ [1/... year]	$Pf_{60.000}$ [1/... year]
0,0	3.100.000	3.000.000
0,5	500.000	680.000
1,0	90.000	120.000
1,5	17.000	24.000
2,0	3.500	4.600

Table A.4: Overview of the calculated failure probabilities for each scenario for dike trajectory 14-2 location 4. For the explanation of the columns and the target failure probability of 14-2 see the caption of Table A.3.

Trajectory 14-2 location 5

Sea level rise [m]	$Pf_{250.000}$ [1/... year]	$Pf_{60.000}$ [1/... year]
0,0	22.000.000	34.000.000
0,5	3.400.000	13.000.000
1,0	520.000	2.500.000
1,5	89.000	400.000
2,0	20.000	74.000

Table A.5: Overview of the calculated failure probabilities for each scenario for dike trajectory 14-2 location 5. For the explanation of the columns and the target failure probability of 14-2 see the caption of Table A.3.

Trajectory 14-2 location 6

Sea level rise [m]	$Pf_{250.000}$ [1/... year]	$Pf_{60.000}$ [1/... year]
0,0	11.000.000	4.300.000
0,5	3.300.000	2.600.000
1,0	500.000	1.200.000
1,5	76.000	210.000
2,0	15.000	36.000

Table A.6: Overview of the calculated failure probabilities for each scenario for dike trajectory 14-2 location 6. For the explanation of the columns and the target failure probability of 14-2 see the caption of Table A.3.

Trajectory 14-3 location 7

Sea level rise [m]	$Pf_{250.000}$ [1/... year]	$Pf_{60.000}$ [1/... year]
0,0	7.500.000.000	5.700.000.000
0,5	1.300.000.000	2.400.000.000
1,0	210.000.000	470.000.000
1,5	33.000.000	77.000.000
2,0	2.000.000	13.000.000

Table A.7: Overview of the calculated failure probabilities for each scenario for dike trajectory 14-3 location 7. The calculated failure probabilities in column $Pf_{83.333}$ are based on a hydraulic load corresponding to a relative contribution of 24 percent and the failure probabilities in column $Pf_{20.000}$ are based on a hydraulic load corresponding to a relative contribution of 100 percent. The probabilities in column $Pf_{83.333}$ are used in this study. In both cases a length effect of 2 was used (N=2). The target failure probability of trajectory 14-3 is 1/83.333 per year.

Trajectory 14-3 location 8

Sea level rise [m]	$Pf_{250.000}$ [1/... year]	$Pf_{60.000}$ [1/... year]
0,0	86.000.000	240.000.000
0,5	14.000.000	82.000.000
1,0	2.000.000	12.000.000
1,5	290.000	2.000.000
2,0	44.000	280.000

Table A.8: Overview of the calculated failure probabilities for each scenario for dike trajectory 14-3 location 8. For the explanation of the columns and the target failure probability of 14-3 see the caption of Table A.7.

B. Duros-plus model

The purpose of this model is to determine the amount of dune erosion after the occurrence of a random, heavy storm. This dune erosion is determined by the coastal profile before the storm, the storm surge conditions and the diameter of the dune sand. The storm surge conditions consist of the storm surge height, h_{max}, and wave height, H_{0s}, and wave period, T_p, at deep water (depth at approximately NAP -20m). The erosion profile is a function of these parameters and the falling velocity of the dune sand in still water of 5 degrees Celsius. For an arbitrary erosion profile, see Figure B.1.

The Duros-plus model uses the following assumptions (Van de Graaff et al. (2006)):

- The upper part of the coastal profile present before the storm is transformed into a erosion profile. Changes to the profile in deeper water are considered negligible.

- The vertical location of the erosion profile is related to the height of the maximum sea level, but the shape of the breakwater profile is not influenced by this water level. The shape is also unaffected by the location of the coastal profile before the storm, the direction of wave attack on the profile and the presence of debris from buildings, beach wall, promenade or dune foot defences.

- The transport of the eroded sand is exclusively in a seaward direction.

- Eventually, a two-dimensional impact profile is determined.

- Usually, the timeline of the water level is also taken into account in the determination of the erosion profile. This results in less erosion for a steep water level gradient at the maximum storm surge level and more erosion for a gradual water level gradient around the maximum storm surge level. This is not taken into account in the DUROS-plus model.

- The maximum values for h_{max}, H_{0s} and T_p occur simultaneously. These maximum values occur when the maximum storm surge level is reached. These values determine the shape and vertical location of the impact profile.

- The total volume of horizontally eroded sand during a storm $[m^3/m]$ is equal to the amount of deposition. So, net losses of sand will not be taken into account.

- In Figure B.1 there are several erosion points. For coastal managers, R* is the most important. In the remainder of this thesis, the erosion point means point R*.
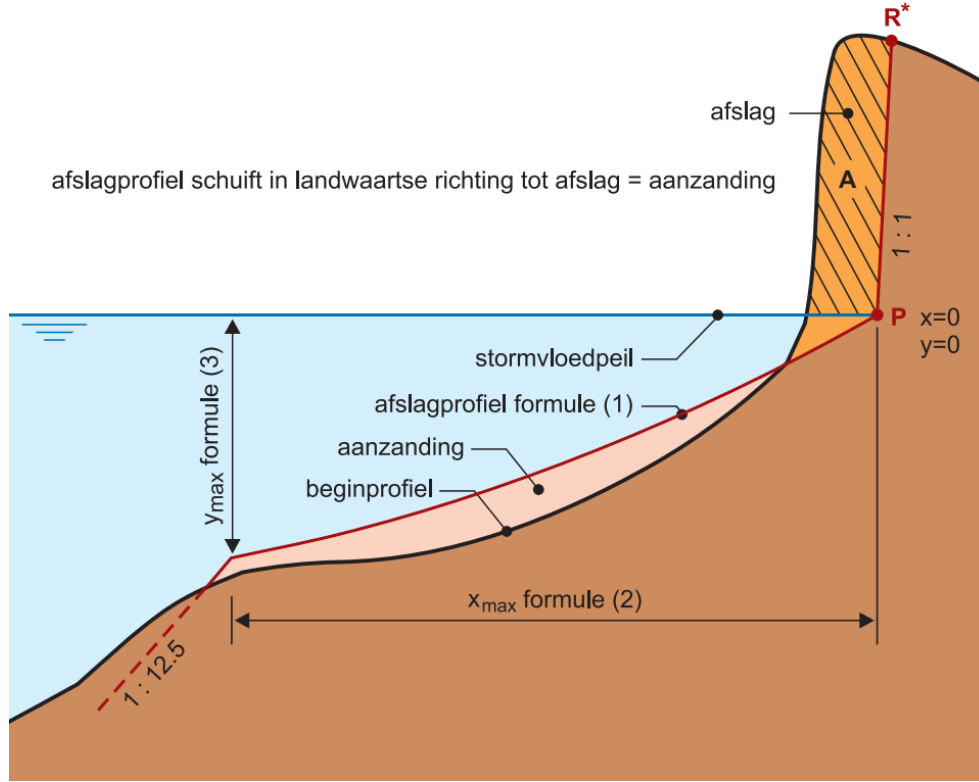
Figure B.1: An overview of the erosion profile of arbitrary dune profile. 'A' is the erosion volume (in Dutch: afslag), 'beginprofiel' = dune profile before the storm, 'afslagprofiel formule' = dune profile after the storm according to the formula, 'stormvloedpeil' = storm surge level, P = erosion point and R* = erosion point at the surface (Van de Graaff et al. (2006)).

The dune foot is at a height of NAP + 3m before the storm, but after the storm this dune foot is at the maximum storm surge level. From this point (x = 0, y = 0) the erosion profile moves parabolic in a seaward direction. For the parabolic course, see Equation B.1.

$$\left(\frac{7.6}{H_{0s}}\right) y = 0.4714 \left(\left(\left(\frac{7.6}{H_{0s}}\right)^{1.28} \left(\frac{12}{T_p}\right)^{0.45} \left(\frac{w}{0.0268}\right)^{0.56} x + 18\right)^{0.5} - 2.0 \tag{B.1}$$

This parabolic gradient holds up to the point x_{max}. This point can be determined by Equation B.2. In a seaward direction from this point there is a straight gradient of 1:12.5 until the erosion profile intersects again with the original profile before the storm.

$$x_{max} = 250 \left(\frac{H_{0s}}{7.6}\right)^{1.28} \left(\frac{0.0268}{w}\right)^{0.56} \tag{B.2}$$

Equation B.1 and Equation B.2 result in Equation B.3.

$$y_{max} = \left(0.4714 \left(250 \left(\frac{12}{T_p}\right)^{0.45} + 18\right)^{0.5} - 2.0\right) \left(\frac{H_{0s}}{7.6}\right) \tag{B.3}$$

The above formulas relate to storm surges with wave periods between 12 and 20 s. For wave periods greater than 20 s, $T_p = 20$ s and for T_p less than 12 s, $T_p = 12$ s is applied. The falling velocity in seawater of 5 degrees of the dune sand can be determined with Equation B.4.

$$\log \frac{1}{w} = 0.476(\log D_{50})^2 + 2.180 \log D_{50} + 3.226 \tag{B.4}$$

These are the calculation rules to determine the shape of the erosion profile. These calculation rules are also used for the MorphAn application, which is discussed in more detail in Section 4.4.

Dune safety model

A simple method has been developed to determine whether a dune meets the safety requirements. The inputs of the parameters that finally determine the erosion are determined so that the erosion as output is equal to the required maximum allowed probability of a dune breach. This amount of dune erosion is also called the normative dune erosion (Van de Graaff et al. (2006)). A point R in the profile with an exceedance probability of 10^{-5} corresponds to the 10^{-5} erosion point. For a safe dune, this point lies so seaward of the landward boundary of the dune area that a boundary profile can still be fitted. In a cross-section, these points are connected to each other to form an erosion line. In the 2-dimensional approach of the DUROS-plus model, an erosion line is thus finally determined which consists of a number of line segments. When narrow dunes are tested for safety, this normative dune erosion must be within the dune profile. Very wide dunes generally have no safety problem. This normative erosion is then important to find out which part of the dune will erode under the design conditions.

The test method with DUROS-plus shows when a dune breach occurs. The results of this method are either no dune breach (safe) or a dune breach (unsafe). In the complex method, the duration of the high water peak is included in the probabilistic calculations. This is not the case in the DUROS-plus model, but is included in an additional factor, T. In addition to the variation in duration of the high water peak, the inaccuracy of the DUROS-plus model is also included in this additional factor. This is an supplement factor to the volume of dune erosion A $[m^3/m]$. The supplement factor is 25 percent of the calculated volume of dune erosion, which therefore includes the duration of the storm surge as well as the accuracy of the model, see Figure B.2.
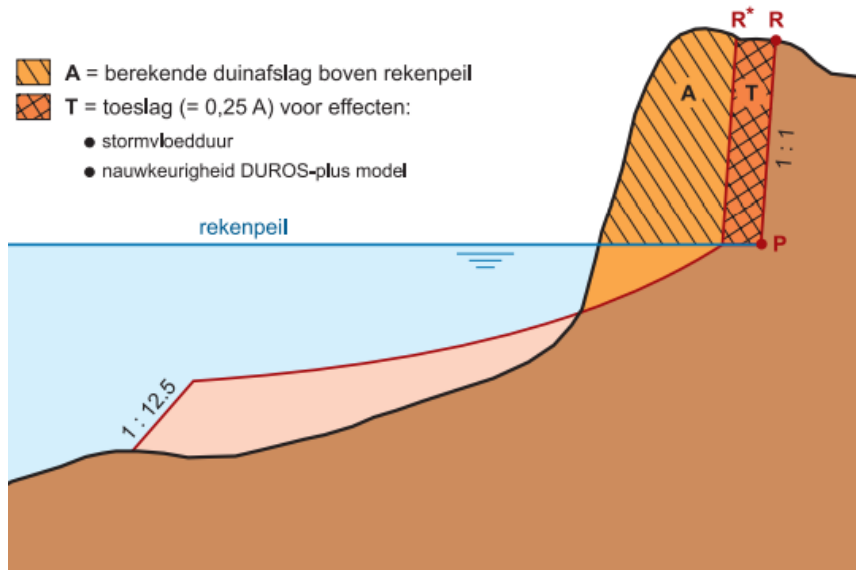
Figure B.2: Application of the surcharge factor, T, due to the variation in duration of the storm surge and the inaccuracy of the DUROS-plus model (Van de Graaff et al. (2006))

Another method of assessing whether the dune is still 'safe' is to compare the erosion profile with the boundary profile. The boundary profile have to fit landward of the critical erosion point for the dune to be considered safe. The boundary profile is determined using the following formula using the design level (RP), the significant wave height and period. The minimum crest height, h_0, must have a minimum height of RP + 2.5 m.

$$h_0 = RP + 0.12T_p\sqrt{H_{0s}} \tag{B.5}$$

The width of the boundary profile is 3m. The rule for the slope of the inner slope is that it is equal or less to 1:2 and the outer slope of the boundary profile is 1:1. An example of a boundary profile is given in Figure B.3.

Figure B.3: Boundary profile in a dune cross section (Van de Graaff et al. (2006)).

The location of the boundary profile is stated in the Legger. In most situations, the dune is much wider than necessary for safety and it is therefore possible to freely choose the position of the boundary profile (Van de Graaff et al. (2006)). This position is then chosen landward of the normative erosion profile.

In case the dune height is too low and a boundary profile is not possible to fit, but there is enough dune width, the alternative bound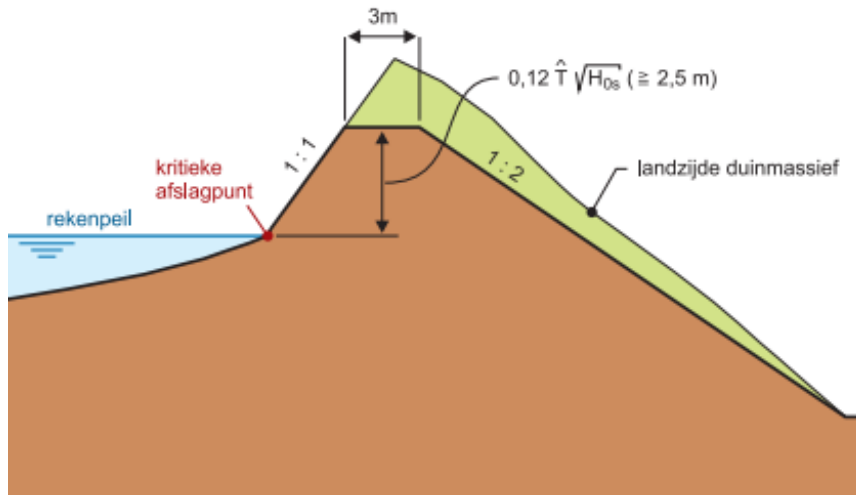ary profile can be used. In this alternative boundary profile, the lack of dune height is compensated by the dune width to still assess the dune as safe. The rule here is that the volume per m above the RP of the alternative boundary profile must be equal to the volume per m of the original boundary profile. In addition, the minimum height above the RP must be 1m (Van de Graaff et al. (2006)). An example of an alternative boundary profile is given in Figure B.4.
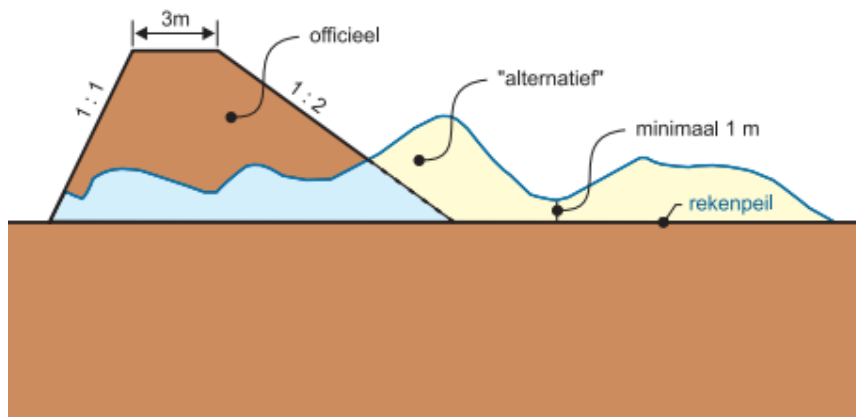
Figure B.4: Alternative boundary profile compared with the original profile (Van de Graaff et al. (2006)).

The coast between Den Helder and Hoek van Holland falls in class 1 of coastal curvature. As a result, this is considered a straight coast in the calculations and the reference value G_0 for the transport difference is 0. With curved coasts there can be losses of sand from the dune profile due to differences in longitudinal profile. Since this is not the case for the dunes of dike ring 14, the underlying theory will not be discussed.

C. Output MorphAn dunes
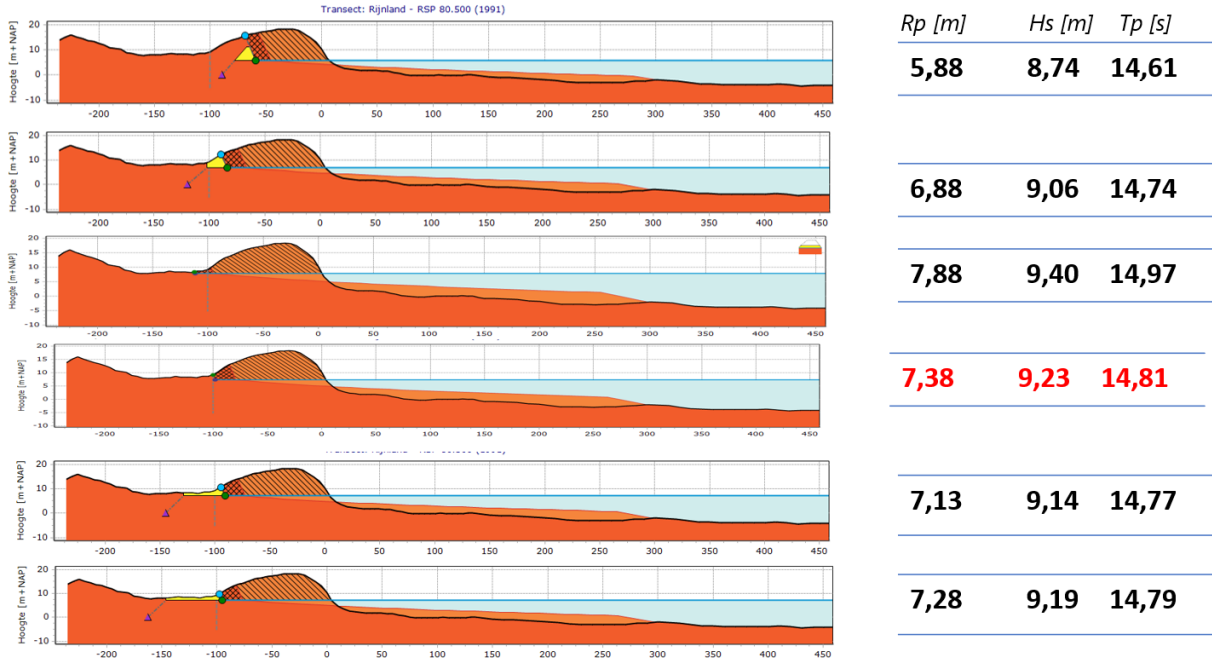
Figure C.1: Overview of the calculations in MorphAn for the location Noordwijk. On the right, the hydraulic loads are mentioned as the sea water level, Rp, significant wave height, Hs, and the wave period, Tp. The hydraulic loads are shown in red for which MorphAn is not able to return a boundary profile. For this sea water level the recurrence levels are determined using Hydra-NL for each different scenario of sea level rise.

	Rp [m]	Hs [m]	Tp [s]
	5,83	8,74	14,61
	6,83	9,06	14,74
	7,83	9,40	14,87
	8,18	9,52	14,92
	8,21	9,53	14,92

Figure C.2: Overview of the calculations in MorphAn for the location Katwijk. On the right, the hydraulic loads are mentioned as the sea water level, Rp, significant wave height, Hs, and the wave period, Tp. The hydraulic loads are shown in red for which MorphAn is not able to return a boundary profile. For this sea water level the recurrence levels are determined using Hydra-NL for each different scenario of sea level rise.

D. Hydrodynamic models
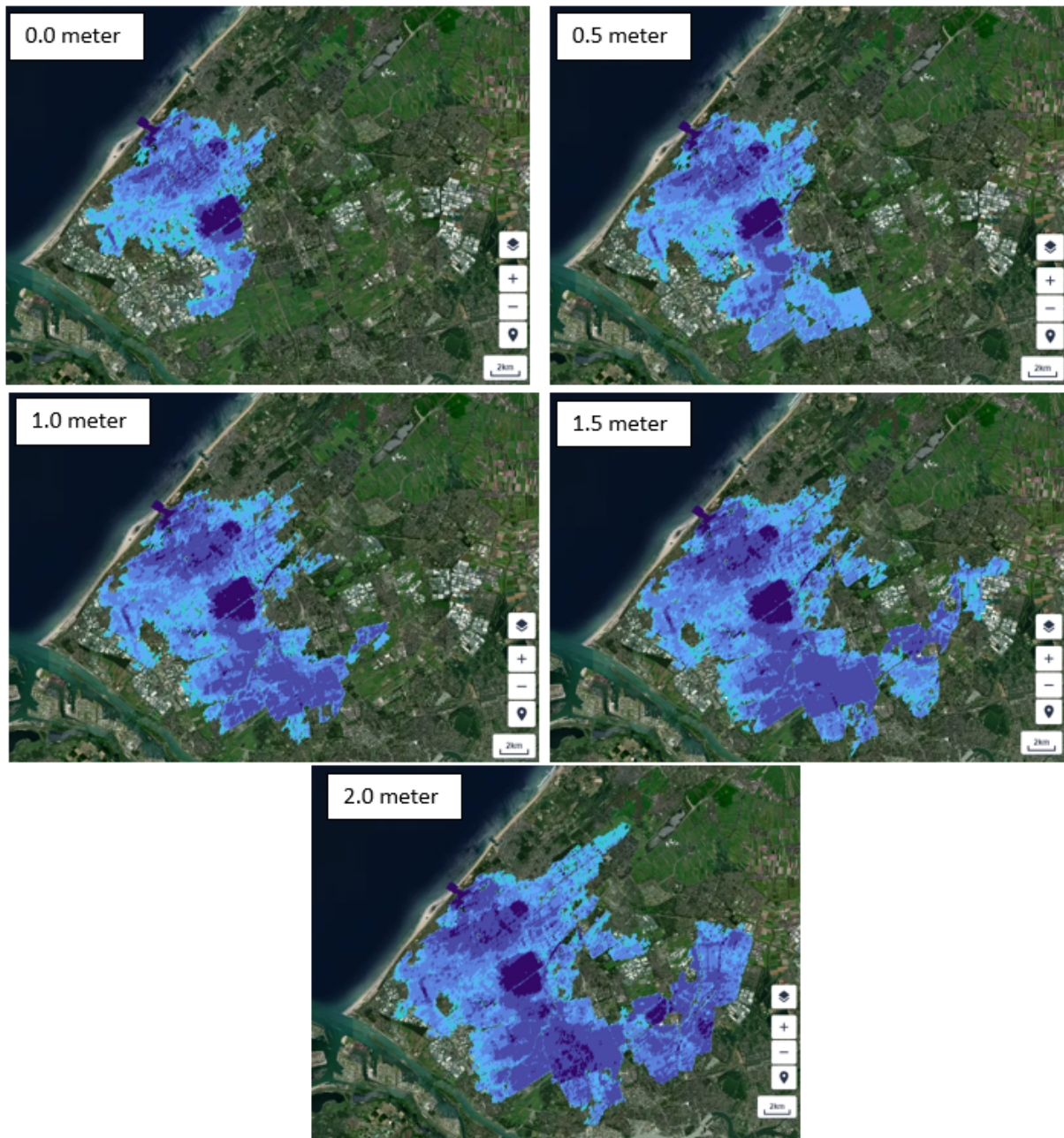
Figure D.1: Hydrodynamic models for the breach location at Kijkduin (Ranneft, 2020).
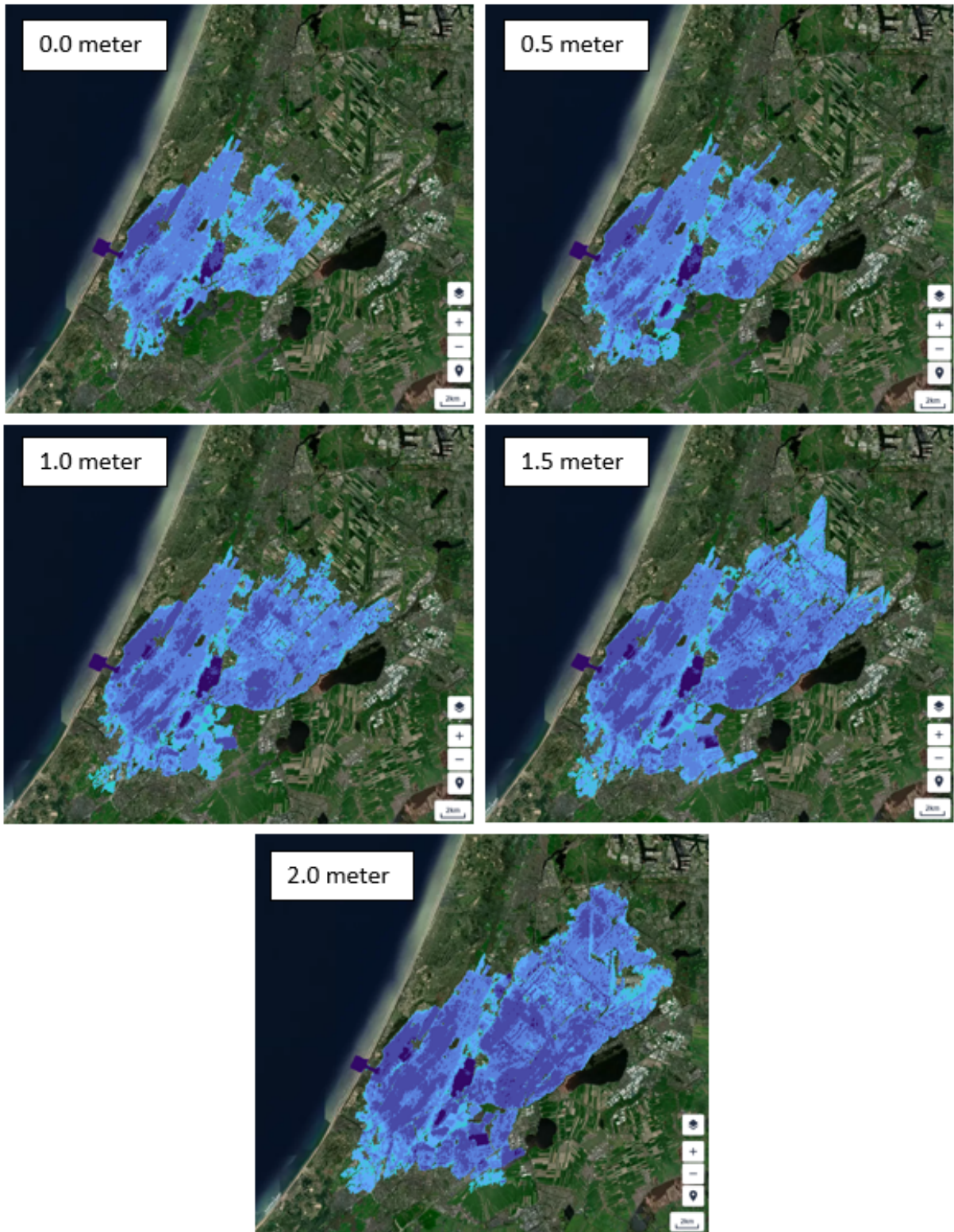
Figure D.2: Hydrodynamic models for the breach location at Noordwijk (Ranneft, 2020).

E. Reinforcement projects

E.1. Cross-sections reinforced profiles

Figure E.1: Cross section of an example of reinforcing profile 1. In this cross-section, the increase in crest level is 0,75 m. On the left side is the river located.
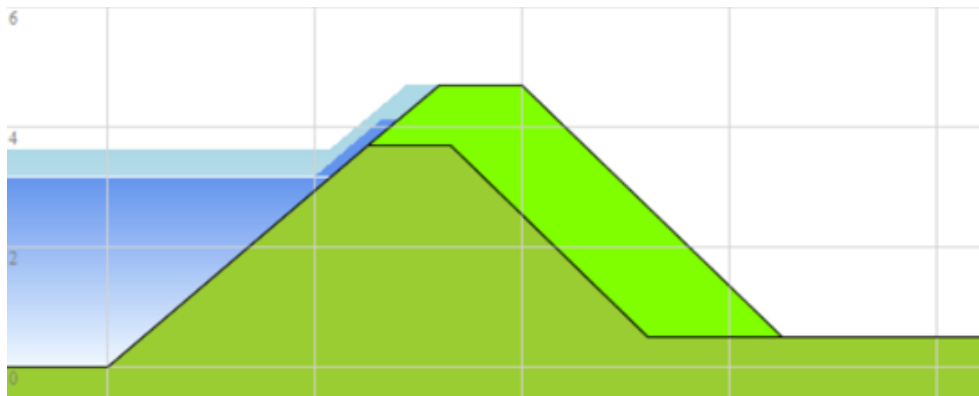
Figure E.2: Cross section of an example of reinforcing profile 2. In this cross-section, the increase in crest level is 1,01 m. On the left side is the river located.

Figure E.3: Cross section of an example of reinforcing profile 3. In this cross-section, the increase in crest level is 0,96 m. On the left side is the river located.
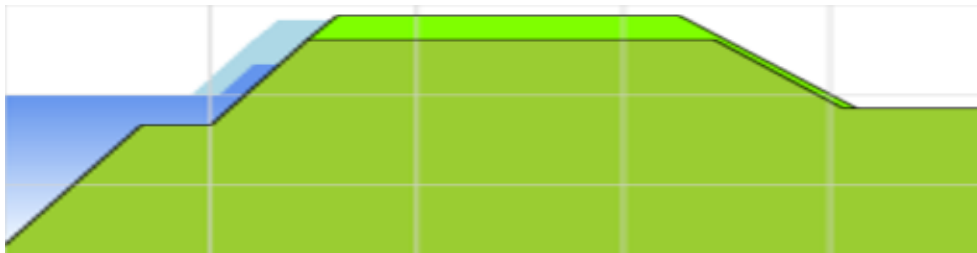
Figure E.4: Cross section of an example of reinforcing profile 4. In this cross-section, the increase in crest level is 0,8 m. On the left side is the river located.
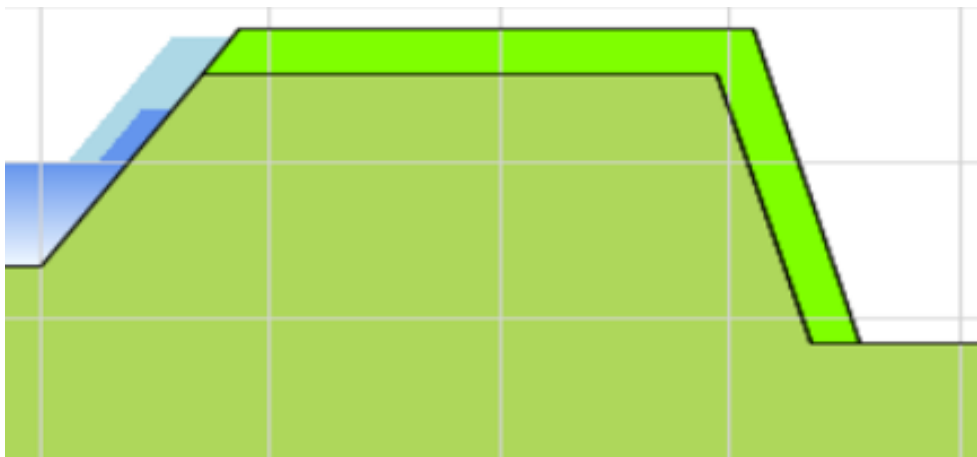
Figure E.5: Cross section of an example of reinforcing profile 5. In this cross-section, the increase in crest level is 0,84 m. On the left side is the river located.
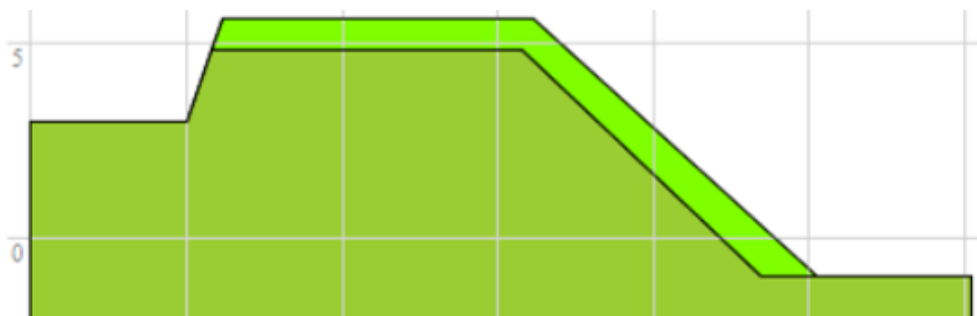
Figure E.6: Cross section of an example of reinforcing profile 6. In this cross-section, the increase in crest level is 0,85 m. On the left side is the river located.
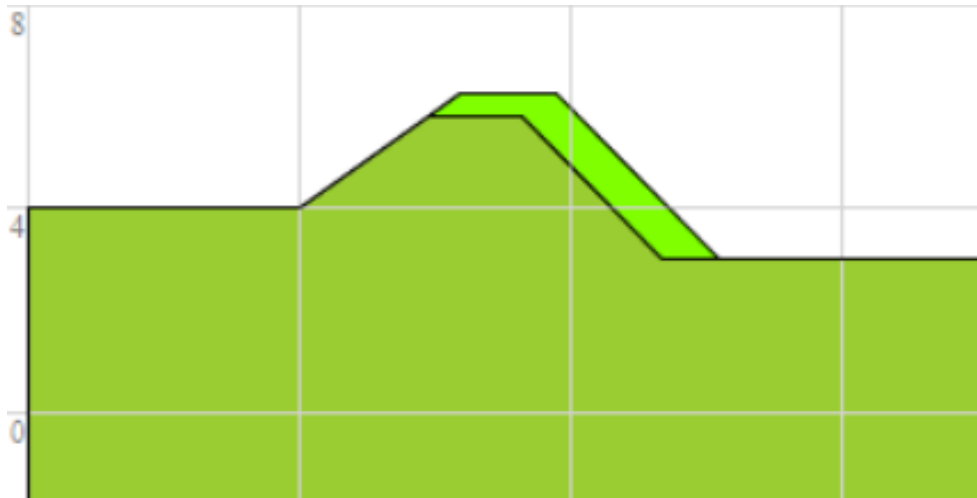
Figure E.7: Cross section of an example of reinforcing profile 7. In this cross-section, the increase in crest level is 0,48 m. On the left side is the river located.
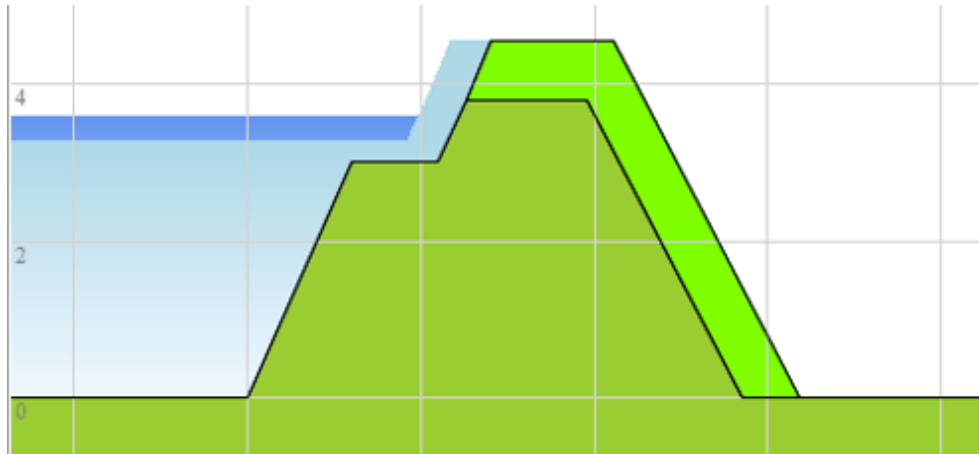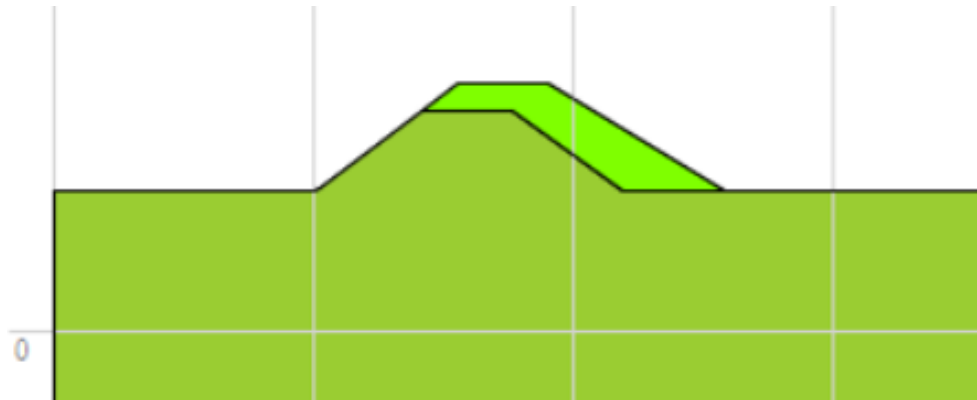

Figure E.8: Cross section of an example of reinforcing profile 8. In this cross-section, the increase in crest level is 0,72 m. On the left side is the river located.

E.2. Total costs compared to probability of failure river dikes

Increasing crest height[m]		Consequences	
Profile 1	Profile 2	Costs [million euros]	Probability of failure [1/... year]
0	0	0	3.500
0,75	0	82,9	15.000
0,75	0,51	228,3	66.000
0,85	0,51	228,9	97.000
1,25	0,51	260,2	110.000
1,25	0,61	264,1	170.000
1,25	1,01	291,9	460.000
1,55	1,01	292,1	790.000
1,55	1,31	303,5	1.500.000
1,75	1,31	304,8	2.500.000
1,75	1,51	309,6	3.200.000
2,15	1,51	340,6	5.500.000

Table E.1: Total costs inflation included corresponding to different probability of failures for trajectory 14-1 in case of the scenario with 1,5m sea level rise.

Increasing crest height[m]		Consequences	
Profile 1	Profile 2	Costs [million euros]	Probability of failure [1/... year]
0	0	0	46.000
0,75	0	82,9	130.000
0,75	0,51	228,3	850.000
0,85	0,51	228,9	950.000
0,85	0,61	232,7	1.200.000
1,25	0,61	264,1	1.400.000
1,25	1,01	291,9	5.900.000
1,55	1,01	292,1	6.600.000

Table E.2: Total costs inflation included corresponding to different probability of failures for trajectory 14-1 in case of the scenario with 1m sea level rise.

Increasing crest height[m]		Consequences	
Profile 1	Profile 2	Costs [million euros]	Probability of failure [1/... year]
0	0	0	140.000
0,75	0	82,9	580.000
0,75	0,51	228,3	2.600.000
0,85	0,51	228,9	3.900.000
1,25	0,51	260,2	4.200.000
1,25	0,61	264,1	6.200.000

Table E.3: Total costs inflation included corresponding to different probability of failures for trajectory 14-1 in case of the scenario with 0,5m sea level rise.

Increasing crest height[m]				Consequences	
Profile 3	Profile 4	Profile 5	Profile 6	Costs [million euros]	Probability of failure [1/... year]
0	0	0	0	0	3.500
0	0,2	0	0	107,1	4.900
0,24	0,2	0	0	141,9	7.600
0,24	0,68	0	0	146,2	12.000
0,48	0,68	0	0	155,3	15.000
0,48	0,68	0	0,24	402,7	20.000
0,48	0,68	0,36	0,24	470,2	32.000
0,72	0,68	0,36	0,24	471,3	38.000
0,72	0,68	0,36	0,72	492,7	49.000
0,72	0,8	0,36	0,72	492,7	78.000
0,72	1,04	0,36	0,72	499,1	80.000
0,96	1,04	0,36	0,72	501,2	81.000
0,96	1,04	0,84	0,72	503,4	200.000
0,96	1,16	0,84	0,72	504,5	210.000
1,08	1,16	0,84	0,72	506,6	250.000
1,08	1,16	0,84	0,84	509,8	320.000

Table E.4: Total costs inflation included corresponding to different probability of failures for trajectory 14-2 in case of the scenario with 2m sea level rise.

Increasing crest height[m]				Consequences	
Profile 3	Profile 4	Profile 5	Profile 6	Costs [million euros]	Probability of failure [1/... year]
0	0	0	0	0	17.000
0	0,2	0	0	107,1	20.000
0,24	0,2	0	0	141,9	38.000
0,24	0,68	0	0	146,2	52.000
0,48	0,68	0	0	155,3	76.000
0,48	0,68	0	0,24	402,7	89.000
0,48	0,68	0,36	0,24	470,2	130.000
0,72	0,68	0,36	0,24	471,3	190.000
0,72	0,68	0,36	0,72	492,7	250.000
0,72	0,8	0,36	0,72	492,7	340.000
0,96	0,8	0,36	0,72	494,8	360.000
0,96	0,8	0,84	0,72	497,0	390.000
0,96	1,04	0,84	0,72	503,4	990.000
0,96	1,16	0,84	0,72	504,5	1.300.000

Table E.5: Total costs inflation included corresponding to different probability of failures for trajectory 14-2 in case of the scenario with 1,5m sea level rise.

Increasing crest height[m]				Consequences	
Profile 3	Profile 4	Profile 5	Profile 6	Costs [million euros]	Probability of failure [1/... year]
0	0	0	0	0	90.000
0	0,2	0	0	107,1	98.000
0,24	0,2	0	0	141,9	200.000
0,24	0,68	0	0	146,2	250.000
0,48	0,68	0	0	155,3	500.000
0,48	0,68	0	0,24	402,7	520.000
0,48	0,68	0,36	0,24	470,2	640.000
0,72	0,68	0,36	0,24	471,3	1.300.000
0,72	0,8	0,36	0,24	471,3	1.300.000
0,72	0,8	0,36	0,72	492,7	1.600.000
0,96	0,8	0,36	0,72	494,8	2.000.000

Table E.6: Total costs inflation included corresponding to different probability of failures for trajectory 14-2 in case of the scenario with 1m sea level rise.

Increasing crest height[m]				Consequences	
Profile 3	Profile 4	Profile 5	Profile 6	Costs [million euros]	Probability of failure [1/... year]
0	0	0	0	0	500.000
0	0,2	0	0	107,1	510.000
0,24	0,2	0	0	141,9	1.100.000
0,24	0,68	0	0	146,2	1.300.000
0,48	0,68	0	0	155,3	3.300.000
0,48	0,68	0	0,24	402,7	3.300.000
0,72	0,68	0	0,24	403,8	3.400.000
0,72	0,68	0,36	0,24	471,3	7.100.000

Table E.7: Total costs inflation included corresponding to different probability of failures for trajectory 14-2 in case of the scenario with 0,5m sea level rise.

Increasing crest height[m]		Consequences	
Profile 7	Profile 8	Costs [million euros]	Probability of failure [1/... year]
0	0	0	44.000
0	0,12	138,5	71.000
0	0,36	186,1	180.000
0	0,48	186,3	290.000
0	0,72	186,7	730.000
0	0,84	213,9	1.200.000
0	0,96	215,1	1.900.000
0	1,32	223,2	2.000.000
0,12	1,32	300,9	3.200.000
0,36	1,32	301,5	7.500.000

Table E.8: Total costs inflation included corresponding to different probability of failures for trajectory 14-3 in case of the scenario with 2m sea level rise. For trajectory 14-3, this has only been done for the scenario with 2m sea level rise. The other scenarios already have very low probabilities of failure and the expectation is that trajectory 14-3 in those scenarios does not need to be reinforced.

E.3.   Total costs compared to probability of failure dunes

Volume reinforcement [m^3/m]	Costs [million euros]	Sea water level dune breach [m+NAP]	Probability of failure [1/... year]
0	0	7,38	34.000
150	47,0	7,63	63.000
400	125,3	7,88	120.000
750	234,9	8,38	710.000

Table E.9: Total costs, inflation included, corresponding to different probability of failures for the Noordwijk profile in case of the scenario with 1,5m sea level rise.

Volume reinforcement [m^3/m]	Costs [million euros]	Sea water level dune breach [m+NAP]	Probability of failure [1/... year]
0	0	7,38	120.000
150	47,0	7,63	250.000
400	125,3	7,88	710.000
750	234,9	8,38	28.000.000

Table E.10: Total costs, inflation included, corresponding to different probability of failures for the Noordwijk profile in case of the scenario with 1m sea level rise.

Volume reinforcement [m^3/m]	Costs [million euros]	Sea water level dune breach [m+NAP]	Probability of failure [1/... year]
0	0	7,38	710.000
150	47,0	7,63	4.400.000
400	125,3	7,88	28.000.000
750	234,9	8,38	1,2E+09

Table E.11: Total costs, inflation included, corresponding to different probability of failures for the Noordwijk profile in case of the scenario with 0,5m sea level rise.

Volume reinforcement $[m^3/m]$	Costs [million euros]	Probability of failure [1/... year]
0	0	9.000
150	27,6	19.000
400	73,6	34.000
750	137,9	120.000

Table E.12: Total costs, inflation included, corresponding to different probability of failures for the Kijkduin profile in case of the scenario with 2m sea level rise.

Volume reinforcement $[m^3/m]$	Costs [million euros]	Probability of failure [1/... year]
0	0	30.000
150	27,6	63.000
400	73,6	120.000
750	137,9	710.000

Table E.13: Total costs, inflation included, corresponding to different probability of failures for the Kijkduin profile in case of the scenario with 1,5m sea level rise. An overview is not given for the scenarios with 0 to 1 meter sea level rise, as it is expected that no reinforcements are needed due to the already low probabilities of failure of the original profiles.

Volume reinforcement $[m^3/m]$	Costs [million euros]	Probability of failure [1/... year]
0	0	9.000
150	11,9	19.000
400	31,7	34.000
750	59,6	120.000

Table E.14: Total costs, inflation included, corresponding to different probability of failures for the Monster profile in case of the scenario with 2m sea level rise.

Volume reinforcement $[m^3/m]$	Costs [million euros]	Probability of failure [1/... year]
0	0	30.000
150	11,9	63.000
400	31,7	120.000
750	59,6	710.000

Table E.15: Total costs, inflation included, corresponding to different probability of failures for the Monster profile in case of the scenario with 1,5m sea level rise. An overview is not given for the scenarios with 0 to 1 meter sea level rise, as it is expected that no reinforcements are needed due to the already low probabilities of failure of the original profiles.

F. Economic optimisations

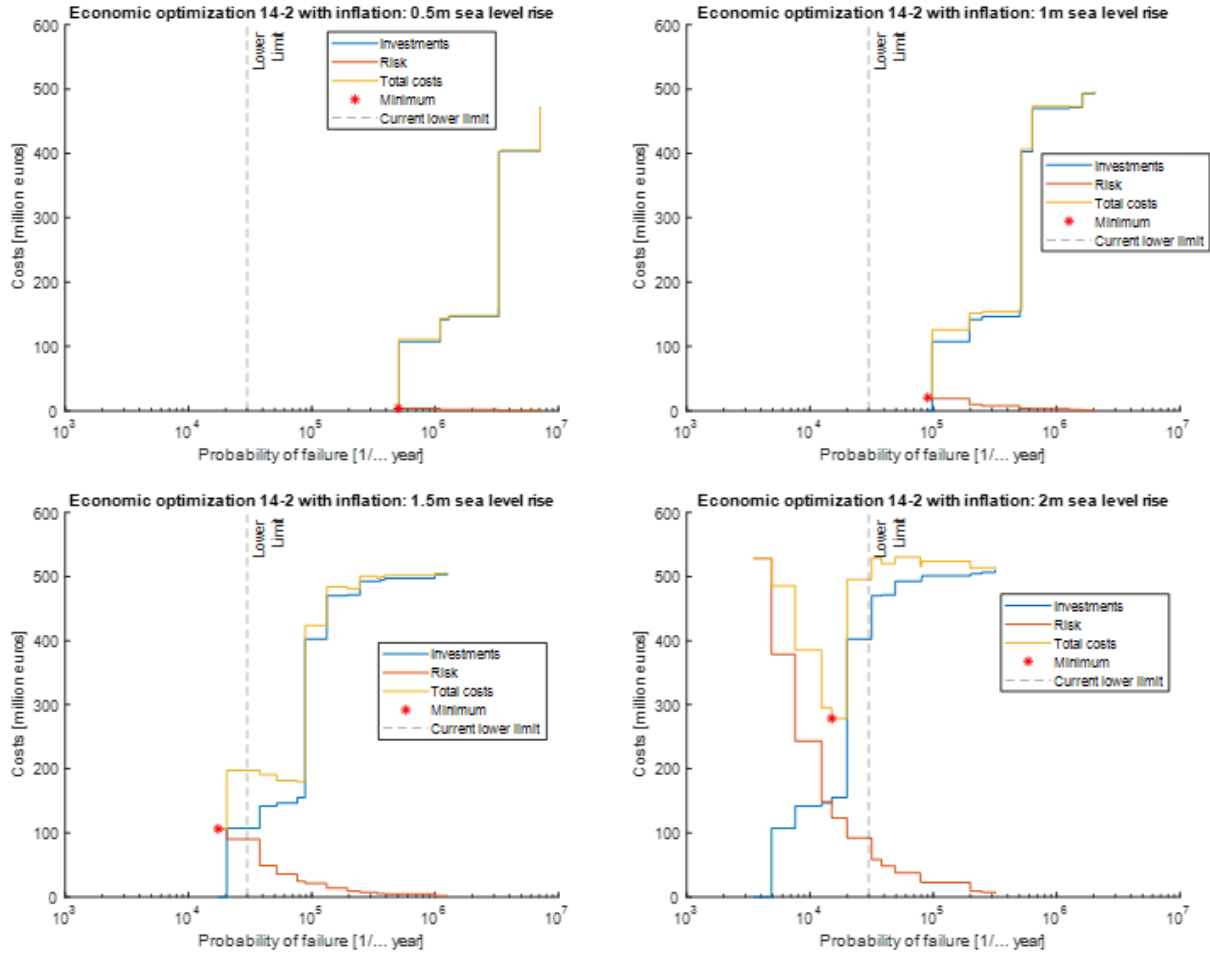## F.1. Graphs economic optimisations

Figure F.1: Overview of the economic optimization for the scenarios of 0,5 to 2 m sea level rise for trajectory 14-2. The threshold / lower limit of the safety level of trajectory 14-2 is 1/30.000 per year.
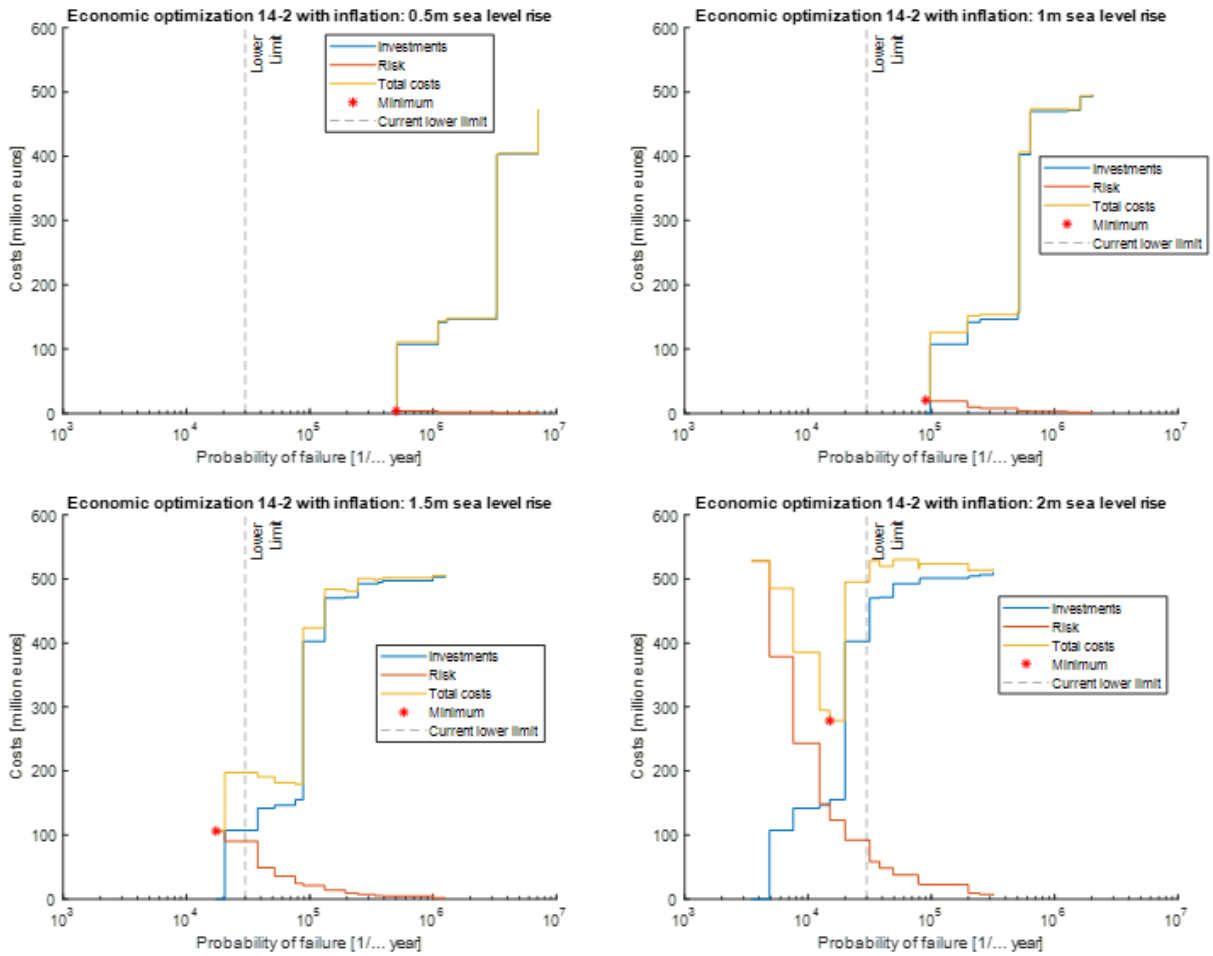
Figure F.2: Overview of the economic optimization for the scenarios 2 m sea level rise for trajectory 14-3. The threshold / lower limit of the safety level of trajectory 14-3 is 1/10.000 per year. This scenario of 2m sea level rise shows that it is not economically efficient to reinforce for trajectory 14-3. Since this will certainly also apply to the other scenarios, the optimisations are not shown for the scenarios with 0,5 to 2 m sea level rise.
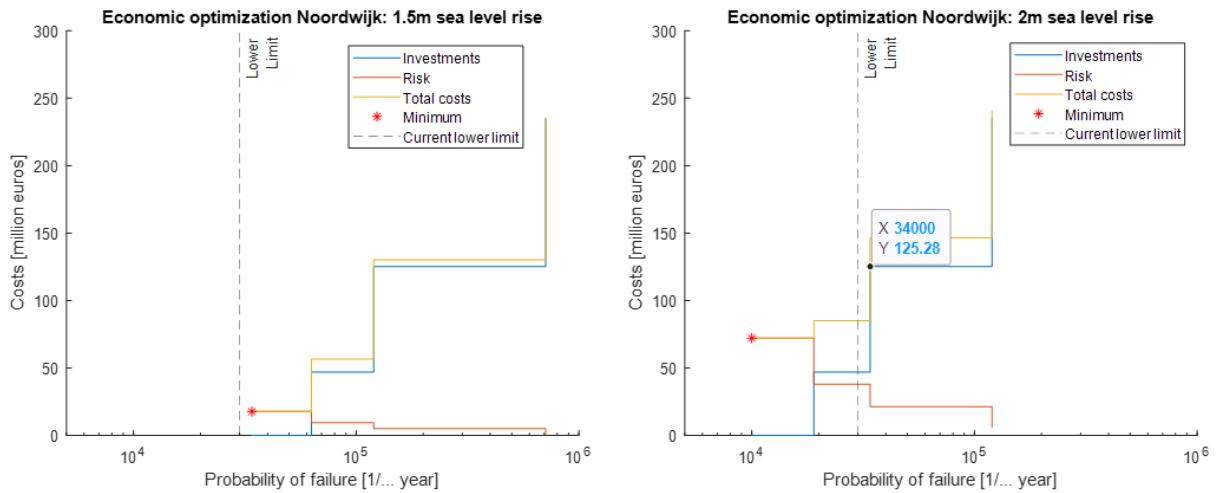
Figure F.3: Overview of the economic optimization for the scenarios 1,5 and 2 m sea level rise for dune breach location Noordwijk. The threshold / lower limit of the safety levelis 1/30.000 per year. The scenarios of 0,5 and 1m sea level rise are not shown, because it is not economically efficient to reinforce for the dunes at these scenarios.
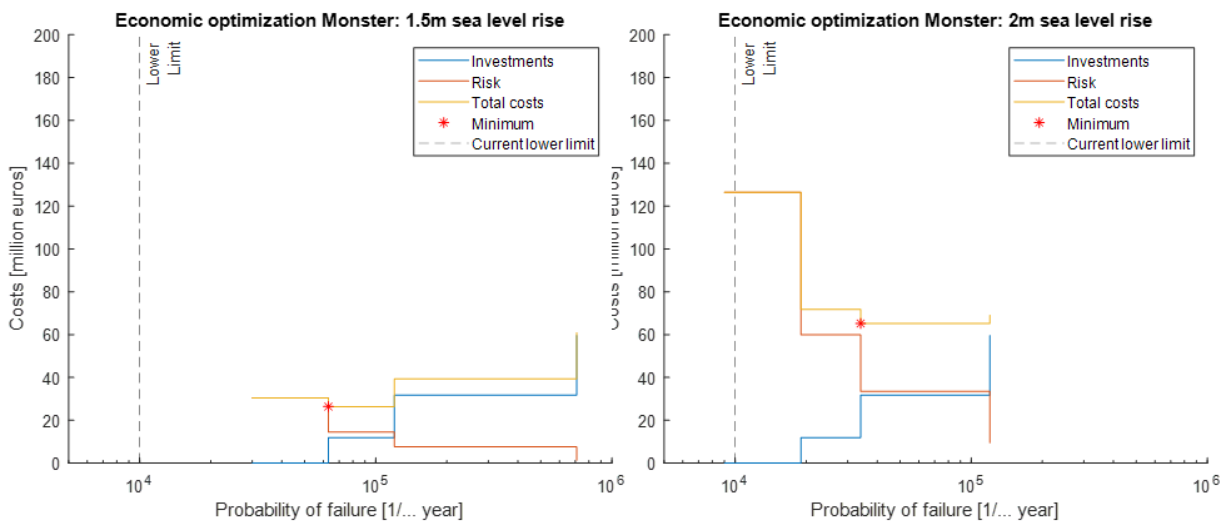

Figure F.4: Overview of the economic optimization for the scenarios 1,5 and 2 m sea level rise for dune breach location Monster. The threshold / lower limit of the safety level is 1/10.000 per year. The scenarios of 0,5 and 1m sea level rise are not shown, because it is not economically efficient to reinforce for the dunes at these scenarios.

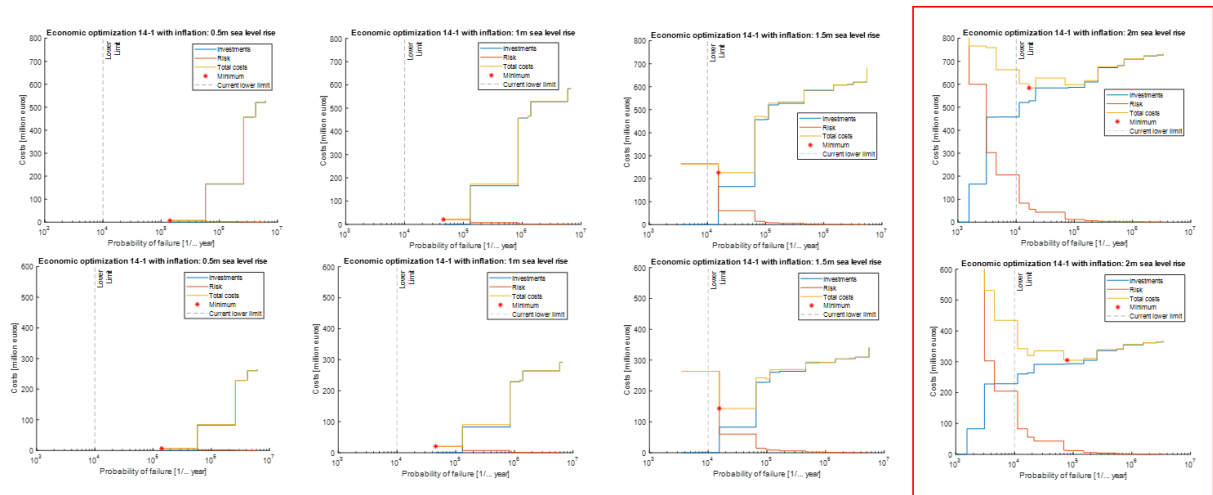## F.2.   Sensitivity analysis KOSWAT

Figure F.5: Sensitivity analysis on the influence of the KOSWAT on the recommended probability of failure. In the upper graphs, the investments necessary for reinforcements are increased with a factor 2. This only changes for the scenario of 2m sea level rise for trajectory 14-1.
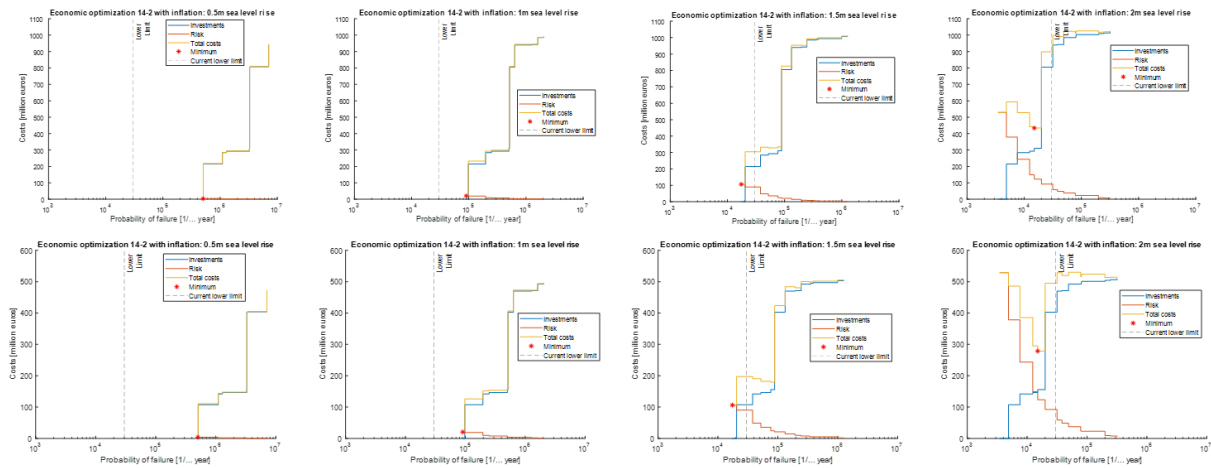

Figure F.6: Sensitivity analysis on the influence of the KOSWAT on the recommended probability of failure. In the upper graphs, the investments necessary for reinforcements are increased with a factor 2. The recommended probability of failure is the same for all scenarios.
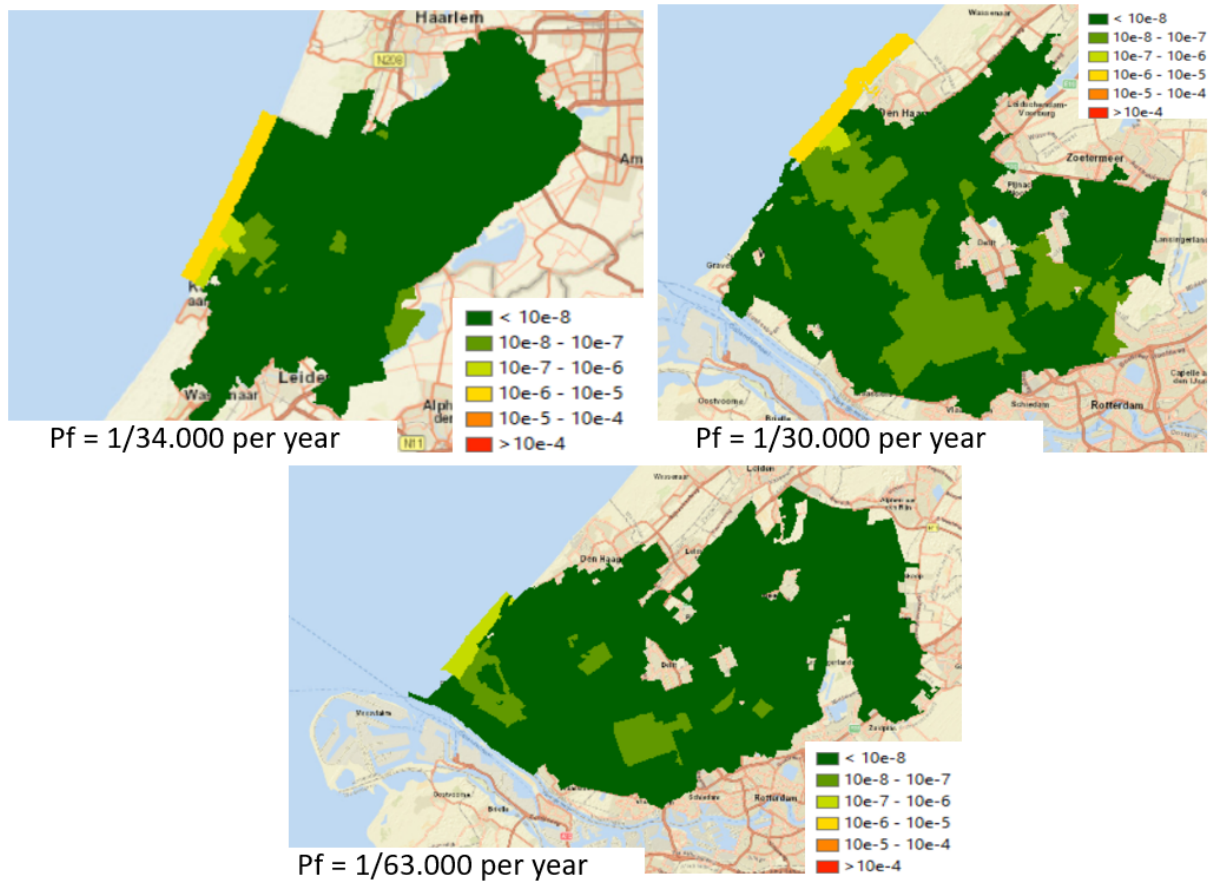
F.3. Local Individual Risk

Figure F.7: Local Individual Risk (LIR) for the coast corresponding to economic optima with the highest probability of failure. The yellow parts at the coast are located within the buffer of the surface bodies. Therefore the LIR for above scenarios do meet the requirement.